11-30-2010

Characterization of the Structure and Function of Nucleotide Pyrophosphatase/Phosphodiesterase 7

Irene Werengekha Wanjala

To the University Council:

The Dissertation Committee for Irene W. Wanjala certifies that this is the approved version of the following electronic dissertation: “Characterization of the Structure and Function of Human Nucleotide Pyrophosphatase/Phosphodiesterase 7”

_____	_____
Daniel L. Baker, Ph.D. Major Professor	Abby L. Parrill, Ph.D. Major Professor

We have read this dissertation and recommend its acceptance

_____
Yongmei Wang, Ph.D.

_____
Theodore J. Burkey, Ph.D.

_____
Richard L. Peterssen, Ph.D.

Accepted for the Graduate Council

_____
Karen D. Weddle-West, Ph.D.
Vice Provost for Graduate Programs

CHARACTERIZATION OF THE STRUCTURE AND FUNCTION OF NUCLEOTIDE PYROPHOSPHATASE/PHOSPHODIESTERASE-7

by

Irene W. Wanjala

A Dissertation

Submitted in Partial Fulfillment of the

Requirements for the Degree of

Doctor of Philosophy

Major: Chemistry

The University of Memphis

December, 2010

Dedication

To my loving mom, Rose Luseno Wanyonyi who taught me lessons I could never have learned in any classroom. You endured all for me and I love you beyond measure. May the Lord reward you abundantly.

Acknowledgements

My sincere appreciation goes to each and everyone that helped me in any way in completing my studies. I would not have done it without every single one of you. I am most indebted to my husband, Shad Nasong'o first for paving the way for me to reach the USA and second for his support and understanding. You stood in the gap in all ways and I would not have managed without you. I commend my sons Amos and Alfred for their patience and understanding when I had to spend long hours in the lab.

Many thanks to my research mentors Dr. Daniel L. Baker and Dr. Abby L. Parrill together with my research committee members Dr. Yongmei Wang, Dr. Theodore Burkey and Dr. Richard Peterssen. Thank you all for your guidance and support and for being easily accessible whenever I needed you.

I specifically wish to thank the Department of Chemistry at The University of Memphis for financial support throughout my program. I acknowledge the Elsa Pardee foundation and the American Heart Association for research funding. Sincere thanks to the great women at P.E.O. for awarding me the International Peace Scholarship in 2006 and 2008. You are a source of inspiration to women from the third world.

Last but not least, I acknowledge all my student peers, faculty and staff in the Chemistry Department for their support. I specifically acknowledge Angela Howard for giving me a thorough orientation at the beginning of my program and for sharing ideas throughout our tenure at the University. Dr. Truc Chi Pham is appreciated for her tireless brainstorming sessions with molecular biology kinks. Thanks to Krista Bearden, Karen

Mosely, Jessica Williams, Kristi Ruddick, Patricia Ranaivo, Benjamin Clayton, Dr. Alexandra Kikonyogo and Dr. Samuel Tekobo, among others, for their friendship.

ABSTRACT

Wanjala, Irene Werengekha. Ph.D. The University of Memphis. December, 2010.
Characterization of the structure and function of nucleotide pyrophosphatase/phosphodiesterase-7
Major Professors: Daniel L. Baker and Abby L. Parrill

Nucleotide pyrophosphatase/phosphodiesterase (NPP) 7, also known as alkaline sphingomyelinase (Alk-SMase) is a membrane-anchored ectoenzyme initially discovered in the rat intestinal tract in 1969. It is the most recently identified NPP isoform. The family currently consists of seven members, NPP1-7, numbered according to the order in which they were first associated with the family. NPP enzymes hydrolyze a wide range of substrates. NPP1and NPP3 are nucleotide pyrophosphatases that cleave inorganic phosphate from nucleotides and their derivatives. In contrast, NPP2, NPP6 and NPP7 are phosphodiesterases that hydrolyze phosphodiester bonds in lysolipids and their derivatives. NPP4 and NPP5 are yet to be characterized in terms of substrate preference and biological function. Numerous lysolipid derivatives have been shown to be hydrolyzed by NPP2 and NPP6 but only three main lysolipid substrates have been previously reported for NPP7. One of the goals of this work was to characterize the substrate preference of NPP7 through more exhaustive kinetic means. Our results show that NPP7, like NPP2 and NPP6, hydrolyzes numerous choline-containing substrates including glycerolipids, lysophosphatidylcholine, platelet activating factor, lyso platelet activating factor and the sphingolipids, sphingomyelin and sphingosylphosphorylcholine. A synthetic small molecule, *para*-nitrophenyl phosphocholine was also identified as a substrate for NPP7. Like NPP6, NPP7 hydrolyzed all identified substrates with a

lysophospholipase C activity and like NPP2, NPP7 preferred larger lipid substrates to the smaller non-lipid substrates tested.

Most hydrolytic activities of NPP isoforms lead to formation of bioactive lipids that affect numerous physiological and pathological processes. This, coupled with their extracellular activity, makes them attractive targets for therapeutic intervention. A major bottleneck to their utilization as therapeutic targets is that very little is known about their structure and function. Although NPP enzymes hydrolyze a wide range of substrates, and sometimes share a common substrate, they exhibit different substrate preference profiles, the factors producing these substrate profiles have not been previously investigated. Our second goal was therefore to employ computational modeling as a rational tool to guide experimental procedures in exploring NPP7 substrate specificity determinants. Our modeling results suggest the presence of a common binding pocket for the different substrate groups of NPP7and presence of essential non covalent interactions between the substrate and specific amino acid residues.

Like alkaline phosphatases, NPP isoforms require two divalent metal cations within their catalytic core and are inactivated when the metals are removed. The amino acid residues that coordinate these metal cations are conserved within NPP and AP isoforms. However, the specific endogenous divalent metal in individual NPP isofomrs is not yet known. It still remains an open question as to the specific role of these divalent metal cations in enzyme activity. Our third goal was therefore to explore the role played by divalent metal cations during the NPP7 catalytic cycle. Our results indicate that the secondary structure of NPP7 is not altered in presence or absence of divalent metal cations. However, its catalytic function is eliminated with prolonged exposure to

sufficient amounts of metal chelators. The current work significantly advances our understanding of NPP7 in terms of preferred substrates, the amino acid determinants that underlie these preferences and the role of divalent catalytic site metal ion in the structure and function of the enzyme.

PREFACE

This dissertation presents a detailed description of our efforts to better understand the structure and function of nucleotide pyrophosphatase/ phosphodiesterase-7 (NPP7). NPP7 was discovered more than 40 years ago and has been associated with a wide range of biological processes. Despite its relatively long history and importance, its structure and function are not yet well understood. NPP7 was choosen as the focus of this work, in part, because it is one of the smaller isoforms within the NPP family and could be used as a model for the larger isoforms that are more difficult to isolate and characterize.

Computational molecular modeling, molecular biology and biochemical methods have been used to study the structure and function of NPP7. The work in chapter 3 is an extensive survey of NPP7 substrates in which three new substrates were identified for the enzyme. This work is submitted to the *Journal of Lipid Research.* Chapter 4 is a discussion of the use of computational homology modeling to identify substrate recognition determinants for NPP7 and the experimental validation of these results by mutagenesis and biochemical analyses. This work is submitted to the *Journal of Molecular Pharmacology*. Chapter 5 presents work on the role of divalent metal cations in NPP7 and was performed as a comparative survey with NPP2 and NPP6. The work is to be submitted as an equally authored paper by Dr. Truc Chi Pham, Irene W. Wanjala and Angela L. Howard to *Biochemical Journal*. Only work specific to NPP7 is presented in chapter 5 of this dissertation. To help maintain continuity, chapters 1 (introduction), 2 (molecular biological strategies and procedures) and 5 (metal ion effects) are also formatted following *Journal of Lipid Research* guidelines.

Table of Contents

List of Tables

List of Figures

List of Abbreviations

Bis-pNPP: bis-*para*-nitrophenyl phosphopate

BVES: baculovirus expression system

E169A: glutamate 169 mutated to alanine

E169Q: glutamate 169 mutated to glutamine

EDTA: ethylenediaminetetraacetic acid

EG: ethylene glycol

F275A: phenylalanine 275 mutated to alalnine

F80A: phenylalanine 80 mutated to alanine

GPC: glycerolphosphocholine

HEK: human embryonic kidney

L107F: leucine 107 mutated to phenylalanine

LPA lysophosphatidic acid

LPC lysophosphatidylcholine

LPLC: lysophospholipase C

LPLD: lysophospholipase D

Lyso SM: lyso sphingomyeline

MPD: 2-methyl-2,4-pentanediol

MWCO: molecular weight cut-off

NPP nucleotide pyrophosphatase/phosphodiesterase

PAF: platelet activating factor

pNPP: *para*-nitrophenyl phosphopate

pNPPC: *para*-nitrophenyl phosphocholine

pNP-TMP: *para*-nitrophenyl thymidine-5-monophosphate

R440: arginine 440

SM sphingomyelin

SPC: sphingosylphosphorylcholine

T415: threonine 415

Y142A: tyrosine 142 mutated to alanine

Y166A: tyrosine 166 mutated to alanine

CHAPTER 1

INTRODUCTION

1.1 NPP7 history

Nucleotide pyrophosphatase/ phosphodiesterase 7 is also known as alkaline sphingomyelinase (alk-Smase) (1-5) and was initially discovered in 1969 by Swedish scientist, Åke Nilsson (6). However, it remained relatively obscure for thirty years due to a lack of understanding of its biological relevance. Initially, sphingomyelin (7) was the only known substrate and no further biological significance was associated with SM hydrolysis (8). However, in the late 1990s, it was shown that sphingomyelin metabolism leads to the formation of both proliferative messengers such as lysosphingomyelin, sphingosine-1-phosphate, and ceramide phosphate and anti-proliferative messengers such as ceramide and sphingosine (9). This revelation led to rejuvenated efforts toward identifying the biological significance of this enzyme. Initial investigations established that although NPP7 hydrolyzed sphingomyelin (SM) at alkaline pH, hence its name alkaline sphingomyelinase, it has no structural similarity with known acid and neutral sphingomyelinases (3). In 1997, alk-SMase was shown to have structural and functional similarity with the NPP subfamily of alkaline phosphatase enzymes (10).

1.2 The NPP isoforms

The NPP family currently consists of seven members named NPP1-7 in the order in which they were first associated with the family (1). All isoforms, with the exception of NPP2, are membrane-anchored ectoenzymes classified as either type I or type II membrane proteins depending on their orientation relative to the cell membrane (1). NPP1 and 3 are type II (extracellular C-terminus) while NPP4-7 are type I (extracellular N-terminus) transmembrane proteins. NPP2 is the only secreted member of the family (11). All seven isoforms have structural and functional similarities described in the following sections.

1.3 Structural similarities among NPP isoforms

1.3.1 Conserved extracellular catalytic domains

All NPP enzymes have a modular structure with a conserved catalytic domain of nearly 400 amino acid residues as shown in Fig. 1.1. The different human isoforms exhibit 24-60% overall conserved amino acid identity (1). In addition to the conserved catalytic domains, NPP4, NPP5, NPP6 and NPP7 also contain a putative N-terminal signal peptide and a C-terminal transmembrane domain. Their C-termini traverse the cell membrane while their catalytic domains face the extracellular space (1, 12). Functionally active, truncated forms of NPP6 (5) and NPP7 (13) that lack this C-terminal membrane anchor, termed Ex-constructs, have been described that are secreted by mammalian cells. NPP1 and NPP3 have N-termini that traverse the cell membrane. Despite this reversed orientation, the catalytic domains of these isoforms also face the extracellular space (12).

The remaining isoform, NPP2, is synthesized as a pre-pro-enzyme that is secreted in active form after proteolytic processing (14).

1.3.2 Nuclease-like domains and somatomedin B-like domains

The larger NPP isoforms, NPP1, NPP2 and NPP3, have nuclease-like domains on the C-terminal side of their catalytic domains. These nuclease-like domains are similar in primary amino acid sequence to DNA and RNA-nonspecific endonucleases but lack this catalytic capacity, and they lack the residues required for endonuclease activity (1). NPP1-3 also contain two somatomedin B-like domains that were initially thought to be involved in homodimerization (1). However, the role of the somatomedin B-like domains in NPP isoforms remains unknown as it has now been shown that none of the NPP isoforms form dimers (15).

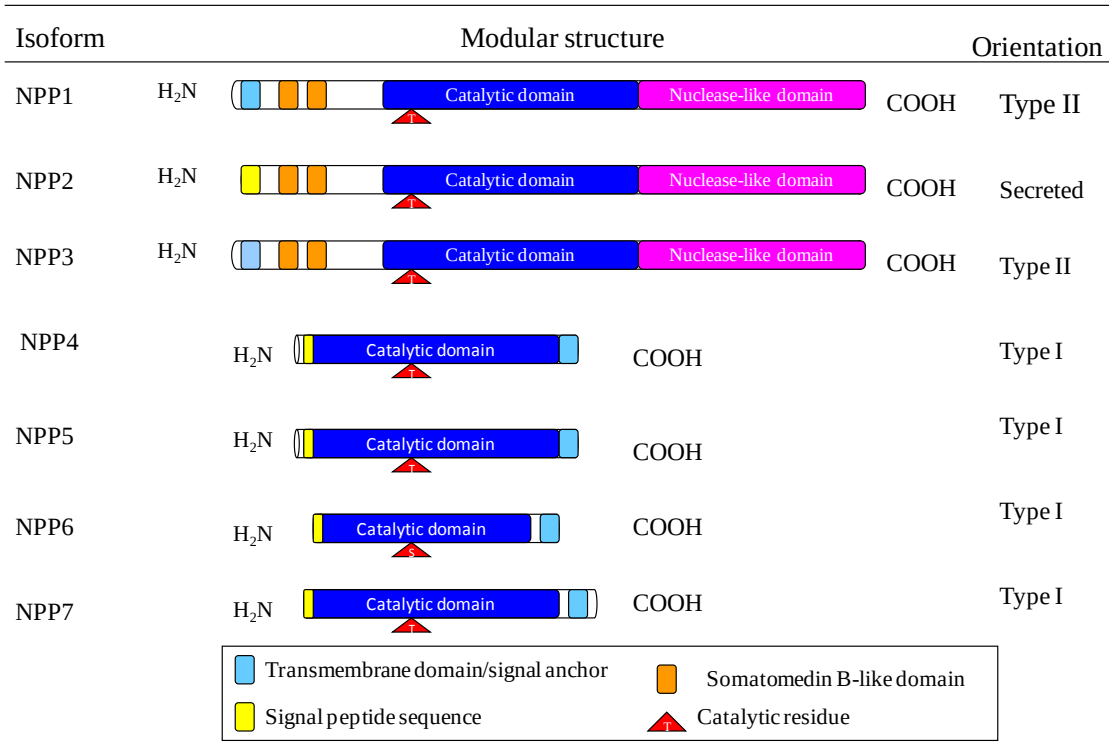

Fig. 1.1. The domain structure of the known NPP isoforms. The seven NPP isoforms are arranged in the order of their initial association with the NPP family. (1)

1.3.3 Conserved catalytic and metal-binding sites

All seven NPP isoforms contain a single conserved nucleophilic alcohol-containing catalytic residue (12). In NPP6 this is a serine (5) while all other NPP family members contain a threonine (12). In close proximity to the single catalytic residue are two divalent metal cations that are important in catalytic function. The residues coordinating these divalent metals are conserved in identity and spatial arrangement as those of other sulfo- and phospho-coordinating metalloenzymes such as alkaline phosphatases (12). However, the metal identity and requirement for each NPP enzyme are still not known. The NPPs are believed to have a similar catalytic mechanism to that

of the closely related alkaline phosphatases (APs) and amino acid residues that coordinate the two metal cations within the catalytic site are conserved in both families of enzymes (12). Sequence comparisons indicate that for all NPPs, metal 1 is coordinated by two histidines and one aspartate while metal 2 is coordinated by two aspartates and one histidine.

1.4 Functional similarities among NPP isoforms

1.4.1 The catalytic cycle of NPP isoforms

The catalytic mechanism for NPP enzymes has been proposed based on that of the extensively studied and closely related alkaline phosphatases (1, 12). The NPP7 catalytic cycle occurs in several steps as shown in Fig. 1.2. In the first step, the phosphate group of the incoming substrate is attacked by a metal-activated hydroxyl group of the catalytic residue, threonine75 (T75) in NPP7. This leads to the formation of a phosphodiester linkage with the substrate phosphate resulting in a metal stabilized enzyme-substrate complex. In the second catalytic step, one of the divalent metal cations activates a water molecule by lowering its pK_a and facilitates a nucleophilic attack on the phosphate atom of the intermediate. This leads to regeneration of the free enzyme with the release of phosphorylcholine, the second catalytic product (16).

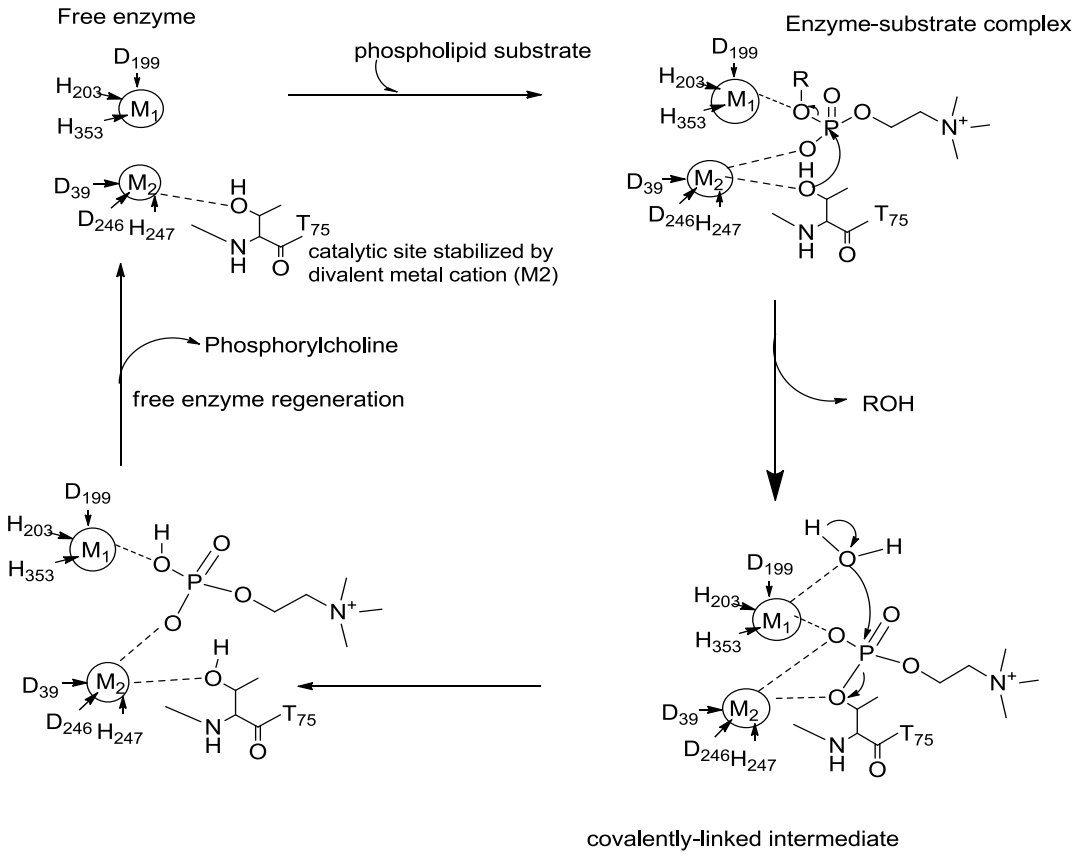

Fig. 1.2. NPP7 catalytic cycle. The metal activated OH of T75 attacks the phosphate group of substrate (SM) in the first step. A stabilized covalent phosphorylated enzyme intermediate is formed. A metal activated water molecule attacks the phosphate group leading to release of product generating free enzyme in the second step. M1 and M2 are divalent metal cations present in the active site of all NPP enzymes (2).

1.4.2 NPP substrate specificity and preferences

NPP enzymes are classified as pyrophosphatases or phosphodiesterases depending on the substrates they hydrolyze. NPP1-3 are pyrophosphatases that cleave inorganic phosphates from nucleotides and their derivatives (17). In contrast NPP2, NPP6 and NPP7 are phosphodiesterases that hydrolyze phosphodiester bonds in lipids and their

derivatives (4, 5). NPP4 and NPP5 are yet to be characterized in terms of substrates and types of activity. NPP2 is the only one of the seven NPP isoforms that is known to possess both pyrophosphatase and phosphodiesterase activities (1). As a phosphodiesterase it exhibits lysophospholipase D (LPLD) activity, in contrast to NPP6 and NPP7 both of which exhibit lysophospholipase C (LPLC) activity. Fig. 1.3 illustrates the two types of activity using a lysophosphatidylcholine (LPC) as an example substrate. Beside these specific activities, NPP isoforms also exhibit differing substrate preference profiles but it is unclear what determines these well-defined characteristics. (12, 18).

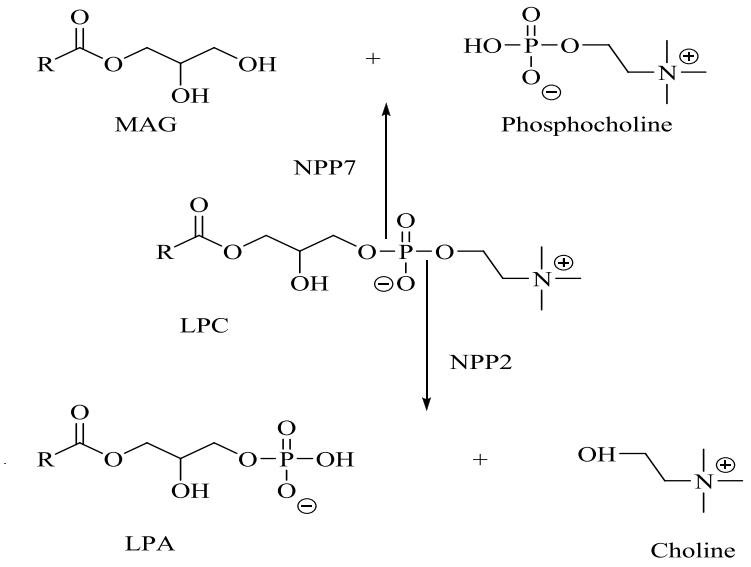

Fig. 1.3. LPLC versus LPLD hydrolysis of LPC. NPP7 generates monoacylglycerol (MAG) and a phosphocholine via LPLC activity while NPP2 generates LPA and choline via LPLD activity.

1.4.3 Biological significance of NPP isoforms

Hydrolytic activities of the NPP enzymes affect a very diverse variety of biological processes as is summarized in Table 1.1. Hydrolysis of several of their substrates (especially lipids) generates messengers that mediate numerous signaling pathways to elicit these biological affects (7, 19, 20).

Table 1.1. Summary of the properties of NPP isoforms

Isoform	**Other names**	**Preferred substrate(s)**	**Enzymatic activity**	**Biological significance**
NPP1	MAFP, NPPase, NPPγ, NTPPPH, PC-1	Nucleotides and derivatives	Nucleotide Pyrophospha tase	Bone mineralization soft tissue calcification insulin signaling
NPP2	Autotaxin, lysoPLD, NPPα, PD-1α	Nucleotides L lysophospholipids and derivatives	Nucleotide pyrophospha tase and lysophospho -lipase D	Normal development Carcinogenesis Cardiovascular disease Neuropathic pain Obesity, among others
NPP3	B10, CD203c, gp130RB13-6, NPPβ, PD-1β	Nucleotides derivatives	Nucleotide Pyrophospha tase	Allergy sensitivity glial cell differentiation
NPP4	N/A	Unknown	Unknown	Unknown
NPP5	N/A	Unknown	Unknown	Unknown
NPP6	N/A	Choline containing lysophospho-lipids	Choline Specific Lysphospho-lipase C	Renal Choline reabsorption
NPP7	Alkaline sphingomyelinase (Alk-SMase)	Choline containing lysophospholipids	Choline specific lysphospho-lipase C	Gastrointestinal Maturation, Cholesterol absorption, Anticancer effects

1.5 Current studies on the characterization of NPP7

The biological activity of NPP7 warrants further study to better understand its function. Likewise, understanding NPP7 structure and function will, by analogy, help understand NPP2 which is an anticancer target. In the current study, we describe the use of a combination of biochemical and computational methods to significantly expand knowledge on the structure and function of NPP7. The following three main areas will be addressed.

1.5.1 Influence of substrate chain length and architecture on NPP7 activity

An extensive investigation of the influence of substrate chain length and architecture within lysolipids on NPP7 catalytic function is described in Chapter 3. Through this work we identified two lysolipids; sphingosylphosphorylcholine (SPC) and lyso platelet activating factor (lyso PAF), and one synthetic small molecule, *para*-nitrophenylphosphocholine (pNPPC), as novel NPP7 substrates. NPP7 activity against each of these newly identified substrates, as well as the previously known substrates has been extensively characterized using Michaelis-Menten enzyme kinetics described in Section 1.5.3.

1.5.2 NPP7 substrate specifying determinants

The use of molecular modeling to investigate substrate recognition by NPP7 and validation of the models using biochemical assays on site-directed mutant proteins is described in Chapter 4. Analysis of mutant activity and comparison of their efficiency relative to wild type enzyme was achieved by applying the Michaelis-Menten kinetics for

each enzyme against several NPP7 substrates. The mathematical and qualitative basis of the Michaelis-Menten's theory of enzyme catalyzed reactions is briefly discussed in Section 1.5.3. The results obtained show that F275 is essential for recognition of all choline phosphodiesters by NPP7. In addition, several residues, including E169 and Y166, were found to play a role in determining NPP7 substrate preferences.

1.5.3 Application of the Michaelis-Menten kinetics to enzyme catalysis

We have applied Michaelis-Menten kinetics to the characterization of the catalytic behavior of NPP7 and its mutants. As such, a detailed description of the theory is necessary. The Michaelis-Menten (MM) theory for enzyme kinetics first assumes that the enzyme, E, and its substrate, S, associate reversibly to form an enzyme-substrate complex, ES as follows;

$$E + S \underset{k_{-1}}{\overset{k_1}{\rightleftharpoons}} ES \qquad (1)$$

This association/dissociation is assumed to be in rapid equilibrium with K_s denoting the the enzyme : substrate dissociation constant (21). Therefore at equilibrium,

$$k_{-1}[ES] = k_1[E][S] \qquad (2)$$

and

$$K_s = ([E][S])/[ES] = k_{-1}/k_1 \qquad (3)$$

The product, P, is formed in a second step when ES yields the free enzyme plus product (E + P). The complete reaction equation therefore becomes;

$$E + S \underset{k_{-1}}{\overset{k_1}{\rightleftharpoons}} ES \xrightarrow{k_2} E + P \qquad (4)$$

After the second step, E is free to interact with another substrate molecule. Briggs and Haldane refined the interpretations above by assuming that the concentration of the enzyme-substrate complex, ES, quickly reaches a constant value in such a dynamic system (22). This means that ES is formed as rapidly from E + S as it disappears through dissociation to generate E + S and reaction to form E + P. This is the steady-state assumption where the change in ES concentration with time (t) is zero and is expressed as

$$d[ES]/dt = 0 \qquad (5)$$

With the steady state assumption the rate of formation and breakdown of ES are defined by rate expressions that involve several rate constants (23). A combination and simplification of these five expressions summarizes the formation of the ES complex as follows

$$[ES] = \frac{[E_t][S]}{[S] + \{(k_1 + k_2)/k_1\}} \qquad (6)$$

The term $(k_{-1} + k_2)/k_1$ is defined as the Michaelis constant, K_m and substituting it in equation (6) gives:

$$[ES] = [E_t][S] / (K_m + [S]) \qquad (7)$$

When k_2 is rate-limiting, $k_2 << k_{-1}$ and K_m reduces to k_{-1} / k_1, which is defined as the dissociation constant, K_d of the ES complex. Where these conditions hold, K_m represents a measure of the affinity of the enzyme for its substrate in the ES complex. However, this

scenario does not hold for most enzymes. In cases where $k_2 >> k_{-1}$ then $K_m = k_2/k_1$. In other cases where k_2 and k_{-1} are comparable K_m remains a more complex function of all three rate constants. In such cases, the Michaelis-Menten equation and the characteristic behavior of the enzyme still apply but the K_m cannot be considered as a simple measure of substrate affinity.

The Michaelis-Menten kinetics of enzyme catalyzed reactions are also simplified by the initial velocity assumption where formation of ES from E + P by the reverse reaction is ignored (24). This is true for the initial velocity for the reaction immediately after E and S are mixed and [P] is essentially zero. With this simplification, the initial velocity (V_o) is then described by the breakdown of ES to form product which is determined by the concentration of the enzyme-substrate complex:

$$V_o = k_2[ES] \quad (8)$$

Initial velocity can also be expressed in terms of the Michaelis constant K_m as follows:

$$V_o = k_2[E_t][S] / (K_m + [S]) \quad (9)$$

The maximal velocity, V_{max}, of an enzyme occurs when the enzyme is saturated with substrate i.e. when $[ES] = E_t$, and can thus be described as $k_2[E_t]$. Therefore equation 9 can also be expressed as:

$$V_o = V_{max}[S] / (K_m + [S]) \quad (10)$$

This is known as the Michaelis-Menten equation, the rate equation for a one-substrate enzyme–catalyzed reaction. This equation is a statement of the qualitative relationship between the initial velocity V_o, the maximal velocity V_{max} and the substrate concentration [S], all related through the Michaelis constant K_m. K_m is expressed in units of

concentration and is described as the concentration of substrate when the initial velocity, V_o equals half the maximal velocity:

$$K_m = [S], \text{ when } V_o = 1/2V_{max} \quad (11)$$

In the work described in Chapters 3 and 4 of this dissertation, enzyme activity was measured either by fluorescence (lipid substrates) or absorbance (paranitrophenol derivative substrates). NPP7 catalytic activity against varying substrate concentrations was measured in relative fluorescence and absorbance units which were converted to product concentrations using standard curves based on resorufin and *para*-nitrophenol, respectively. The initial velocity (V_o) of the enzyme was determined by taking the slope (within the linear range) of the activity curve for each substrate concentration. The linear fit equation from a plot of signal (fluorescence or absorbance) against standard (resorufin or *para*-nitrophenol) concentration was used to convert all relative fluorescence and absorbance units to product concentrations. The resulting initial reaction velocities were plotted against substrate concentration and rectangular hyperbolic curve fitting *[y = m1 * m2x(1+ m2x)]* was done with KaleidaGraph 4.0 (Synergy software, Reading, PA, USA). In this equation, m1 = V_{max} and 1/m2 = K_m.

To describe the limiting rate of any enzyme-catalyzed reaction at saturation, a more general rate constant, k_{cat} is used (23). If the enzyme-catalyzed reaction has several steps and one is clearly rate-limiting, then k_{cat} is equivalent to the rate constant for that limiting step (25). When several steps are partially rate-limiting, k_{cat} can become a complex function of several of the rate constants that define each individual step. In the Michaelis-Menten equation, $k_{cat} = V_{max} / [E_t]$ and equation 10 thus becomes

$$V_o = k_{cat}[E_t][S] / (k_m + [S]) \quad (12)$$

k_{cat} is also called the turnover number and it is equivalent to the number of substrate molecules converted to product in a given unit time by a single enzyme active site when the enzyme is saturated with substrate. The first order rate constant, k_{cat} and has units of reciprocal time. The kinetic parameters, k_{cat} and K_m, are useful in studying and comparing different enzymes. Each enzyme will have values of k_{cat} and K_m that reflect the cellular environment such as the concentration of substrate normally encountered in vivo by the enzyme and the chemistry of the reaction being catalyzed. In the results described herein, the turnover number (k_{cat}) was calculated by dividing the V_{max} value by the final enzyme concentration used in all assays (8.33 nM). This value represents the number of catalytic cycles or turnovers per enzyme active site per unit time when enzyme is saturated with substrate (22). The kinetic parameters, k_{cat} and K_m also allow the evaluation of the kinetic efficiency of enzymes although either parameter alone is insufficient for this task. For instance, two enzymes catalyzing different reactions may have the same k_{cat} value yet the rates of the uncatalyzed reactions may be different and thus the rate enhancements brought about by the enzymes may be greatly different (22). The best way to compare catalytic efficiencies of different enzymes or turnover of different substrates by the same enzyme is to compare the ratio k_{cat} / K_m for the two reactions. This ratio is also called the specificity constant (23) and is the rate constant for the conversion of E + S to E + P. When $[S] << K_m$ equation 12 reduces to the form

$$V_o = k_{cat} / K_m [E_t][S] \quad (13)$$

V_o in this case depends on the concentration of two reactants, $[E_t]$ and [S] making k_{cat}/K_m a second order rate constant with units of $M^{-1}s^{-1}$. The higher the ratio, the more efficient the enzyme is for a given substrate (21) however, there is an upper limit to k_{cat} / K_m, imposed by the rate at which E and S can diffuse together in aqueous environment. The diffusion-controlled limit is 10^8 to 10^9 $M^{-1}s^{-1}$. Enzymes that have a specificity constant value near this range are said to have achieved catalytic perfection. In this dissertation, we shall use all these parameters to characterize the catalytic activity of NPP7 and its mutants against several substrates.

1.5.4 The role of divalent metals in NPP7 catalytic function

The role of divalent metal cations in NPP7 catalytic function is described in Chapter 5. We have employed both functional (biochemical assays) and structural (circular dichroism) methods to investigate NPP7 behavior in the presence and absence of divalent metal cations. Although previous reports indicated that EDTA is necessary for NPP7 catalytic activity, our findings indicate the opposite is true. In fact, we successfully used EDTA to significantly reduce the catalytic function of NPP7. Addition of biologically relevent divalent metals (cobalt, zinc, and nickel) to the inactivated enzyme restored catalytic activity. In all cases the secondary structure of EDTA and metal ion treated enzyme did not significantly deviate from untreated controls.

1.6 References

1. Stefan, C., S. Jansen, and M. Bollen. 2005. NPP-type ectophosphodiesterases: unity in diversity. *Trends Biochem Sci* **30**: 542-550.
2. Zalatan, J. G., and D. Herschlag. 2006. Alkaline phosphatase mono- and diesterase reactions: comparative transition state analysis. *J Am Chem Soc* **128**: 1293-1303.
3. Nyberg, L., R. D. Duan, J. Axelson, and A. Nilsson. 1996. Identification of an alkaline sphingomyelinase activity in human bile. *Biochim Biophys Acta* **1300**: 42-48.
4. Duan, R. 2003. Identification of human intestinal alkaline sphingomyelinase as a a novel ecto-enzyme related to the nucleotide phosohodiesterase family. *Biological chemistry* **278**: 38528-38536.
5. Sakagami, H., J. Aoki, Y. Natori, K. Nishikawa, Y. Kakehi, and H. Arai. 2005. Biochemical and molecular characterization of a novel choline-specific glycerophosphodiester phosphodiesterase belonging to the nucleotide pyrophosphatase/phosphodiesterase family. *J Biol Chem* **280**: 23084-23093.
6. Nilsson. 1969. The presence of sphingomyelin- and ceramide-cleaving enzymes in the small intestinal tract. *Biochimica biophysica Acta* **176**: 339-347.
7. Andersson, D., K. Kotarsky, J. Wu, W. Agace, and R. D. Duan. 2009. Expression of alkaline sphingomyelinase in yeast cells and anti-inflammatory effects of the expressed enzyme in a rat colitis model. *Dig Dis Sci* **54**: 1440-1448.

8. Hertervig, E., A. Nilsson, L. Nyberg, and R. D. Duan. 1997. Alkaline sphingomyelinase activity is decreased in human colorectal carcinoma. *Cancer* **79**: 448-453.

9. Nilsson, A., and R. D. Duan. 1999. Alkaline sphingomyelinases and ceramidases of the gastrointestinal tract. *Chem Phys Lipids* **102**: 97-105.

10. Liu, J. J., A. Nilsson, and R. D. Duan. 2000. Effects of phospholipids on sphingomyelin hydrolysis induced by intestinal alkaline sphingomyelinase: an in vitro study. *J Nutr Biochem* **11**: 192-197.

11. Clair, T., H. Y. Lee, L. A. Liotta, and M. L. Stracke. 1997. Autotaxin is an exoenzyme possessing 5'-nucleotide phosphodiesterase/ATP pyrophosphatase and ATPase activities. *J Biol Chem* **272**: 996-1001.

12. Gijsbers, R., H. Ceulemans, W. Stalmans, and M. Bollen. 2001. Structural and catalytic similarities between nucleotide pyrophosphatases/phosphodiesterases and alkaline phosphatases. *J Biol Chem* **276**: 1361-1368.

13. Cheng, Y. 2002. Purification, localization and expression of human intestinal alkaline sphingomyelinase. *Lipid Research* **44**: 316-324.

14. Jansen, S., C. Stefan, J. W. Creemers, E. Waelkens, A. Van Eynde, W. Stalmans, and M. Bollen. 2005. Proteolytic maturation and activation of autotaxin (NPP2), a secreted metastasis-enhancing lysophospholipase D. *J Cell Sci* **118**: 3081-3089.

15. Cimpean, A., C. Stefan, R. Gijsbers, W. Stalmans, and M. Bollen. 2004. Substrate-specifying determinants of the nucleotide pyrophosphatases/phosphodiesterases NPP1 and NPP2. *Biochem J* **381**: 71-77.

16. Gijsbers, R., H. Ceulemans, and M. Bollen. 2003. Functional characterization of the non-catalytic ectodomains of the nucleotide pyrophosphatase/phosphodiesterase NPP1. *Biochem J* **371**: 321-330.

17. Gijsbers, R., J. Aoki, H. Arai, and M. Bollen. 2003. The hydrolysis of lysophospholipids and nucleotides by autotaxin (NPP2) involves a single catalytic site. *FEBS Lett* **538**: 60-64.

18. Bollen, M., R. Gijsbers, H. Ceulemans, W. Stalmans, and C. Stefan. 2000. Nucleotide pyrophosphatases/phosphodiesterases on the move. *Crit Rev Biochem Mol Biol* **35**: 393-432.

19. Duan, R. D., and A. Nilsson. 2009. Metabolism of sphingolipids in the gut and its relation to inflammation and cancer development. *Prog Lipid Res* **48**: 62-72.

20. Wu, J., F. Liu, A. Nilsson, and R. D. Duan. 2004. Pancreatic trypsin cleaves intestinal alkaline sphingomyelinase from mucosa and enhances the sphingomyelinase activity. *Am J Physiol Gastrointest Liver Physiol* **287**: G967-973.

21. Paula, P. A. a. J. D. 2006. Physical Chemistry. 8th ed. Freeman and company.

22. Grisham, R. H. G. a. C. M. 1995. Biochemistry Saunders College Publishing.

23. Cox, D. L. N. a. M. M. 2008. Lehninger Principles of Biochemistry. 5th ed. W. H. Freeman and Company.

24. Voet, D. V. a. J. 2004. Biochemistry. 3rd ed. John Wiley and sons, Inc.

25. Cornish-Bowden, A. 1979. Fundamentals of Enzyme kinetics Butterworths.

CHAPTER 2

GENETIC ENGINEERING, SUB-CLONING, PROTEIN EXPRESSION AND PURIFICATION OF HUMAN NPP7

This project required the ability to express small amounts of wild type and site-directed mutants of NPP7 for activity determination, as well as the ability to express and purify larger amounts of native enzyme for biochemical, structural and functional characterization. To accomplish these diverse goals we utilized two complementary systems, transient transfection in mammalian cells (HEK293) and baculovirus expression in insect cells (Sf9). The rationale and methodology used to generate functional enzyme from these mammalian and insect cell expression systems is detailed in the following sections.

2.1 Rationale

DNA encoding full length, human NPP7 (Genebank number AY20633) was generously provided by Dr. Rui-Dong Duan (Lund University, Lund, Sweden). This gene was supplied in the pcDNA 4/TO/myc–his B mammalian expression vector cloned between KpnI and NotI restriction sites (Fig. 2.1). The work described herein for NPP7 is part of a larger project to characterize lysophospholipid preferring NPP isoforms. Thus, the NPP7 expression plasmid provided was modified prior to subcloning to achieve several goals common to the overall project. First, changes were made to the cloning sites so that a single insert could be subcloned into both the desired mammalian

expression vector (pcDNA3.1(+)) and baculovirus transfer vector (pFASTBac1). Second, a stop codon was inserted after residue 415 (threonine) to remove the 41 C-terminal residues including the transmembrane anchor to generate a soluble version of the protein that could be collected from conditioned cell culture medium. Finally, a FLAG affinity tag (DYKDDDDK) was inserted downstream of the protein sequence (between T415 and the stop codon) to allow for easy purification. The protein expressed from the resulting modified insert was a shortened version of the human NPP7 enzyme that was truncated after the FLAG affinity tag during expression. This modified protein was referred to as NPP7ExFLAG owing to its extracellular (Ex) localization, as well as the presence of the FLAG affinity tag. A similarly truncated NPP construct was previously generated and shown to retain catalytic function (1, 2).

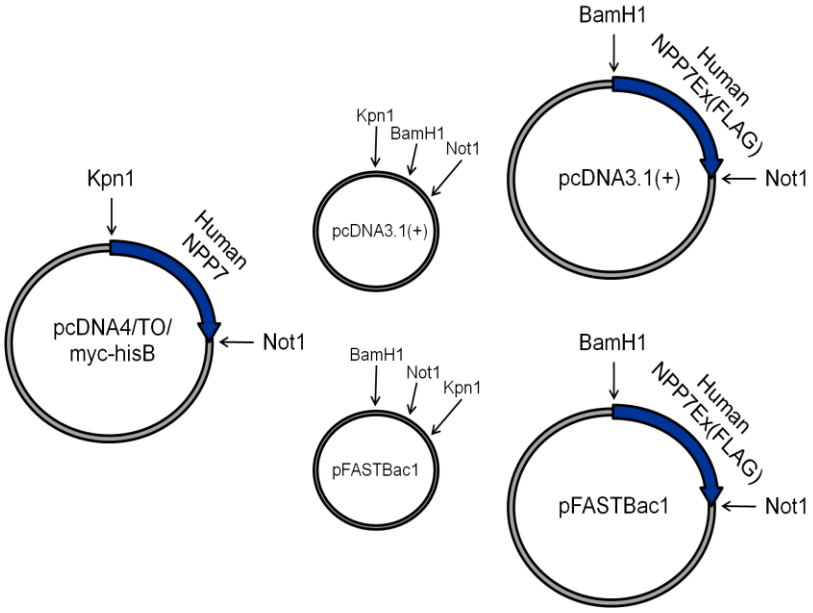

Fig. 2.1. NPP7ExFLAG genetic engineering scheme. Full length human NPP7 was provided in the pcDNA4/TO/myc-hisB plasmid (left) cloned between Kpn1 and Not1 restriction sites. Final constructs for NPP7 transient transfection into mammalian cells (pcDNA3.1+, top right) and baculovirus-mediated infection of insect cells (pFASTBac1, bottom right). Empty vectors for pcDNA3.1+ (top middle) and pFASTBac1 (bottom middle) show the relative orientation of Kpn1, BamH1 and Not1 restriction sites.

2.2 Genetic Engineering

All site-directed mutations and PCR insertions were accomplished using the QuickChange PCR kit (Stratagene, La Jolla, CA, USA) according to the manufacturer's protocols. The KpnI site (GGTACC) in the parent vector was mutated to a BamH I recognition sequence (GGATCC) using the sense primer 5'-GCGTTTAAACTTAAG CTTGGATCCGAAATGAGAG-3' and antisense primer 5'-CTCTCATGCTTTCG GATCCAAGCTTAAGTTTAAACGC-3'. In a separate PCR reaction, the FLAG

affinity-tag (DYKDDDDK) and a stop codon were incorporated at position 416 using the sense primer 5'-CCCATGCTGCACACAGACTACAAGGACGACGATGACAAGTAG GAATCTG CTCTTCCG-3' and antisense primer 5'-CGGAAGAGCAGATTCCT ACTTGTCATCG TCGTCCTTGTAGTCTGTGTGCAGCATGGG-3'. Plasmids were isolated from ampicillin resistant colonies using Miniprep kits from Qiagen (Valencia, CA, USA) according to the manufacturer's protocols and were verified by complete nucleotide sequencing of the insert. Fig. 2.2 shows complete amino acid sequences for the parent, full length NPP7 insert and for the modified truncated FLAG fusion protein.

Human NPP7(wild type)

MRGPAVLLTV ALATLLAPGA GAPVQSQGSQ NKLLLVSFDG FRWNYDQDVD
TPNLDAMARD GVKARYMTPA FVTMTSPCHF TLVTGKYIEN HGVVHNMYYN
TTSKVKLPYH ATLGIQRWWD NGSVPIWITA QRQGLRAGSF FYPGGNVTYQ
GVAVTRSRKE GIAHNYKNET EWRANIDTVM AWFTEEDLDL VTLYFGEPDS
TGHRYGPESP ERREMVRQVD RTVGYLRESI ARNHLTDRLN LIITSDHGMT
TVDKRAGDLV EFHKFPNFTF RDIEFELLDY GPNGMLLPKE GRLEKVYDAL
KDAHPKLHVY KKEAFPEAFH YANNPRVTPL LMYSDLGYVI HGRINVQFNN
GEHGFDNKDM DMKTIFRAVG PSFRAGLEVE PFESVHVYEL MCRLLGIVPE
ANDGHLATLL PMLHTESALP PDGRPTLLPK GRSALPPSSR PLLVMGLLGT
VILLSEVA

Human NPP7ExFLAG

MRGPAVLLTV ALATLLAPGA GAPVQSQGSQ NKLLLVSFDG FRWNYDQDVD
TPNLDAMARD GVKARYMTPA FVTMTSPCHF TLVTGKYIEN HGVVHNMYYN
TTSKVKLPYH ATLGIQRWWD NGSVPIWITA QRQGLRAGSF FYPGGNVTYQ
GVAVTRSRKE GIAHNYKNET EWRANIDTVM AWFTEEDLDL VTLYFGEPDS
TGHRYGPESP ERREMVRQVD RTVGYLRESI ARNHLTDRLN LIITSDHGMT
TVDKRAGDLV EFHKFPNFTF RDIEFELLDY GPNGMLLPKE GRLEKVYDAL
KDAHPKLHVY KKEAFPEAFH YANNPRVTPL LMYSDLGYVI HGRINVQFNN
GEHGFDNKDM DMKTIFRAVG PSFRAGLEVE PFESVHVYEL MCRLLGIVPE
ANDGHLATLL PMLHTDYKDD DDK

Fig. 2.2. Amino acid sequences for full length NPP7 and truncated NPP7ExFLAG. The catalytic residue T75 is highlighted in black and the FLAG affinity sequence is highlighted in grey.

2.3 Mammalian cell expression

Mammalian protein expression was used to generate relatively small amounts of wild type and mutant, human NPP7ExFLAG protein for *in vitro* functional analysis.

2.3.1 Subcloning of NPP7ExFLAG into pcDNA 3.1(+)

The modified human NPP7ExFLAG insert was subcloned from the parental pcDNA 4/TO/myc–his B vector into pcDNA3.1(+) (Invitrogen, Carlsbad, CA, USA) using standard molecular biology techniques. Inserts were liberated using double digestions with BamH1 and Not1 (New England Biolabs, Ipswich, MA, USA), purified by Qiagen's gel extraction protocol (Valencia, CA, USA), and ligated into target vector that had been digested with BamH1 and Not1 using T4 DNA ligase (New England Biolabs, Ipswich, MA, USA). Plasmids were isolated from ampicillin-resistant colonies using Miniprep kits from Qiagen (Valencia, CA, USA) according to the manufacturer's protocols and were verified first by agarose gel electrophoresis of NotI and BamHI double digests and finally by complete nucleotide sequencing of the insert (data not shown).

2.3.2 NPP7ExFLAG expression in HEK293 cells

Expression of human NPP7ExFLAG protein and site directed mutants was done by transient transfection in human embryonic kidney (HEK293T) cells using the Polyfect transfection reagent (Qiagen, Valencia, CA, USA) according to the manufacturer's protocols. Briefly, HEK293T cells were seeded in Dulbecco's Modified Eagle's Medium (DMEM) containing 10% heat inactivated fetal calf serum and 2 mM L-glutamine and

100 U/ml penicillin/streptomycin. The cells were grown overnight at 37°C and 5% CO_2 to 80% confluence before transfection with the appropriate NPP7-pcDNA3.1(+) construct and polyfect reagent. Eight hours after trasfection, the culture medium was changed to serum-free DMEM, and cells were incubated for an additional 48 hours. Conditioned medium containing secreted NPP7ExFLAG protein was collected and concentrated using Centricon 10,000 molecular weight cutoff filters (Millipore, Billerica, MA, USA) by centrifugation at 3,073 x g for 20 minutes at 4°C. Expression of protein was verified by Western blot (detailed protocols can be found in section 2.3.3). Concentrated protein was buffer-exchanged three times into NPP7 assay buffer (10 mM Tris-HCl, 150 mM NaCl, 10 mM taurocholate pH 8.0) using Centricon 10,000 molecular weight cutoff filters (Millipore, Billerica, MA, USA) by centrifugation at 3,073 x g for 20 minutes at 4°C. Proteins were stored as 0.5-1.0 µM stocks at 4°C without the addition of adjuvants or preservatives prior to functional characterization (see discussion in section 2.5).

2.3.3 Verification of NPP7ExFLAG expression

Western blots with the Anti-FLAG M2 antibody (Sigma-Aldrich, St. Louis, MO, USA) were used to verify protein expression of NPP7ExFLAG and its mutants in conditioned media of transiently transfected HEK293T cells. Following separation of proteins using sodium dodecyl sulfate polyacrylamide gel electrophoresis (SDS-PAGE) on 4-15% gradient gels (Bio-Rad, Hercules, CA, USA), proteins were transferred to polyvinylidene difluoride (PVDF) membranes (Bio-Rad, Hercules, CA, USA) by electroblotting at 100V in Tris/Glycine buffer containing 1% SDS and 20% methanol for 1 hour. Nonspecific binding sites were blocked using Tween containing 50 mM Tris

buffered saline (TBST) (2.7 mM KCl, 138 mM NaCl, 0.5% (v/v) Tween®20 and 5% (w/v) non-fat dry milk (NFDM). After appropriate washes, the membrane was treated with Anti-FLAG M2 antibody (Sigma-Aldrich, St. Louis, MO, USA) (1:2000 dilution in TBST + 3% NFDM). Following additional washes, the membrane was treated with goat anti-mouse IgG antibody (Sigma-Aldrich, St. Louis, MO, USA) (1:5000 dilution in TBST + 3 % NFDM). After a final wash, SuperSignal Pico West chemiluminescent substrate (ThermoScientific, Rockford, IL, USA) was used in conjunction with a digital imaging system (Fotodyne, Hartland, WI, USA) for detection. Fig. 2.3 shows a sample Western blot of NPP7ExFLAG proteins expressed in HEK293 cells.

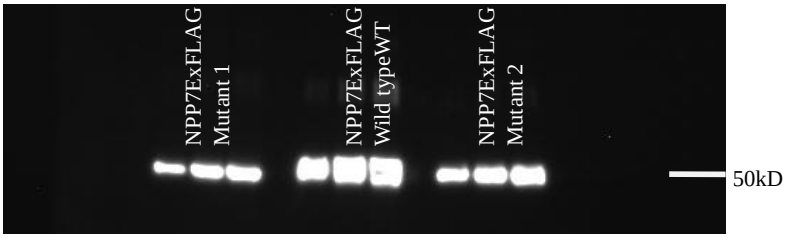

Fig. 2.3 Sample Western blot image for NPP7 expression verification. Three different concentrations (2X, 3X and 5X) of each protein sample were run and the band intensities obtained reflect the concentration differences.

2.4 Baculovirus expression of NPP7ExFLAG

Baculovirus expression was used to generate large amounts of wild type protein for structural and functional characterization. Previous research established that NPP7 is a glycoprotein that lacks activity in the absence of glycoslylation (2, 3). Although insect

cells lack the ability to perform the complete array of complex glycosylation available in mammalian cells, they do have the ability to perform simple glycosylation, as well as the ability to perform other post-translational modifications possible in mammalian systems (4, 5). Here we chose to use the Bac-to-Bac baculovirus expression system (Invitrogen, Carlsbad, CA, USA) and Sf9 insect cells.

2.4.1 Subcloning NPP7ExFLAG into pFastBac1

The Kpn1 and Not1 restriction sites present in the parent vector had a reversed orientation to those in the pFastBac1 transfer vector as shown in Figure 2.1. As was described in sections 2.1 and 2.2, the Kpn1 site was mutated to a BamH1 recognition sequence which solved this issue. The NPP7ExFLAG insert was subcloned into pFASTBac1 in parallel with pcDNA3.1(+) using the same protocols described in section 2.3.1. Bacmid was prepared according to the manufacterer's protocols. Briefly, after successful subcloning to generate the pFastBac-NPP7ExFLAG plasmid, the system required the introduction of a viral expression construct into the pFastBac1 donor vector. Bacmid DNA is a baculovirus shuttle vector contained in specialized DH10Bac™ *E. coli* (Invitrogen, Carlsbad, CA, USA), which also contain a low-copy number mini-F replicon, kanamycin resistance marker, LacZ gene and a helper plasmid. All of these components are required to transpose the Tn7 element from the pFastBac donor plasmid to the mini-*att*Tn7 attachment site on the bacmid to generate a recombinant bacmid (4-7). The resulting recombinant bacmid DNA was purified using the PureLink HiPure Plasmid Maxiprep Kit (Invitrogen, Carlsbad, CA, USA) with subsequent verification by PCR (data not shown).

2.4.2 NPP7ExFLAG expression in Sf9 insect cells

Sf9 insect cells were seeded in 6-well plates at a density of 9 x 10^5 cells per well in 2 ml of Sf-900 III serum free medium (Invitrogen, Carlsbad, CA, USA) supplemented with 50 µg/mL streptomycin and 50 units/mL penicillin (complete growth medium). The cells were incubated at 27°C and allowed to attach to the bottom of the wells for 1 hour. Transfection complexes were prepared using 2 µg bacmid DNA and 9 mL Cellfectin transfection reagent (Invitrogen, Carlsbad, CA, USA) diluted in 100 mL of unsupplemented Grace's medium (Invitrogen, Carlsbad, CA, USA). The complexes were gently mixed and incubated at room temperature for 30 minutes. Cells were incubated with the complexes at 27°C for 5 hours after which the DNA/lipid complexes were removed and replaced with 2 mL of complete growth medium. Following incubation at 27°C for 144 hours, a P1 viral stock resulted. To isolate the P1 viral stock, the conditioned cell culture medium was collected and centrifuged at 500 x g for five minutes. The clarified supernatant was then transferred to fresh sterilized tubes, and FBS was added up to a concentration of 2%. The viral stocks were stored at 4°C protected from light for up to 2 months.

The P1 viral stock was amplified to a higher titer P2 stock using fresh Sf9 cells. Sf9 cells were seeded in 6-well plates at a density of 9 x 10^5 cells per well in 2 mL of Sf-900 III serum free medium supplemented with 50 µg/mL streptomycin and 50 units/mL penicillin (complete growth medium). The cells were incubated at 27°C and allowed to attach to the bottom of the wells for one hour. 50 µL of P1 viral stock were added, and the cells were incubated at 27°C for 144 hours to generate P2 viral stocks.

To express large amounts of human NPP7ExFLAG protein, Sf9 cells were amplified in suspension culture (27°C with orbital shaking at 140 rpm) up to 1 liter in a 3 liter flask. Cells were grown in suspension up to a density of 2 x 10^6 cells/ mL of medium before infection with 15 mL of P2 viral stock. Following infection, cells were incubated at 27°C with shaking at 140 rpm for 72 hours for protein expression. After 72 hours, the conditioned medium was collected and centrifuged at 3,073 x g for 10 minutes to harvest NPP7ExFLAG. The supernatant was filtered using sterile filtering cups before protein purification using an Anti-FLAG affinity column (described in section 2.4.3).

2.4.3 Affinity purification of NPP7ExFLAG expressed in sf9 cells

Secreted NPP7ExFLAG protein was purified from conditioned cell culture medium from baculovirus infected Sf9 cells by affinity chromatography using Anti-FLAG M2 agarose beads (Sigma-Aldrich, St. Louis, MO, USA). Clarified conditioned medium was passed over an Anti-FLAG M2 Gel affinity column (5 mL column volume, Sigma-Aldrich, St. Louis, MO, USA) equilibrated in TBS buffer (50 mM Tris-HCl, 150 mM NaCl, pH 7.4). Bound protein was washed with 20 column volumes of TBS and then eluted with TBS containing 50 µg/mL FLAG peptide. The purified protein was concentrated using Centricon 10,000 molecular weight cutoff filters (Millipore, Billerica, MA, USA) by centrifugation at 3,073 x g for 20 minutes at 4°C. The concentrated protein was buffer exchanged into 10 mM Tris-HCl, 10 mM NaCl, pH 7.4 and stored at 4°C without addition of adjuvants or preservatives (see discussion in section 2.5). After purification, protein expression was verified by SDS-PAGE on 4-15% gradient gels (Bio-Rad, Hercules, CA, USA), as shown in Fig. 2.4. The purified protein is truncated after

residue 415 (threonine) and the FLAG sequence and has a molecular mass of approximately 50 kDa, as opposed to the 60kDa molecular mass for the full length enzyme. It is also noteworthy that the total mass obtained by the sum of all amino acids including the FLAG-tag is about 48 kDa, but the band obtained on SDS-PAGE is slightly above 50 kDa, most likely due to post-translational modification(s). Mature human NPP7 is known to be glycosylated at five positions (1) and insect cells are capable of such post-translational modifications (5, 7).

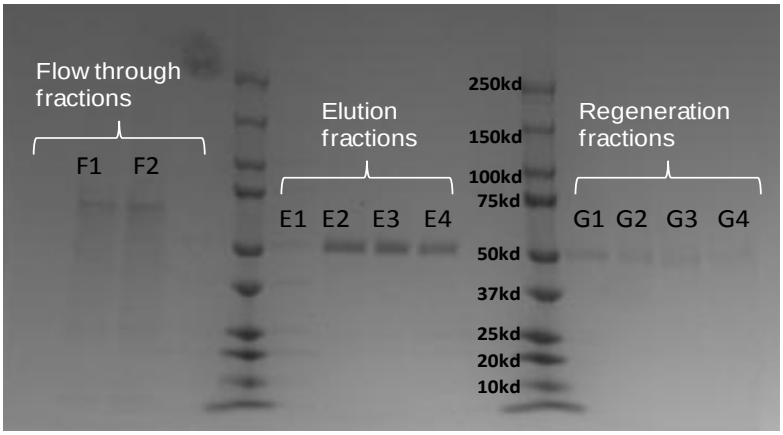

Fig. 2.4. SDS-PAGE of affinity purified NPP7ExFLAG. Flow-through fractions were collected after protein binding onto the column. Elution fractions were collected using 5ml aliquots of FLAG peptide. Regeneration fractions were collected with 5ml aliquots of glycine-HCl buffer (pH 3.5).

2.5 Storage of expressed protein

In parallel work on the NPP2 isoform, it was determined that 20% ethylene glycol was required to stabilize purified enzyme stocks for storage. The use of preservatives

and/or adjuvants during storage of NPP7 had not been previously reported in the literature. Thus, we examined the effect of several adjuvants including ethanol, 2-methyl-2,4-pentanediol (MPD), and ethylene glycol (EG) (8) on the stability of purified NPP7 stocks. All three adjuvants tested resulted in interference with assays to assess NPP7 function. In contrast, samples of NPP7 stored without additives remained stable and fully active for more than two months at a minimum concentration of 0.5 μM when stored at 4°C in NPP7 assay buffer (50 mM tris-HCl 150 mM NaCl, pH 8.0) or circular dichroism (CD) buffer (10 mM tris-HCl, 10 mM NaCl, pH 7.4). Working stocks (25 nM enzyme) were prepared immediately prior to use for all activity assays.

2.6 References

1 Duan, R., 2003. Identification of human intestinal alkaline sphingomyelinase as a a novel ecto-enzyme related to the nucleotide phosohodiesterase family, *Biological chemistry*, **278**: 38528-38536,

2 Wu, J., G. H. Hansen, A. Nilsson and R. D. Duan. 2005. Functional studies of human intestinal alkaline sphingomyelinase by deglycosylation and mutagenesis, *Biochem J*, **386**: 153-60,

3 Duan, R. D., 2006. Alkaline sphingomyelinase: an old enzyme with novel implications, *Biochim Biophys Acta*, **1761**: 281-91,

4 Philipps, B., M. Forstner and L. M. Mayr. 2004. Baculovirus expression system for magnetic sorting of infected cells and enhanced titer determination, *Biotechniques*, **36**: 80-3,

5 Philipps, B., M. Forstner and L. M. Mayr. 2005. A baculovirus expression vector system for simultaneous protein expression in insect and mammalian cells, *Biotechnol Prog*, **21**: 708-11,

6 McCall, E. J., A. Danielsson, I. M. Hardern, C. Dartsch, R. Hicks, J. M. Wahlberg and W. M. Abbott. 2005. Improvements to the throughput of recombinant protein expression in the baculovirus/insect cell system, *Protein Expr Purif*, **42**: 29-36,

7 Invitrogen. 2004. Bac-to-Bac Baculovirus Expression System,

8 Ferry, G., N. Moulharat, J. P. Pradere, P. Desos, A. Try, A. Genton, A. Giganti, M. Beucher-Gaudin, M. Lonchampt, M. Bertrand, J. S. Saulnier-Blache, G. C. Tucker, A. Cordi and J. A. Boutin. 2008. S32826, a nanomolar inhibitor of autotaxin: discovery, synthesis and applications as a pharmacological tool, *J Pharmacol Exp Ther*, **327**: 809-19,

CHAPTER 3

THE INFLUENCE OF SUBSTRATE CHAIN LENGTH AND ARCHITECTURE ON NPP7 CATALYTIC FUNCTION

3.1 Abstract

Nucleotide pyrophosphatase/phosphodiesterase (NPP) 7 is a member of the NPP family of ectoenzymes. The NPP family consists of seven known isoforms that have been associated with a wide range of biological effects. NPP7 was discovered 40 years ago but slow progress has been made toward its structural and functional characterization. It has previously been shown to hydrolyze three lipid substrates, lysophosphatidylcholine, platelet activating factor, and sphingomyelin. NPP7 activity against these three substrates has been associated with human diseases including cancer, atherosclerosis, and inflammatory bowel disease. In this study, we identify additional NPP7 substrates and characterize the effect of substrate chain length and architecture on their hydrolysis through kinetic analysis. Two bioactive lipids (sphingosylphosphorylcholine and lyso platelet activating factor) and one synthetic small molecule (para-nitrophenylphosphocholine) were identified as novel NPP7 substrates. A new absorbance-based assay method using the identified synthetic substrate is also described.

3.2 Introduction

Nucleotide pyrophosphatase/ phosphodiesterase 7 (NPP7) has previously been shown to hydrolyze three endogenous lipid substrates, lysophosphatidylcholine (LPC),

platelet activating factor (PAF), and sphingomyelin (SM) with a lysophospholipase C activity (1). NPP7 is localized mostly to the GI tract (2) and its activity leads to generation of signaling messengers implicated in various biological processes associated with this organ system (1). The hydrolysis of SM is important in the breakdown and absorption of dietary SM, maturation of the intestinal tract and cholesterol absorption (3). Hydrolysis of PAF is thought to play a role in suppression of PAF-induced inflammation in the intestinal tract (4). The hydrolysis of LPC by NPP7 reduces the generation of LPA by distinct lysophospholipase D enzymes and likely plays a role in decreasing cancer risk (5). NPP7 is an enzyme with a growing biology that merits understanding in terms of structure and function. Unfortunately, the substrate profile of NPP7 is limited to these three known substrates without complete kinetic characterization. Unlike NPP2 (6) and NPP6 (7), the other known lysolipid preferring phosphodiesterases of the NPP family, a detailed survey of possible substrates has not been published for NPP7. Such a study would help elucidate structure–activity relationships to help better understand the functions of this enzyme.

In the current study, a survey of possible lysolipid substrates of NPP7 has been conducted. Substrate candidates were selected with varied chain lengths, linkage functionality, and linker region. All candidates were subjected to full kinetic analysis of their hydrolysis by human NPP7.

3.3 Materials and Methods

3.3.1 NPP7 plasmid design

The gene coding for full length, human NPP7 contained within the pcDNA 4/TO/myc–his B mammalian expression vector was generously donated by Dr. Rui-Dong Duan of Lund University (Lund, Sweden). The insert originally contained Kpn1 (upstream) and Not1 (downstream) cloning sites. To make this insert compatible with the pFASTBac1 vector, the KpnI site (GGTACC) in the parent vector was mutated to a BamH I recognition sequence (GGATCC) using the sense primer 5'-GCGTTTAAAC TTAAGCTTGGATCCGAAATGAGAG-3' and antisense primer 5'-CTCTCATGCTT TCGGATCCAAGCTTAAGTTTAAACGC-3'. In a separate PCR reaction the FLAG affinity-tag (DYKDDDDK) and a stop codon were incorporated at amino acid position 416 using the sense primer 5'-CCCATGCTGCACACAGACTACAAGGACGACG ATGACAAGTAGGAATCTGCTCTTCCG-3' and antisense primer 5'-CGGAAGAGCAGATTCCTACTTGTCATCGTCGTCCTTGTAGTCTGTGTGCA GCATGGG-3'. The Quickchange PCR kit (Stratagene, La Jolla, CA, USA) was used for all mutagenesis according to the manufacturer's protocols. All mutants were verified through complete nucleotide sequencing before further manipulation. Truncation of NPP7 at amino acid position 416 (to generate the construct NPP7ExFLAG) has previously been shown to generate functional, extracellularly localized protein (8). To allow for high capacity protein production and purification, the NPP7ExFLAG insert was used to generate a recombinant bacmid using the Bac-to-Bac system (Invitrogen, Carlsbad, CA, USA) according to the manufacturer's protocols. Bacmid DNA was purified using the PureLink HiPure Plasmid Maxiprep Kit (Invitrogen K2100-06,

Carlsbad, CA, USA) and verified by PCR. Recombinant Bacmid DNA was transfected into Sf9 cells in the presence of Cellfectin transfection reagent (Invitrogen, Carlsbad, CA, USA) to generate viral stocks. High titer viral stocks were obtained after a second 7 day infection.

3.3.2 NPP7 protein expression and purification

For protein expression, Sf9 cells were amplified to a density of 2 x 10^6 cells/mL in a 1L cell culture suspension before the addition of high titer viral stock (15 mL). After 72 hours of infection, conditioned medium was collected and clarified by centrifugation at 3,073 x g for 10 minutes. The supernatant was filtered using 0.22 μm sterile filtering cups (Millipore, Billerica, MA, USA) before protein purification.

The filtered media was purified using an Anti-FLAG M2 Gel affinity column (Sigma-Aldrich, St. Louis, Mo, USA) equilibrated in TBS buffer (50 mM Tris, 150 mM NaCl, pH 7.4). Bound proteins were washed with 20 column volumes of TBS and then eluted with TBS containing 500 μg/mL FLAG peptide (Sigma-Aldrich, St. Louis, MO, USA). Purified proteins were concentrated and buffer exchanged into 10 mM Tris, 10 mM NaCl, pH 7.4 using Centricon 10,000 MWCO filters (Millipore, Billerica, MA, USA). Protein purity was verified by SDS-PAGE with Coomassie staining and Western blot.

3.3.3 NPP7 catalytic activity assays

Fluorescence-based assay: Hydrolysis of all lipid substrates was monitored using a modification of Invitrogen's Amplex Red phospholipase C assay to detect released

phosphatidylcholine. NPP7ExFLAG catalytic activity was monitored via fluorescence determination (excitation 571 nm and emission 585 nm) every minute for 1 hour using a Synergy2 multiwell plate reader (BioTek Instruments Inc., Vermont, USA). Each well on the plate was loaded with a total of 60 µL consisting of substrate, Amplex Red cocktail (10 µM Amplex Red reagent, 0.1 U/mL choline oxidase, 1 U/mL horseradish peroxidase, 4 U/mL alkaline phosphatase) and recombinant, purified NPP7ExFLAG (8.33 nM). All components were prepared in NPP7 assay buffer containing 50 mM Tris-HCl, pH 8.0, 150 mM NaCl, and 10 mM sodium taurocholate (2) without the previously described 2 mM EDTA.

***Absorbance-based assay*:** Hydrolysis of all synthetic, *para*-nitrophenol containing substrates was done using an absorbance assay based on the *para*-nitrophenolate product that has a maximum absorbance at 405 nm. Each well on the plate was loaded with a total of 60 µL consisting of substrate and enzyme in NPP7 assay buffer. NPP7ExFLAG activity was monitored by the level of absorbance at 405 nm for a 1 hour period using a Synergy2 multiwell plate reader (BioTek Instruments Inc., Vermont, USA).

3.3.4 Calculation of kinetic parameters

NPP7 catalytic activity against varying substrate concentrations was measured in relative fluorescence and absorbance units which were converted to product concentrations using standard curves based on resorufin and *para*-nitrophenol, respectively. The initial velocity of the enzyme-catalyzed reaction was determined by taking the slope (within the linear range) of the activity curve for each substrate

concentration. The linear fit equation from a plot of signal (fluorescence or absorbance) against standard (resorufin or *para*-nitrophenol) concentration was used to convert all relative fluorescence and absorbance units to product concentrations. The resulting initial reaction velocities were plotted against substrate concentration and rectangular hyperbolic curve fitting *[y = m1 * m2x(1+ m2x)]* was done with KaleidaGraph 4.0 (Synergy software, Reading, PA, USA). In this equation, m1 = V_{max} and 1/m2 = K_m. The turnover number (k_{cat}) was calculated by dividing the V_{max} value by the final enzyme concentration used in all assays (8.33 nM). This value represents the number of catalytic cycles or turnovers per enzyme active site per unit time when enzyme is saturated with substrate (9). We further calculate the enzyme's catalytic efficiency for each substrate hydrolyzed using k_{cat}/K_m ratio. The higher the ratio, the more efficient the enzyme is for a given substrate (10).

3.4 Results

3.4.1 Expression and purification of human NPP7ExFLAG

The expression and localization of human NPP7 in Sf9 insect cells was analyzed at 48, 72, and 96 hours after infection with high titer baculoviorus stocks by Western blot as shown in Fig. 3.1A. The majority of the expressed protein was localized within the cell pellet but a significant minority was localized to the less complex concentrated conditioned medium (CCM) For the experiments outlined herein, only that material localized to the CCM was purified by anti-FLAG affinity chromatography and used for enzyme assays (Fig. 3.1B). The truncated NPP7ExFLAG protein band has a predicted

molecular weight of 48 kDa but the protein bands appear slightly above 50 kDa probably due to post-translational modifications.

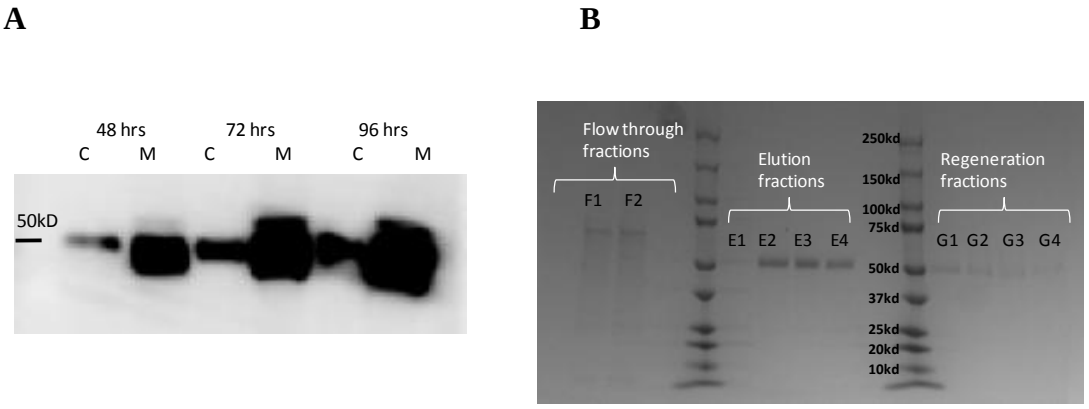

Fig. 3.1. Western blot of NPP7ExFLAG expressed in sf9 cells. (A). Trial expressions were performed to obtain the optimal expression time in Sf9 insect cells. The amount of truncated NPP7ExFLAG secreted in the medium was analyzed after 48, 72, and 96 hours. (B). Coomassie stained SDS-PAGE of purified NPP7ExFLAG.

3.4.2 Effect of EDTA on NPP7 activity

Previously, Duan et al. suggested that zinc inhibited NPP7 activity and that EDTA reversed this effect (2). These results are difficult to rationalize based on the knowledge that NPP7, like all NPP isoforms, is a metalloenzyme (11) that is presumed to require divalent metals in its active site for catalytic activity. We have recently shown that EDTA is an effective inhibitor of all known lysolipid preferring NPP isoforms (Pham et al., manuscript in preparation). Here we show that treatment with EDTA at 2 mM

significantly blocks NPP7ExFLAG activity using the substrates LPC (16:0), PAF (16:0), and SM (Fig. 3.2). This figure shows single concentration data at a single assay time point in which hydrolysis of substrate versus time was linear in the absence of EDTA.

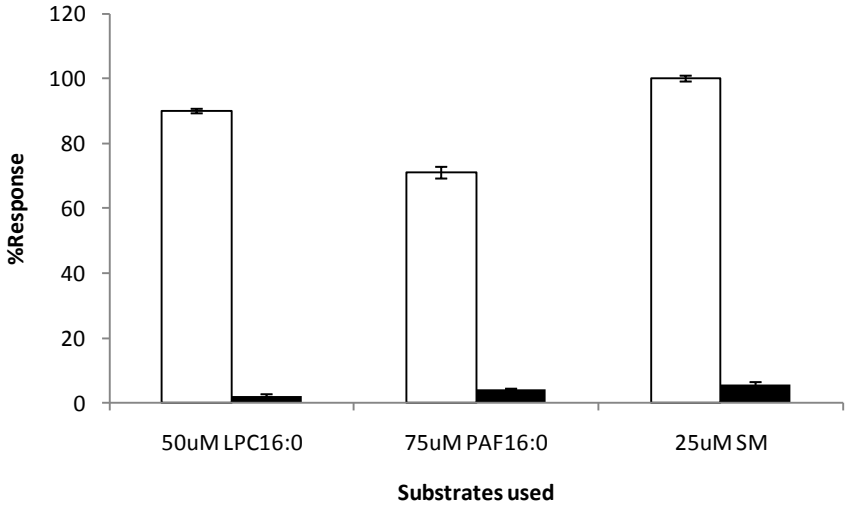

Fig. 3.2. Effect of EDTA on NPP7ExFLAG catalytic activity. Hydrolysis of PAF16:0, LPC16:0 and SM by 8.33nM NPP7 was analyzed using the Amplex Red assay, in the presence (black bars) and absence (white bars) of 2 mM EDTA in the assay buffer. All activities are normalized to that of SM without EDTA.

3.4.3 Hydrolysis of SM and SPC

Fig. 3.3 shows Michaelis-Menten plots of initial velocity versus substrate concentration for NPP7ExFLAG mediated hydrolysis of both SM and SPC using the Amplex Red fluorescence method as described in materials and methods. A panel of kinetic parameters determined experimentally for the hydrolysis of SM and SPC are

shown in Table 3.1. The K_m values of 23 ± 1.3 μM for SM and 56 ± 1.4 μM for SPC indicate a 2.4-fold greater affinity for SM by NPP7ExFLAG. The maximal velocity (V_{max}) and the relative turnover number (k_{cat}) for hydrolysis of SPC were approximately 10% higher than SM. Based on these data the calculated specificity constant (k_{cat}/K_m) for SM was twice that of SPC meaning that NPP7 exhibits a higher catalytic efficiency against SM than SPC at physiological conditions (12).

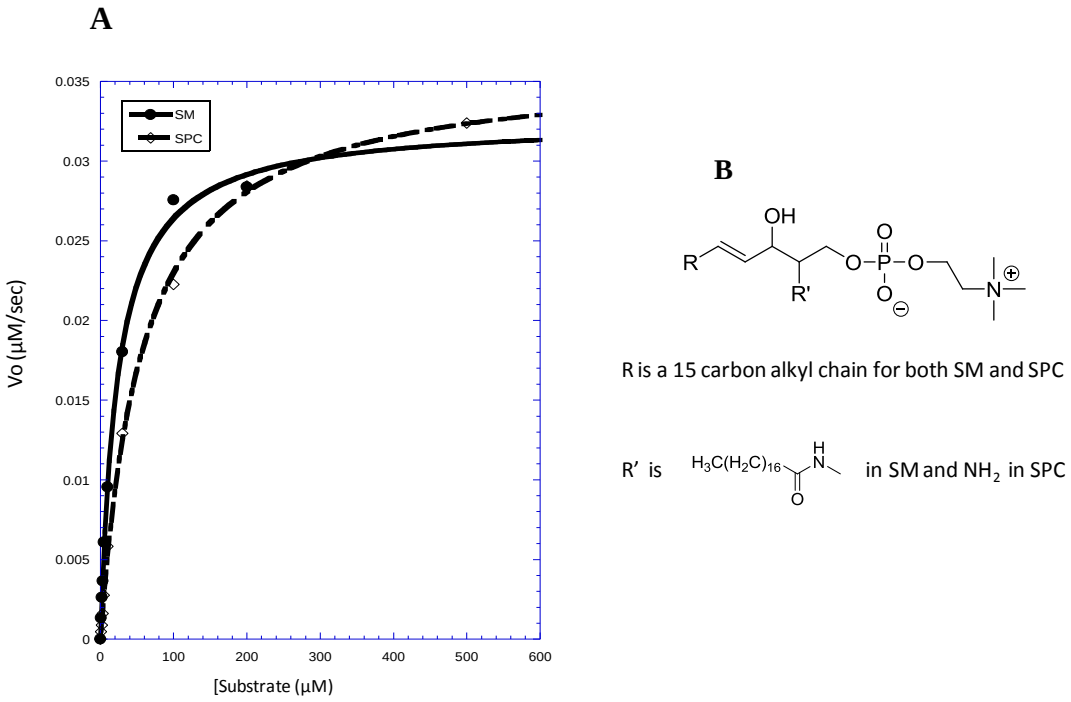

Fig. 3.3. Hydrolysis of SM and SPC by NPP7ExFLAG. (A). Varying concentrations of SM and SPC were used to obtain initial velocities using the Amplex Red assay. Plots of substrate concentration versus initial velocity were generated using the KaleidaGraph software package. The equation of each nonlinear curve, $y= m_1m_2x/(1+m_2x)$, was used to obtain values for K_m and V_{max} for each substrate (Table 3.1). Final values were obtained from the average of three triplicate runs. Both SM and SPC have the basic structure shown in panel B.

Table 3.1. Kinetic parameters for the hydrolysis of SM and SPC.

Substrate	K_m (μM)	V_{max} (μM/sec) ($x10^{-2}$)	k_{cat} (sec^{-1})	k_{cat}/K_m ($M^{-1}sec^{-1}$) ($x10^4$)
SM	23 ± 1.3	3.3 ± 0.1	3.9 ± 0.11	17.0 ± 5.8
SPC	56 ± 1.4	3.6 ± 0.02	4.3 ± 0.02	8.0 ± 2.6

3.4.4 Hydrolysis of LPC

Plots of initial velocity versus substrate concentration for NPP7ExFLAG mediated hydrolysis of LPC species are shown in Fig. 3.4A. Summaries of kinetic parameters obtained for each LPC species are compiled in Table 3.2. GPC, the smallest LPC species (where the *sn*-1 fatty acid has been replaced with a hydrogen), had the smallest K_m value of 25 μM but its turnover number (k_{cat}) was at least eight times less than the other LPC species examined. LPC14:0, LPC16:0 and LPC18:0 had similar affinities (K_m = 38 μM, 41 μM and 33 μM, respectively) and a one way ANOVA statistical analysis followed by the Bonferroni's post test showed no significant difference in the K_m values for these three substrates. LPC14:0 had a slightly larger k_{cat} value of 2.1 sec^{-1} compared to that of LPC16:0 and LPC18:0 (1.6 sec^{-1} for both). The k_{cat}/K_m values (5.5 x 10^4, 4.0 x 10^4, and 4.8 x 10^4 $M^{-1}sec^{-1}$ for LPC14:0, LPC16:0, and LPC18:0, respectively) show that NPP7 hydrolyzed LPC14:0 more effectively. The specificity constants for LPC14:0 and LPC16:0 were statistically different with a p value of <0.0001. For the shorter chain lengths of LPC tested (LPC10:0 and LPC12:0), the rate of hydrolysis decreased with decreasing chain length as shown by the kinetic parameters. LPC10:0 had the highest K_m value of 371 μM and a specificity constant six times smaller than the longer chained LPC species.

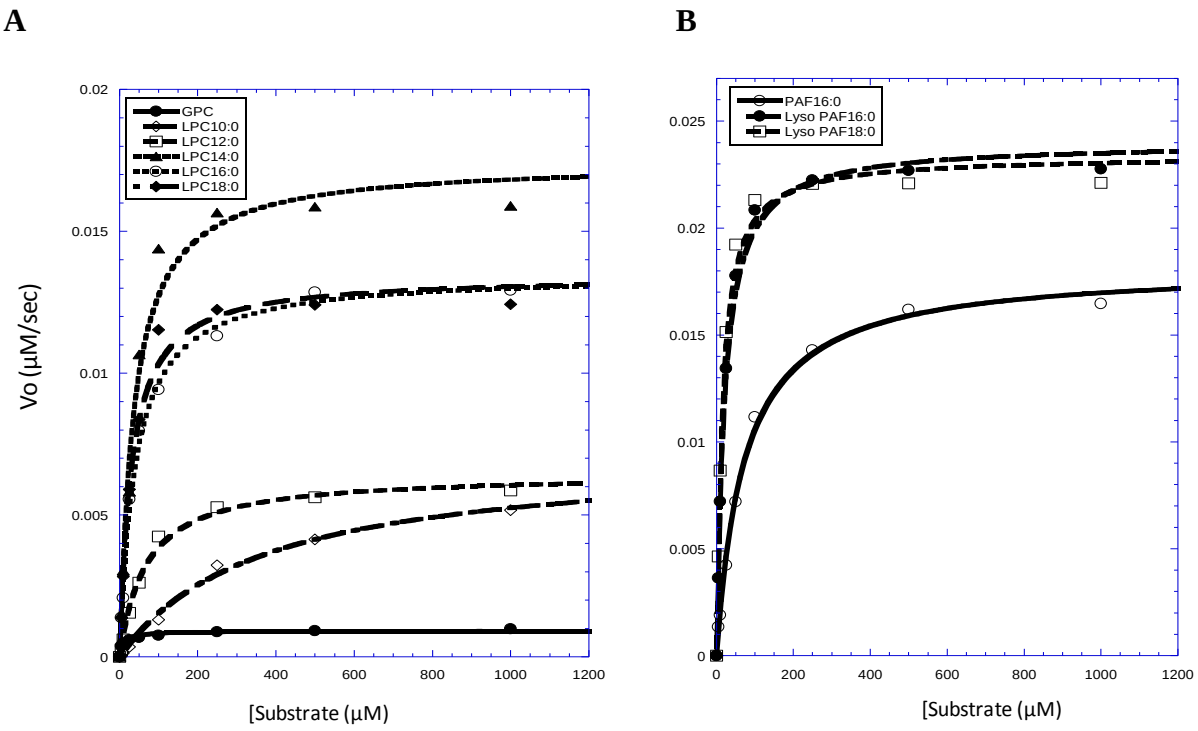

Fig. 3.4. Hydrolysis of LPC by NPP7ExFLAG. Glycerophospholipids of varying chain length and linker functionality were used to obtain initial velocities with 8.33 nM of NPP7ExFLAG. Panel A is comparison of the hydrolysis of LPC species. Panel B is a comparison of PAF versus LPAF hydrolysis

Table 3.2. Kinetic parameters for hydrolysis of glycerophospholipids

Substrate	K_m (μM)	V_{max} (μM/sec) ($x10^{-2}$)	k_{cat} (sec^{-1})	k_{cat}/K_m ($M^{-1}sec^{-1}$) ($x10^4$)
GPC	25 ± 1.0	0.1 ± 0.084	0.1 ± 0.01	0.4 ± 0.11
LPC10:0	371 ± 6.0	0.7 ± 0.002	0.9 ± 0.02	0.2 ± 0.12
LPC12:0	68 ± 1.0	0.6 ± 0.003	0.8 ± 0.03	1.2 ± 0.14
LPC14:0	38 ± 0.7	2.0 ± 0.029	2.1 ± 0.02	5.5 ± 2.1
LPC16:0	41 ± 0.3	1.3 ± 0.012	1.6 ± 0.01	4.0 ± 0.6
LPC18:0	33 ± 0.7	1.3 ± 0.033	1.6 ± 0.04	4.8 ± 1.8
PAF16:0	73 ± 1.0	1.8 ± 0.030	2.2 ± 0.03	3.0 ± 1.2
LPAF16:0	21 ± 0.3	2.2 ± 0.180	2.7 ± 0.22	12 ± 5.8
LPAF18:0	14 ± 0.03	2.3 ± 0.050	2.8 ± 0.07	20 ± 4.8

3.4.5 Hydrolysis of PAF and lysoPAF

PAF16:0 has previously been shown to be a substrate for NPP7 (4). Here a complete kinetic analysis of NPP7ExFLAG mediated hydrolysis of PAF 16:0 and two lysoPAF species (16:0 and 18:0) were completed. Representative Michaelis-Menten plots of initial velocity versus substrate concentrations for the hydrolysis of these substrates are shown in Figure 3.4B. The kinetic parameters determined from this analysis are compiled in Table 3.2. LysoPAF species had affinities that were approximately 3.5 to 5 times better (K_m values lower) than PAF 16:0. Likewise, the lysoPAF species had apparent affinities better by a factor of about two when compared to their corresponding LPC analogs. Maximal reaction velocities were the highest for

lysoPAF 16:0 and 18:0, as compared to both PAF and corresponding LPC analogues. NPP7 also exhibited a significantly higher catalytic efficiency for lysoPAF as shown by higher k_{cat}/K_m valuesin Table 3.2.

3.4.6 Hydrolysis of synthetic compounds

Several synthetic substrates previously tested as substrates for either NPP2 (6, 13, 14) or NPP6 (7) were selected and examined as substrates for NPP7ExFLAG. No NPP7ExFLAG catalytic activity was detected with FS-3 and *para*-nitrophenyl phenyl phosphate (*p*NPPP) (data not shown). Likewise, only minimal activity was observed when bis-*para*-nitrophenylphosphate (bis-*p*NPP) or *para*-nitrophenylthymidine monophosphate (*p*NP-TMP) were used as substrates as evidenced by the very low *para*-nitrophenolate signal determined at 405 nm (Fig. 3.5 A).

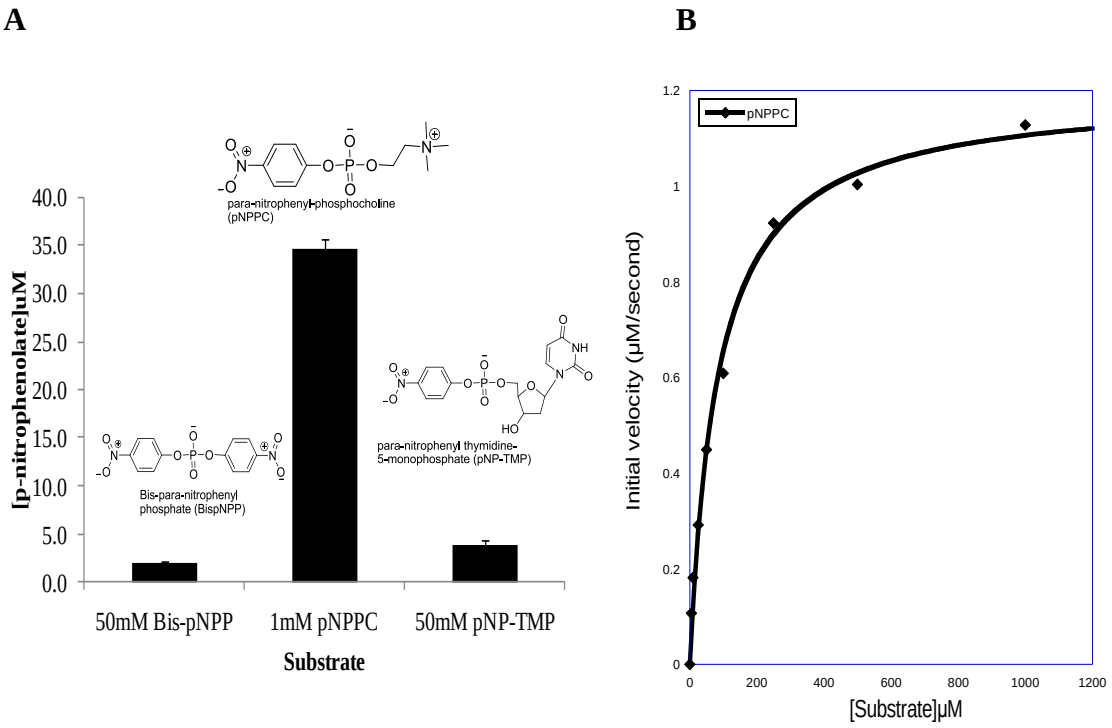

Fig. 3.5. Hydrolysis of synthetic nitrophenyl substrates by NPP7EXFLAG. Accumulation of the p-nitrophenolate anion from hydrolysis of 1mM pNPPC and 50mM bis-pNPP and pNP-TMP after 1 hour (A). The saturation curve for NPP7 hydrolysis of pNPPC (B).

Table 3.3 Kinetic parameters for the hydrolysis of synthetic substrates.

Substrate	K_m (µM)	V_{max} (µM/sec) ($x10^{-2}$)	k_{cat} (sec^{-1})	k_{cat}/K_m ($M^{-1}sec^{-1}$) ($x10^4$)
pNPPC	83 ± 5	2.0 ± 0.02	2.4 ± 0.022	2.9 ± 0.8
pNP-TMP	N/A: Minimal activity			
Bis-pNPP	N/A: Minimal activity			

It is evident from Fig. 3.5A that *para*-nitrophenyl phosphocholine (pNPPC) is a much better substrate for NPP7ExFLAG than the other para-nitrophenyl containing compounds tested. Here single concentrations of each substrate (1 mM pNPPC and 50 mM of either bis-pNPP or pNP-TMP) are compared at a single assay time where the pNPPC hydrolysis rate was linear. Due to low activity, no kinetic parameters could be determined for bis-pNPP or pNP-TMP. In contrast, a Michaelis-Menten saturation curve for the hydrolysis of pNPPC is shown in Fig. 3.5(B) and Table 3.3 shows the calculated kinetic parameters. pNPPC had an apparent K_m value of 83 μM and V_{max} of 0.2 $\mu M \cdot sec^{-1}$. The V_{max}, k_{cat} and specificity constant values obtained for pNPPC were comparable to those obtained for the hydrolysis of PAF16:0 (Table 3.2).

The catalytic effiency for the hydrolysis of each tested substrate by NPP7 was compared by a plot of k_{cat}/ K_m shown in Figure 3.6. The graph shows the k_{cat}/ K_m values obtained for the hydrolysis of each substrate by NPP7 arranged based on the substrate groups tested. The enzyme exhibited greater catalytic efficiency against SM than SPC. Both lysoPAF species were hydrolyzed more efficiently than PAF16:0, the previously known substrate, but lysoPAF18:0 was the most efficiently utilized substrate by this enzyme. Statistical significance of the k_{cat}/ K_m values for lysoPAF18:0 and SM were calculated by the one way ANOVA software followed by the Bonferroni's post test (KnowWare International, Inc, Denver, CO, USA) and gave a p value of <0.0001. Catalytic efficiency against various LPC chain lengths is also shown and the statistical analysis confirmed higher efficiency for the hydrolysis of LPC14:0 than LPC16:0. There was no statistical difference in catalytic efficiency against LPC16:0 and LPC18:0.

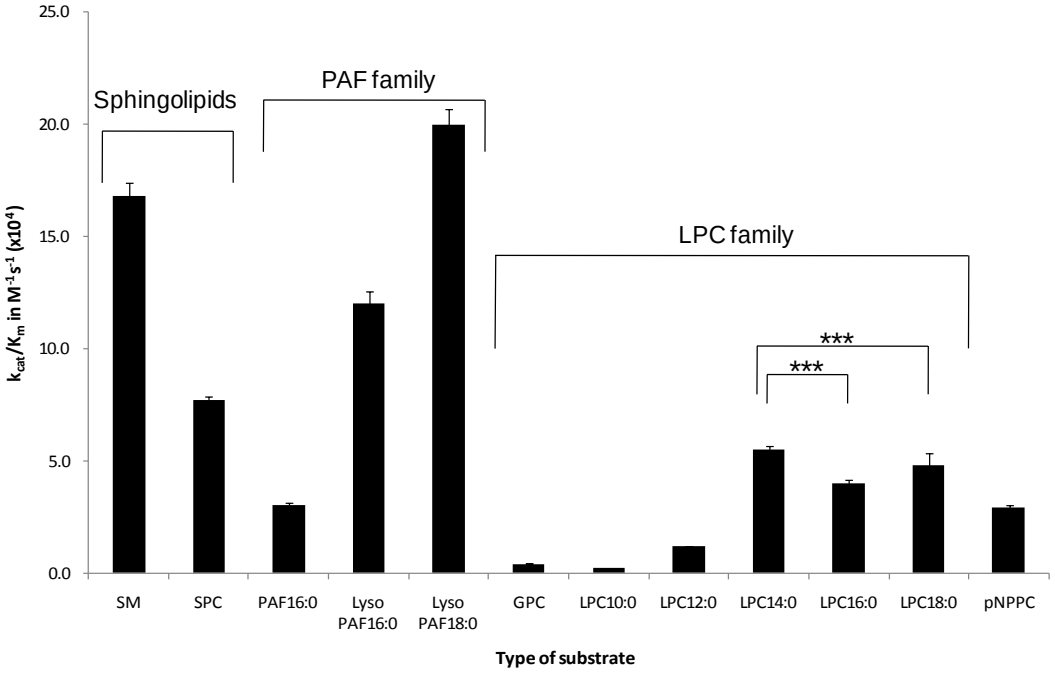

Fig. 3.6. Comparison of NPP7 catalytic efficiency against all substrates. The catalytic efficiency of NPP7 against previously known and newly identified substrates as depicted by the k_{cat}/K_m values is plotted on the y-axis. The statistical difference between the k_{cat}/K_m values for LPC14:0 and LPC16:0 was calculated using the one way ANOVA analysis followed by the Bonferroni post test analysis. The p value obtained was <0.0001 as represented by the three asterisks (***) in the graph.

3.5 Discussion

NPP isoforms have been reported to possess overlapping substrate specificity (6, 15). NPP2 is known to hydrolyze LPC and SPC but not PAF or SM (16). Similarly, NPP6 has been shown to hydrolyze LPC, SPC, and lysoPAF but not PAF or SM (7). Here, we have shown that NPP7 is a more promiscuous lipid preferring isoform within the NPP family that is capable of hydrolyzing glycerolipids (LPC, PAF, lysoPAF) and

sphingolipids (SPC and SM), as well as *para*-nitrophenol containing substrates. This makes NPP7 the only NPP isoform that has the ability to utilize substrates with more than one long hydrocarbon chain in their structures. The results show that NPP7 has a preference for large lipid substrates. NPP7ExFLAG showed very little activity toward GPC, the smallest natural substrate tested. Likewise, NPP7ExFLAG failed to utilize bis-pNPP, pNPPP, and pNP-TMP as substrates even in the mM concentration range. In contrast, NPP7ExFLAG did utilize pNPPC as a substrate despite its small size. The hydrolysis of pNPPC was similar to that of PAF 16:0 based on the panel of kinetic parameters determined. The calculated specificity constants (k_{cat}/K_m values) indicate that lysoPAF 18:0 was the best NPP7ExFLAG substrate, while lysoPAF 16:0 and SM followed closely.

Further research is needed to identify the biological implications, if any, that these newly identified NPP7 substrates present. SPC is a bioactive lipid known to activate a number of signaling cascades via G protein-coupled receptors although it is present in relatively low concentrations in human serum (17, 18). Synthetic and degradative pathways for SPC are not well understood but Xin et al. recently presented several theories (from SM, sphingosine and S1P) by which SPC accumulation could be possible (17). SPC is an effective mitogen for various cell types and its levels are upregulated in several pathological conditions including Niemann-Pick disease and ovarian cancer (17, 18). The hydrolysis of SPC by NPP7 generates sphingosine, an antiproliferative messenger. In contrast, the hydrolysis of SPC by NPP2 generates sphingosine-1-phosphate, a regulator of migration (16). This finding again presents NPP7 as the anticancer NPP isoform as opposed to NPP2 which is a mediator of cancer development

and progression (19). Our finding has thus identified a possible SPC catabolic pathway for which the biological importance remains to be understood.

LysoPAF is the main metabolite and precursor for the biosynthesis of PAF via the remodeling pathway under normal, as well as inflammatory conditions (20). Recently lysoPAF was reported as a bioactive lipid with effects opposing those of PAF (21). NPP7ExFLAG hydrolyzed lysoPAF five times more effectively than PAF. The physiological levels and bioactivity of PAF are tightly controlled by inter conversion to lysoPAF by PAF acetylhydrolases (20). Our findings suggest that NPP7 might play a role in the regulation of PAF by contributing to the clearance of its main metabolite and precursor but further studies are needed to analyze the effects of NPP7 on PAF/lysoPAF metabolism and bioactivity.

Conversion of LPC16:0 to monoacylglycerol and phosphorylcholine by NPP7 has been known for some time but the influence of chain length on hydrolysis has not been explored in this type of kinetic analysis (22). LPC16:0 has been predominantly used in previous work to characterize NPP7 (3, 5, 23, 24). For the first time, this work has established that LPC14:0 is the preferred chain length for NPP7ExFLAG. For LPC chain lengths shorter than 12, affinity was decreased based on the K_m values obtained. NPP7ExFLAG had the highest apparent affinity for GPC, the LPC substrate completely lacking an acyl chain. However, GPC displayed the poorest conversion to products as indicated by the lowest k_{cat} value of 5×10^3 $M^{-1}sec^{-1}$. NPP6 is the only other lysophospholipase C in the NPP family and was previously reported to hydrolyze LPC12:0 and GPC with the highest preference (7).

Para-nitrophenylphosphocholine (pNPPC) is a synthetic NPP7 substrate identified here for the first time. Kinetic parameters for the NPP7ExFLAG mediated hydrolysis of pNPPC were similar to those obtained for PAF16:0. NPP7 cleaves pNPPC with a lysophospholipase C activity, generating phosphocholine which can be monitored by fluorescence (Amplex Red assay) and *para*-nitrophenolate anion which can be monitored by absorbance at 405 nm. We have thus described a new assay method for monitoring NPP7 catalytic activity using this novel substrate. The use of radio-labeled lipid substrates has been the predominant method for monitoring NPP7 activity (4, 5, 8, 25) but this method is labor intensive, time consuming and expensive. These new, alternative methods are an improvement over the previous method in both cost and ease of use. The Amplex Red fluorogenic assay indirectly measures phosphocholine production via a series of exogenous enzymatic reactions to generate resorufin. The absorbance assay based on pNPPC is inexpensive and is based on a direct NPP7 product (para-nitrophenolate anion). Both approaches provide for multiplex, multiwell plate analysis that allows for the type of complete kinetic analysis provided here for NPP7.

Successful baculovirus expression of a truncated, biologically active NPP7ExFLAG construct has been described herein. NPP7 has been suggested to have five glycosylation sites and that mature enzyme is inactive without appropriate N-glycosylation (5). Insect cells are capable of expressing protein with post-translational modifications similar to mammalian cells (26). The molecular weight of the NPP7ExFLAG construct is approximately 48 kDa. The expressed protein migrated to a position slightly above 50 kDa on SDS-PAGE and Western blots, indicating post-translational modification occurs in Sf9 insect cells.

NPP7 has been reported to be inhibited by zinc and the inhibitory effects were prevented by 2 mM EDTA (2). Since this report, 2 mM EDTA has been a component of the NPP7/Alk-SMase assay buffer in all published NPP7 experiments (4, 24, 27). Contrary to previous reports, we establish here that NPP7/Alk-SMase catalytic activity is greatly hampered by EDTA. The current finding is not unusual considering NPP7 is a metalloenzyme which depends on the presence of divalent cations for its catalytic function (24). The chelating abilities of EDTA may disrupt the metal enzyme interactions leading to reduced catalytic activity. Further investigations are underway to find out if this effect is dependent on EDTA concentration and/or time of exposure.

In conclusion, two cheaper, easier and multiplex methods for the assay of NPP7 catalytic activity have been established as alternatives to the common use of radio-labeled substrates. Through these methods, we have extensively characterized and compared the kinetics of this enzyme against all its substrates. Several new substrates have been identified that may have biological implications but further research is needed to identify and characterize such effects.

3.6 References

1. Duan, R. D. 2006. Alkaline sphingomyelinase: an old enzyme with novel implications. *Biochim Biophys Acta* **1761**: 281-291.
2. Nyberg, L., R. D. Duan, J. Axelson, and A. Nilsson. 1996. Identification of an alkaline sphingomyelinase activity in human bile. *Biochim Biophys Acta* **1300**: 42-48.

3. Duan, R. D., E. Hertervig, L. Nyberg, T. Hauge, B. Sternby, J. Lillienau, A. Farooqi, and A. Nilsson. 1996. Distribution of alkaline sphingomyelinase activity in human beings and animals. Tissue and species differences. *Dig Dis Sci* **41**: 1801-1806.

4. Wu, J., A. Nilsson, B. A. Jonsson, H. Stenstad, W. Agace, Y. Cheng, and R. D. Duan. 2006. Intestinal alkaline sphingomyelinase hydrolyses and inactivates platelet-activating factor by a phospholipase C activity. *Biochem J* **394**: 299-308.

5. Wu, J., G. H. Hansen, A. Nilsson, and R. D. Duan. 2005. Functional studies of human intestinal alkaline sphingomyelinase by deglycosylation and mutagenesis. *Biochem J* **386**: 153-160.

6. Stefan, C., S. Jansen, and M. Bollen. 2005. NPP-type ectophosphodiesterases: unity in diversity. *Trends Biochem Sci* **30**: 542-550.

7. Sakagami, H., J. Aoki, Y. Natori, K. Nishikawa, Y. Kakehi, and H. Arai. 2005. Biochemical and molecular characterization of a novel choline-specific glycerophosphodiester phosphodiesterase belonging to the nucleotide pyrophosphatase/phosphodiesterase family. *J Biol Chem* **280**: 23084-23093.

8. Cheng, Y. 2002. Purification, localization and expression of human intestinal alkaline sphingomyelinase. *Lipid Research* **44**: 316-324.

9. Grisham, R. H. G. a. C. M. 1995. Biochemistry Saunders College Publishing.

10. Paula, P. A. a. J. D. 2006. Physical Chemistry. 8th ed. Freeman and company.

11. Gijsbers, R., H. Ceulemans, W. Stalmans, and M. Bollen. 2001. Structural and catalytic similarities between nucleotide pyrophosphatases/phosphodiesterases and alkaline phosphatases. *J Biol Chem* **276**: 1361-1368.

12. Cornish-Bowden, A. 1979. Fundamentals of Enzyme kinetics Butterworths.

13. van Meeteren, L. A., P. Ruurs, E. Christodoulou, J. W. Goding, H. Takakusa, K. Kikuchi, A. Perrakis, T. Nagano, and W. H. Moolenaar. 2005. Inhibition of autotaxin by lysophosphatidic acid and sphingosine 1-phosphate. *J Biol Chem* **280**: 21155-21161.

14. Durgam, G. G., T. Virag, M. D. Walker, R. Tsukahara, S. Yasuda, K. Liliom, L. A. van Meeteren, W. H. Moolenaar, N. Wilke, W. Siess, G. Tigyi, and D. D. Miller. 2005. Synthesis, structure-activity relationships, and biological evaluation of fatty alcohol phosphates as lysophosphatidic acid receptor ligands, activators of PPARgamma, and inhibitors of autotaxin. *J Med Chem* **48**: 4919-4930.

15. Cimpean, A., C. Stefan, R. Gijsbers, W. Stalmans, and M. Bollen. 2004. Substrate-specifying determinants of the nucleotide pyrophosphatases/phosphodiesterases NPP1 and NPP2. *Biochem J* **381**: 71-77.

16. Clair, T., J. Aoki, E. Koh, R. W. Bandle, S. W. Nam, M. M. Ptaszynska, G. B. Mills, E. Schiffmann, L. A. Liotta, and M. L. Stracke. 2003. Autotaxin hydrolyzes sphingosylphosphorylcholine to produce the regulator of migration, sphingosine-1-phosphate. *Cancer Res* **63**: 5446-5453.

17. Xin, C., S. Ren, W. Eberhardt, J. Pfeilschifter, and A. Huwiler. 2007. Sphingosylphosphorylcholine acts in an anti-inflammatory manner in renal mesangial cells by reducing interleukin-1beta-induced prostaglandin E2 formation. *J Lipid Res* **48**: 1985-1996.

18. Boguslawski, G., D. Lyons, K. A. Harvey, A. T. Kovala, and D. English. 2000. Sphingosylphosphorylcholine induces endothelial cell migration and morphogenesis. *Biochem Biophys Res Commun* **272**: 603-609.

19. Mulder, J., A. Ariaens, F. P. van Horck, and W. H. Moolenaar. 2005. Inhibition of RhoA-mediated SRF activation by p116Rip. *FEBS Lett* **579**: 6121-6127.

20. Harayama, T., H. Shindou, R. Ogasawara, A. Suwabe, and T. Shimizu. 2008. Identification of a novel noninflammatory biosynthetic pathway of platelet-activating factor. *J Biol Chem* **283**: 11097-11106.

21. Welch, E. J., R. P. Naikawadi, Z. Li, P. Lin, S. Ishii, T. Shimizu, C. Tiruppathi, X. Du, P. V. Subbaiah, and R. D. Ye. 2009. Opposing effects of platelet-activating factor and lyso-platelet-activating factor on neutrophil and platelet activation. *Mol Pharmacol* **75**: 227-234.

22. Hertervig, E., A. Nilsson, L. Nyberg, and R. D. Duan. 1997. Alkaline sphingomyelinase activity is decreased in human colorectal carcinoma. *Cancer* **79**: 448-453.

23. Nilsson, A., and R. D. Duan. 1999. Alkaline sphingomyelinases and ceramidases of the gastrointestinal tract. *Chem Phys Lipids* **102**: 97-105.

24. Duan, R. 2003. Identification of human intestinal alkaline sphingomyelinase as a a novel ecto-enzyme related to the nucleotide phosohodiesterase family. *Biological chemistry* **278**: 38528-38536.

25. Liu, J. J., A. Nilsson, and R. D. Duan. 2000. Effects of phospholipids on sphingomyelin hydrolysis induced by intestinal alkaline sphingomyelinase: an in vitro study. *J Nutr Biochem* **11**: 192-197.

26. Philipps, B., M. Forstner, and L. M. Mayr. 2004. Baculovirus expression system for magnetic sorting of infected cells and enhanced titer determination. *Biotechniques* **36**: 80-83.

27. Andersson, D., K. Kotarsky, J. Wu, W. Agace, and R. D. Duan. 2009. Expression of alkaline sphingomyelinase in yeast cells and anti-inflammatory effects of the expressed enzyme in a rat colitis model. *Dig Dis Sci* **54**: 1440-1448.

CHAPTER 4

COMPUTATIONAL IDENTIFICATION AND BIOCHEMICAL CHARACTERIZATION OF SUBSTRATE BINDING DETERMINANTS OF NUCLEOTIDE PYROPHOSPHATASE/ PHOSPHDIESTERASE-7

4.1 Abstract

The nucleotide pyrophosphatase/phosphodiesterase (NPP) subfamily of alkaline phosphatases currently consists of seven human isoforms that are related in structure and function. They are all ectoenzymes that hydrolyze a wide variety of substrates to generate lipid messengers that mediate a range of physiological and pathological processes. NPP isoforms have been associated with conditions such as cancer, obesity, bone mineralization, allergy, growth, and development. Thus, they are attractive targets in drug discovery and development, however, they are not well understood in terms of their structure and function. NPP7 is a recent addition to this important family of enzymes. It hydrolyzes lipid substrates that lead to generation of both proliferative and antiproliferative messengers such as ceramide, sphingosine, and sphingosine 1-phosphate. Like other NPPs, NPP7 recognizes a spectrum of substrates preferentially but it is not well understood what determines its well-defined substrate preferences. The aim of this work is to identify and characterize amino acid residues that contribute to substrate recognition by NPP7.

4.2 Introduction

Nucleotide pyrophosphatase/phosphodiesterase-7 (NPP7) is a 60kDa membrane anchored ectoenzyme that hydrolyzes sphingomyelin (SM) (Nilsson 1969), platelet activating factor (PAF) (Wu et al. 2006), lysophosphatidylcholine (LPC) (Wu et al. 2005), sphingosylphosphorylcholine (SPC) and lyso platelet activating factor (lyso PAF) (Wanjala I.W., A.L. Parrill and D.L. Baker, manuscript in preparation) to generate multiple signaling molecules. The enzyme has been implicated in pathological conditions such as cancer and atherosclerosis, as well as in normal physiological processes such as cholesterol absorption and maturation of the intestinal tract (Wu et al. 2006). However, NPP7 has not been well characterized in terms of its structure and function (Duan 2006). The nucleotide pyrophosphatase/phosphodiesterase (NPP) enzymes comprise a seven member subfamily of enzymes (Bollen et al. 2000). Individual NPP isoforms are classified as either pyrophosphatases or phosphodiesterases depending on the specific substrates they hydrolyze (Kanda et al. 2008). NPP1, NPP2, and NPP3 are nucleotide pyrophosphatases that cleave inorganic phosphate from nucleotides and their derivatives (Clair et al. 1997; Gijsbers et al. 2003). In contrast, NPP2, NPP6, and NPP7 are phosphodiesterases that hydrolyze phosphodiester bonds in lipids and their derivatives, (Duan 2003; Sakagami et al. 2005; Umezu-Goto et al. 2002). NPP4 and NPP5 are yet to be characterized in terms of substrate preferences. NPP2 is the only member of the seven known NPP isoforms that possesses both pyrophosphatase and phosphodiesterase activities (Stefan et al. 2005). As a phosphodiesterase, NPP2 exhibits lysophospholipase D (LPLD) (Umezu-Goto et al. 2002) activity which contrasts with the lysophospholipase C (LPLC) activities of NPP6 and NPP7. Besides these specific activities, no previous

experimental evidence is available to explain differences in substrate preference among the known lipid preferring NPP isoforms. (Bollen et al. 2000; Gijsbers et al. 2001)

NPP7 has been previously shown to hydrolyze SM, LPC, and recently, we have also identified lyso platelet activating factor (lysoPAF), sphingosyl-phosphorylcholine (SPC), and para-nitrophenylphosphorylcholine (pNPPC) as additional NPP7 substrates (Wanjala, I.W., A.L.Parrill and D.L. Baker, manuscript in preparation). Here we have used a combination of computational homology modeling, substrate docking, site-directed mutagenesis and kinetic analysis of enzyme activity to examine the role of specific amino acid residues within the NPP7 active site in determining substrate recognition. Homology modeling has not previously been applied to the analysis of NPP7 structure and function relationships and this work could open a new approach in the analysis of this important isoform. Our results suggest an overlapping binding pocket for all substrates examined and show that NPP7 activity against four of its substrates was differentially affected by specific site-directed mutations.

4.3 Materials and Methods

4.3.1 Generation of the NPP7 homology model

The bacterial *Xac* NPP structure (2gso) (Zalatan et al. 2006) was used as the template sequence and the human NPP7 nucleotide sequence (Genbank code AY20633) (Duan 2003) as the target for homology modeling. *Xac* NPP is the most closely related analog of human NPP isoforms with a solved crystal structure, similar function, and relatively high sequence homology. The Molecular Operating Environment (MOE 2008) software package (Chemical Computing Group, Montreal, Canada) was used for all

homology modeling and docking. A database of eleven homology models was generated and each model was analyzed using a Ramachandran plot to identify those models with phi/psi angles outside the range represented in known crystal structures (outliers). Models were ranked based on the number of outliers and their proximity to the catalytic residue (threonine 75). The best models were those with fewer outliers that were located more than 10Å from the active residue. The selected model was then energy minimized using the Assisted Model Building and Energy Refinement (AMBER99) force field (Asada et al. 2002; Hornak et al. 2006; Wang et al. 2000) to generate the final model with which subsequent substrate docking was performed.

4.3.2 Substrate docking

Substrate docking was used to study interactions between NPP7 and its previously known substrates and their closely related analogs. pNPPC was directly docked into the active site as a whole molecule since it is small and has limited flexibility. The substrates LPC, PAF, and SM are highly flexible because of long fatty acyl chains in their structures. For this reason stepwise docking was done starting with the polar head groups of each substrate. Wall restraints were also used to keep the substrate phosphate group in close proximity to the enzyme's active residue, threonine 75. The hydrophobic chains were then extended three carbon atoms at a time followed by energy minimization for the newly added atoms at each step. The protein surface feature within MOE was used to visualize the various channels that could accommodate the substrates during binding. After extending the full chains, chain rotations were done followed by energy minimization to explore the best positions for each chain and thus the

minimum energy conformation for each substrate. The lowest energy conformation was then selected for each substrate and their interactions with the protein analyzed.

4.3.3 Analysis of protein-substrate interactions

Protein residues within 4.5 Å of the substrate atoms were analyzed to determine the presence of non-covalent interactions. Presence of such interactions was taken as evidence of higher affinity binding than complexes lacking such stabilizing interactions. All protein residues around the common substrate groups were identified and the distances separating them from the possible interaction points analyzed. The maximum interaction distance was set at 4.5 Å. All residues more than 4.5 Å away from their possible interaction points in all substrates were eliminated as noncovalent interaction strengths become weaker with increasing distance. The type of interaction formed by each residue was also analyzed. Stronger noncovalent interactions such as H-bonding, π-stacking and cation-π interactions were considered more important than weaker interactions such as Van der Waal's forces. Six mutation candidates were selected and the type of effect expected with a given type of single point mutation predicted.

4.3.4 Site-directed mutagenesis of NPP7

The full length, human NPP7 insert (Genbank AY20633) contained within the mammalian expression vector pcDNA4/TO/myc his B, was kindly provided by Dr. Rui Dong-Duan (Lund University, Lund, Sweden). The upstream cloning site was mutated from the Kpn1 to a BamH1 recognition sequence using the sense primer 5'-GCGTTTAAACTTAAGCTTGGATCCGAAATGAGAG-3' and antisense primer 5'-

CTCTCATGCTTTCGGATCCAAGCTTAAGTTTAAACGC-3' and the Quickchange site-directed mutagenesis kit (Stratagene, La Jolla, CA, USA) according to the manufacturer's protocols. The NPP7 insert was subcloned into the pcDNA3.1(+) mammalian expression vector using standard molecular biology approaches. Next, a truncated, secreted version of NPP7 containing a FLAG affinity tag was generated by adding the sequence DYKDDDDK after T415 and before a stop codon using the sense primer 5'-CCCATGCTGCACACAGACTACAAGGACGACGATGACAAGTAG GAATCTGCTCTTCCG-3' and antisense primer 5'-CGGAAGAGCAGATTCCTA CTTGTCATCGTCGTCCTTGTAGTCTGTGTGCAGCATGGG-3' with the Quickchange site-directed mutagenesis kit (Stratagene, La Jolla, CA, USA) according to the manufacturer's protocols. This truncated NPP7 construct lacked the C-terminal transmembrane anchor but has previously been shown to be functional and expressed as a secreted enzyme (Wu et al. 2005). The complete affinity tagged fusion was termed NPP7ExFLAG. All proposed site directed mutants were generated from this customized plasmid using standard PCR techniques and the multi site-directed mutagenesis kit (Stratagene, La Jolla, CA, USA) according to the manufacturer's protocols. Table 4.1 lists all the sense primers used to prepare all site directed mutants.

Table 4.1 Sense primers for NPP7ExFLAG mutants

Mutation	Sense primer
F80A	5'-TGACCAGCCCCTGCCACGCCACCCTGGTCACCGGC-3'
L107F	5'-ACCACCAGCAAGGTGAAGTTCCCCTACCACGCCAC-3'
Y142A	5'-TGGCTCCTTCTTCGCCCCGGGCGGGAACGT-3'
Y166A	5'-GGCATCGCACACAACGCCAAAAATGAGACG-3'
E169A	5'-TCGCACACAACTACAAAAATGCGACGGAGTGGAGAG-3'
E169Q	5'-TCGCACACAACTACAAAAATGAGACGGAGTGGAGAG-3'
F275A	5'-CGGGACATCGAGTTTGAGCTCCTGGACTAC-3'

4.3.5 Mutant protein expression and normalization

Wild type NPP7ExFLAG and all mutant proteins were expressed via transient transfection in human embryonic kidney cells (HEK293T). HEK293T cells were grown in Dulbecco's modified Eagle's medium (DMEM) containing 10% heat-inactivated fetal calf serum and 2 mM L-glutamine and 100 U/ml penicillin-streptomycin at 37 ^{o}C and 5% CO_2 up to 80% confluence. Transient transfections with wild type or mutant NPP7ExFLAG insert subcloned in the pcDNA3.1(+) mammalian expression vector were done using the Polyfect transfection reagent (Qiagen, Valencia, CA, USA) according to the manufacturer's protocols. Eight hours after transfection, the culture medium was changed to serum-free DMEM and cells were incubated for an additional 48 additional hours. Conditioned media containing secreted NPP7 protein was collected and concentrated using 10,000 molecular weight cutoff (10K MWCO) filters (Millipore, Billerica, MA, USA) by centrifugation at 3073xg for 20 minutes. NPP7 proteins (wild type and mutants) present in concentrated conditioned medium (CCM) were stored at 4^{o}C

in NPP7 assay buffer, pH 8 without addition of adjuvants until functional activity was determined.

Western blots were used to verify expression of NPP7ExFLAG and all its mutants. The M2 Anti-FLAG antibody (Sigma-Aldrich, St. Louis, MO, USA) was utilized following standard protocols. Following separation by SDS-PAGE on Tris-HCl-gradient gels (4-15%, Bio-Rad, Hercules, CA, USA) proteins were transferred onto polyvinylidene difluoride (PVDF) membrane (Bio-Rad, City, State, USA) by electroblotting at 100V in Tris/Glycine SDS buffer for 1 hour. Nonspecific binding sites were blocked with 50 mM Tris buffered saline, 2.7 mM KCl, 138m M NaCl, 0.5% (v/v) Tween®20 (TBST) and 5% (w/v) non-fat dry milk (NFDM). The membrane was then treated with M2 Anti-Flag antibody (Sigma-Aldrich, St. Louis, MO, USA) (1:2000 in TBST + 3% NFDM) and horseradish peroxidase conjugated goat anti-mouse IgG antibody (Sigma-Aldrich, St. Louis, MO, USA) (1:5000 in TBST + 3 % NFDM). Finally, SuperSignal Pico West chemiluminescent substrate (ThermoScientific, Rockford, IL, USA) allowed for chemiluminescence detection using a Luminary imaging system (Fotodyne, Hartland, WI, USA).

All enzyme activity assays were performed with CCM that had been quantified at least twice by Western blot analysis. First, a scanning Western blot was run with varying dilutions of the CCM to assess the differences in the amounts of protein that could arise due to differing expression levels of mutants. Based on the results of the first Western blot, all samples were diluted to the same concentration and were verified by a second independent immunoblot. To quantify the amounts of protein expressed for each sample, a known concentration of the carboxy-terminal FLAG-BAP fusion protein (Sigma

Aldrich, St. Louis, MO, USA) was included on the second Western blot as a standard. All protein bands were normalized relative to the FLAG-BAP standard using the TotalLab software program in conjunction with the Luminary imager (Fotodyne, Hartland, WI, USA).

4.3.6 Assay of NPP7 catalytic activity

Fluorescence-based assay: Hydrolysis of LPC, PAF and SM by NPP7 was monitored using a modification of Invitrogen's Amplex® Red phosphatidylcholine-specific phospholipase C assay kit (Invitrogen, Carlsbad, CA, USA). NPP7 assay buffer was prepared as previously described (containing 50 mM tris-HCl, pH 8.0, 150 mM NaCl, and 10mM taurocholic acid (Nyberg et al. 1996). Unlike the previous work of Nyberg et al. we have determined that EDTA is an inhibitor of the hydrolytic activity of NPP7ExFLAG as one would expect for a metalloenzyme (Wanjala et al., manuscript in preparation). Each well on a 96-well plate (half area, Corning, City State, USA) was loaded with a total of 60 µL consisting of 20 µL each of substrate, Amplex Red cocktail (10 µM Amplex Red reagent, 0.1 U/ml choline oxidase, 1 U/ml horseradish peroxidase, 4 U/ml alkaline phosphatase) and normalized concentrations of enzyme diluted from CCM. The activity of wild type NPP7ExFLAG or mutants was determined by monitoring fluorescence (excitation 571 nm and emission 585 nm) every minute for two hours using a Synergy 2 multi-well plate reader (BioTek, Winooski, VT, USA).

***Absorbance-based activity assay*:** Hydrolysis of pNPPC as a function of NPP7ExFLAG activity was monitored via an absorbance assay based on the generation of *para*-nitrophenolate. This hydrolytic product has a maximum absorption at 405 nm.

Each well of a 96 well plate (half area, Corning, City State, USA) was loaded with a total of 60 µl consisting of NPP7 assay buffer, 400 µM of substrate and normalized amounts of enzyme from CCM. Wild type NPP7ExFLAG or mutant activity was monitored by measuring absorbance at 405 nm every minute for two hours using a Synergy 2 multi-well plate reader (BioTek, Winooski, VT, USA).

Dose response assays were run with varying substrate concentrations using the fluorescence-based (LPC, PAF, SM) or the absorbance-based assay (pNPPC). Relative fluorescence or absorbance units were converted to product concentrations using standard curves. For the fluorescence assay, varying concentrations of resorufin (the ultimate fluorescent product) were used to monitor the level of fluorescence in the presence of all other assay components with the exception of NPP7ExFLAG to generate a standard curve. For the absorbance assay, varying concentrations of *para*-nitrophenol were used in the presence of all other assay components with the exception of NPP7ExFLAG to obtain absorbance values at 405 nm for the standard curve. The trend line equations from these calibration curves were generated using Microsoft Excel (2007) and were used to convert all relative fluorescence and absorbance units to product concentrations. Initial rates for all reactions were determined from the slopes of the linear ranges in the product versus time plots. Curve fitting on Michaelis-Menten initial rate versus substrate concentration plots was done using the KaleidaGraph 4.0 software package (Synergy software, Reading, PA, USA) data was fitted to the following equation $y = m1 \times m2x(1 + m2x)$ ($K_m = 1/m2$ and $V_{max} = m2$). The catalytic constant (k_{cat}) was calculated by dividing V_{max} by the enzyme concentration used in all assays.

4.4 Results

4.4.1 Generation of the NPP7 homology model

Fig. 4.1 shows the energy minimized NPP7 homology model obtained using the Xac crystal structure, PDB (Berman et al. 2000) entry 2gso (Zalatan et al. 2006), as template. The white circle highlights our designated binding pocket, an 8Å radius around the active site residue, threonine 75. The 8Å radius was selected because it was large enough to accommodate the polar headgroup of the large lipid substrates hydrolyzed by NPP7. In close proximity to the active residue are two divalent metal cations transferred directly from the *Xac* template. Like all NPP isoforms, NPP7 requires divalent metal cations for its phosphodiesterase activity.The resulting NPP7 homology model displayed strong interactions between known metal ion coordinating residues (Asp 39, Asp 199, His 203, Asp 246, His 247, His 353) and the two zinc ions (see Fig. 4.2). All six of these residues are approximately 2Å away from one of the metals in the refined model.

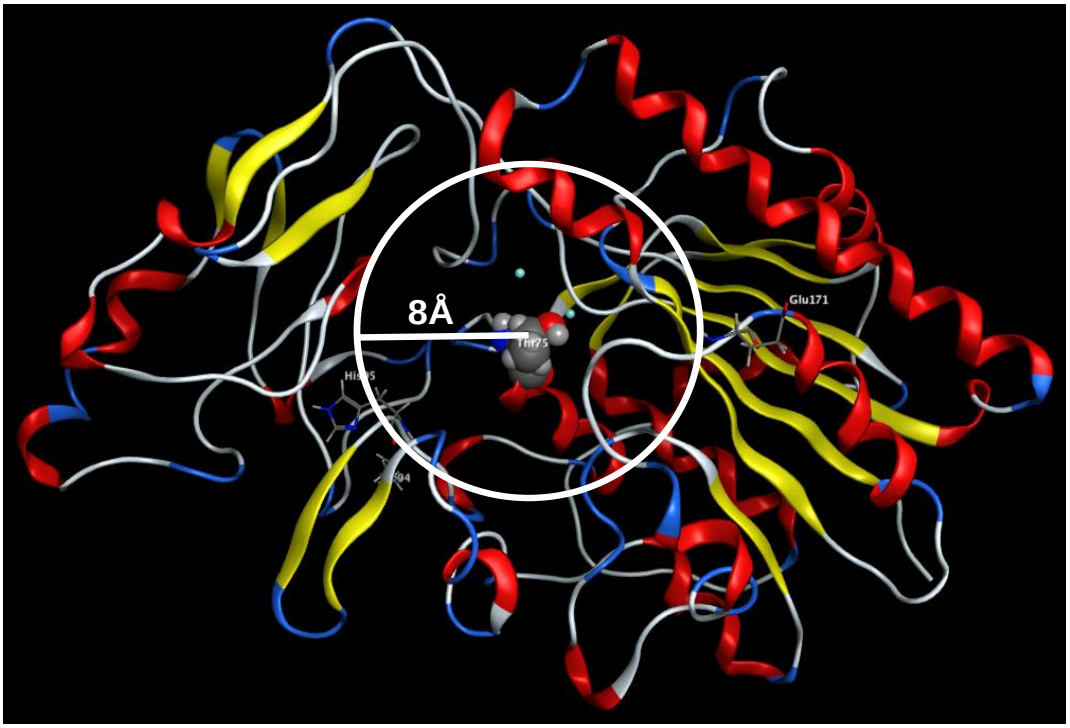

Fig. 4.1. NPP7 homology model. The homology model was generated in MOE using the general bacterial *Xac* NPP crystal structure (PDB entry 2GSO) as the modeling template and human NPP7 nucleotide sequence (Genbank Id AY20633) as the modeling target. The white circle highlights the proposed phosphate target area within the NPP7 active site, an 8Å radius around the active residue threonine75, which is shown as a space filling model. Residues shown in stick models were identified as outliers by the Ramachandran plot.

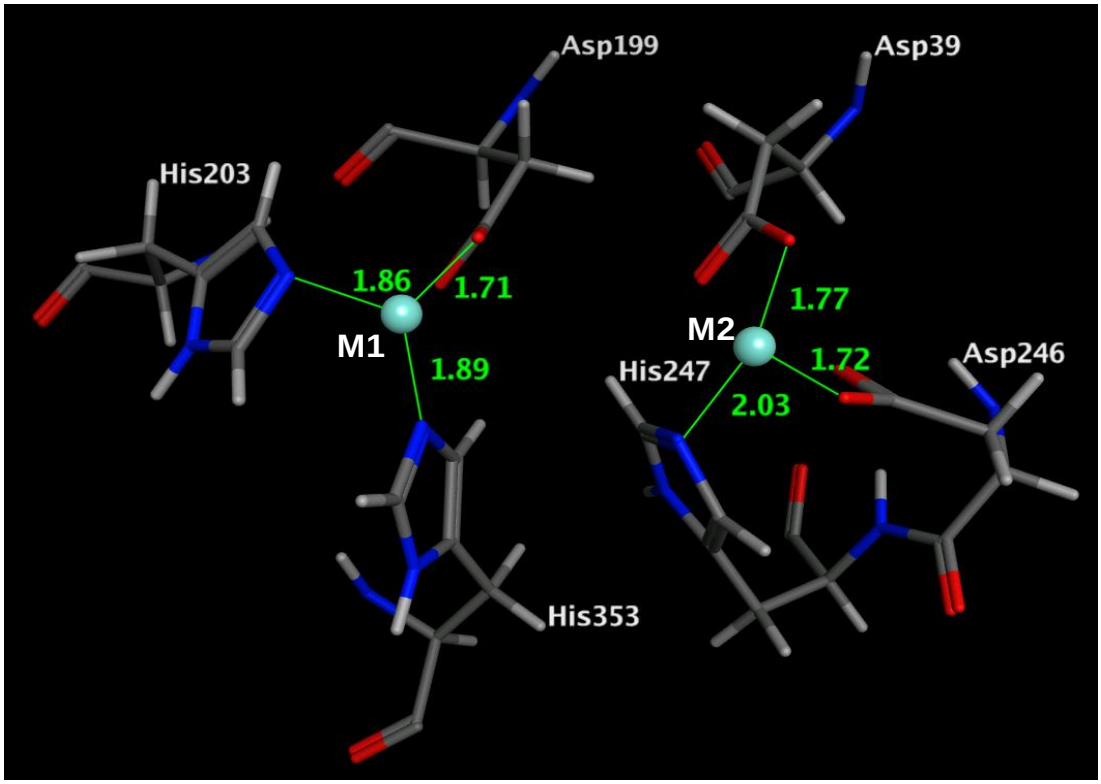

Fig. 4.2. NPP7 homology model metal coordination sites. In close proximity to the active site residue threonine 75 are two divalent metal cations speculated to be present in NPP7 that result from homology modeling based on the *Xac* template. Each metal coordinating residue is approximately 2Å away from the metal it coordinates

4.4.2 Substrate docking

Fig. 4.3 shows the results of stepwise docking for each of the three previously identified lysolipid substrates of NPP7. All three choline groups are in close proximity and all phosphate groups docked within the same vicinity. However, as one might reasonably expect due to the weaker, non-directional van der Waals interactions, the hydrophobic chains adopted different positions. Since there are no structural differences in the hydrophobic chains of the three substrates, we manually placed the chains for LPC

and SM to follow the same shape as that of PAF. Energy minimizing these manually created poses gave conformations with drastically reduced energies and moved the common groups closer. Fig. 4.3 shows a superposition of these conformations which were used for analyzing interactions.

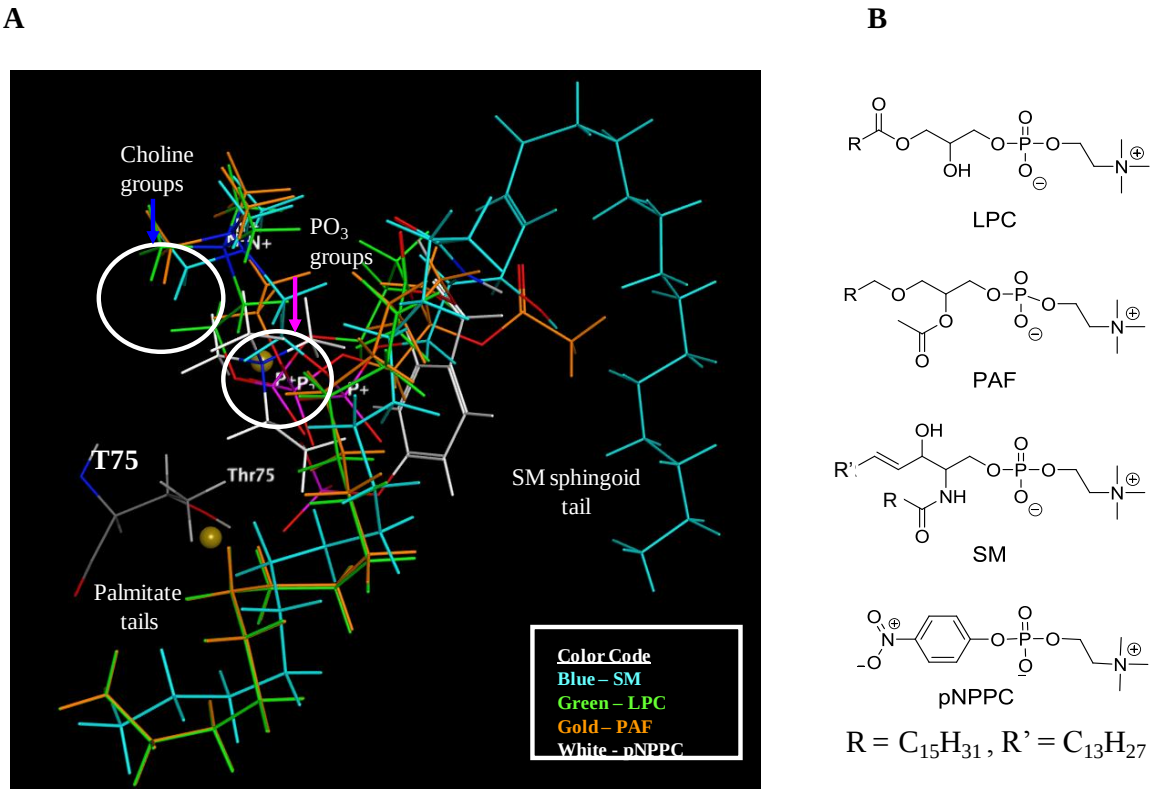

Fig. 4.3. Final docked conformations for LPC, PAF, SM and pNPPC in human NPP7. Minimized poses of all substrates have significant overlap within the active site. All common groups on different substrates are located within close proximity (A). The lipid substrates have a common basic structure whereas pNPPC is quite different (B) but the phosphocholine head groups for all docked in the same area.

4.4.3 Analysis of protein-substrate interactions

Table 4.2 summarizes the predictions made from the complexes of all docked substrates with the human NPP7 homology model. The left column lists all residues within 4.5 Å of each substrate. It is noteworthy that the same residues were identified for most substrates since their common functional groups were located within close proximity. Only the second hydrophobic tail of SM gave unique interacting residues. Residues selected for mutation after analyzing the types and distances of predicted interactions are shown. Predicted effects on enzyme activity based on these interactions are included.

Table 4.2 Modeled substrate interactions with NPP7.

Interactions	**Proposed Mutation**	**Interaction Distance (Å)**			**Predicted Effect of Mutation**
		LPC	**PAF**	**SM**	
LPC/SM/PAF palmitate tail F80, H110, W119, F141, Y142, P143, Y166	F80A Y142A Y166A	3.9 8.2 4.0	3.9 8.2 4.0	3.5 8.4 3. 9	Lose VDW, decrease activity Minimal effect Lose VDW, decrease activity
Choline group N96, L107, H203, F275	F275A L107F	4.3, 3.8 3.4, 4.0	4.3, 3.6 4.0	4.7, 4.0 5.3	Lose +/π, decrease activity Gain +/π, slightly enhanced
SM sphingoid tail F141, N168, E169, W172, Y194, F195, E19	E169A E169Q	5.9 5.9	3.2 3.2	3.2, 3.9 3.2, 3.9	SM: Lose H-bond, decrease activity Eliminate negative charged side chain - Increase activity

4.4.4 Effect of mutations on the hydrolysis of LPC

Fig. 4.4 shows the lowest energy docked conformation of LPC16:0 (shown in white ball and stick) in the NPP7 active site with mutated residues displayed as stick. All mutants of residues colored green hydrolyzed LPC (16:0) with a higher overall k_{cat}/K_m than wild type NPP7ExFLAG enzyme. Mutants of the residues colored red hydrolyzed LPC16:0 with a lower k_{cat}/K_m than did wild type NPP7ExFLAG. All kinetic parameters obtained from activity assays are presented in Table 4.3. Wild type NPP7ExFLAG had an apparent V_{max} of 2.5 μM/sec and a k_{cat} value of 2.9 sec^{-1}. Three mutants (F80A, Y166A and E169A) displayed lower V_{max} and k_{cat} values than the wild type enzyme. These mutants also exhibited a lower affinity for LPC16:0 as seen from their K_m values which are all higher than that of wild type enzyme. Accordingly, their k_{cat}/K_m values are lower than the wild type enzyme. In the model, F80 and Y166 are located 4Å or less from the nonpolar palmitate chain of LPC. Mutation to the smaller alanine residue would increase this contact distance and was predicted to have a detrimental effect on enzyme function (Table 4.2). In contrast, E169 is located almost 6Å from the polar glycerol backbone of LPC, and mutation was not predicted to have a detrimental impact on hydrolysis of this substrate. This apparent contradiction (especially with E169A mutation) between modeling predictions and experimental results might be mitigated if a water-bridged interaction occurs as water molecules were not included in these gas-phase docking studies. One mutant (F275A) had no observable catalytic activity against LPC16:0. This residue is located less than 4.5Å from the choline headgroup of LPC, and is oriented to make a cation-pi interaction. Such an interaction is not possible in the alanine mutant, consistent with the loss of activity upon mutation. Three mutants (L107F, Y142A and

E169Q) exhibited higher V_{max} and k_{cat} values than the wild type enzyme. Interestingly, these three mutants also had higher K_m values than the wild type enzyme. The combination of these values gives L107F a higher k_{cat}/K_m value while giving E169Q a lower k_{cat}/K_m value than wild type enzyme. In the model L107 is located 3.5 Å from the methyl of LPC choline group and 3.99 Å from the palmitate tail where it would potentially have hydrophobic interactions with both LPC regions. Mutation to a phenylanine introduces a phenyl ring with a favorable pi cloud to potentially form a cation-pi interaction with the positively charged LPC choline group and stronger hydrophobic interactions with the palmitate tail than the leucine. This led to the observed increase in catalytic activity of the L107F mutant as was computationally predicted. Y142 was selected as a control mutation site as it is located too far away from any of the substrates to have an effect on their hydrolysis. It is located 8.2 Å away from LPC palmitate tail (the closest interaction point). The unexpected results of an increase in V_{max} with an alanine replacement may be due to an allosteric effect that led to better and faster product release. The increase in the K_m value however, led to a k_{cat}/K_m value similar to that of the wild type enzyme as predicted by the model. As noted previously, E169 is located about 6 Å away from the hydroxyl group on the polar glycerol backbone of LPC and its replacement with a glutamine led to a minimal effect in contrast to an alanine replacement. This result further indicates the possibility of a water-bridged interaction which was maintained with a glutamine replacement though the interaction would be weaker than with a glutamate, hence the slight decrease in k_{cat}/K_m.

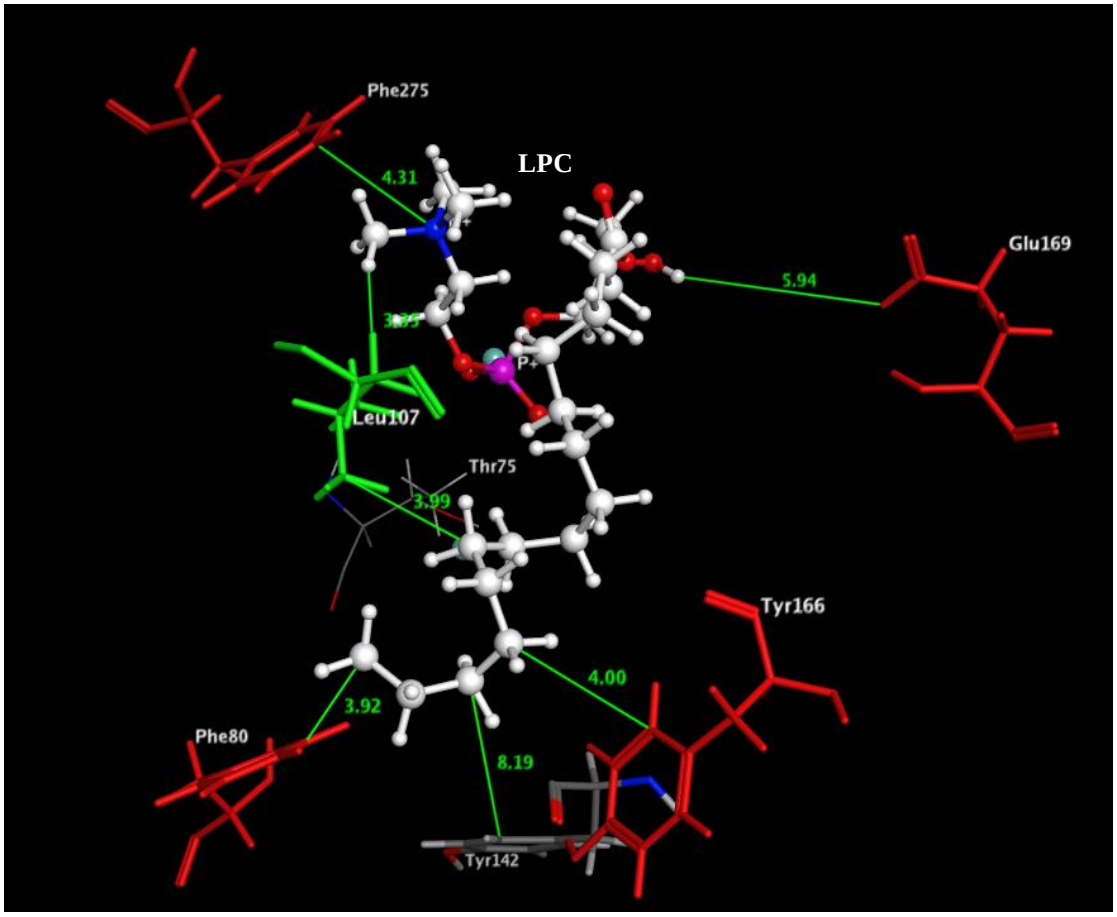

Fig. 4.4. LPC docked into the NPP7 homology model. LPC (16:0) is shown as white ball and stick. Only mutated residues are shown (sticks) with mutation sites that increased k_{cat}/K_m in green and those that decreased k_{cat}/K_m in red. The distance (Å) of each residue from the closest interaction point on the substrate is also shown.

Table 4.3 Kinetic parameters for hydrolysis of LPC 16:0.

Enzyme	K_m (μM)	V_{max} (μM/sec) (x 10^{-2})	k_{cat}(sec^{-1})	k_{cat}/K_m ($M^{-1}sec^{-1}$) (x 10^4)
L107F	61 ± 2.8	3.5 ± 0.03	4.2 ± 0.03	6.8 ± 1.6
Y142A	69 ± 0.9	3.0 ± 0.01	3.6 ± 0.01	5.2 ± 0.05
Wild type	57 ± 0.7	2.5 ± 0.01	2.9 ± 0.01	5.1 ± 0.1
E169Q	88 ± 6.8	3.3 ± 0.02	3.8 ± 0.03	4.3 ± 0.4
E169A	100 ± 15	1.0 ± 0.04	1.2 ± 0.05	1.2 ± 0.2
F80A	120 ± 3.0	0.7 ± 0.01	1.4 ± 0.01	1.2 ± 0.3
Y166A	100 ± 5.0	0.9 ± 0.03	1.1 ± 0.03	1.0 ± 0.2
F275A	No activity			

4.4.5 Effect of mutations on hydrolysis of PAF

Fig. 4.5 shows the lowest energy docked conformation of PAF16:0 (shown in gold ball and stick) in the NPP7 active site with mutated residues displayed as stick. All mutants of residues shown in green hydrolyzed LPC (16:0) with a higher overall k_{cat}/K_m than wild type NPP7ExFLAG enzyme. Mutants of the residues shown in red hydrolyzed LPC16:0 at a lower k_{cat}/K_m than did NPP7ExFLAG. All kinetic parameters obtained from activity assays are presented in Table 4.4. Wild type NPP7ExFLAG had an apparent V_{max} of 1.3 μM/sec and a k_{cat} value of 1.6 sec^{-1}. Three mutants (F80A, Y166A and E169A) exhibited slightly lower V_{max} and k_{cat} values and higher K_m values than the wild type enzyme. Accordingly, these substrates also had lower specificities for the substrate as seen from their k_{cat}/K_m values. In the model, F80 and Y166 are both less than 4 Å from

the non polar palmitate chain of PAF16:0. As for LPC, mutation to the smaller alanine residue would increase these contact distances and was predicted to have a detrimental effect on enzyme function (Table 4.2). Unlike LPC, E169 is located 3.15 Å from the acetyl group of PAF, and mutation was not predicted to have a detrimental impact on hydrolysis of this substrate due to a possible unfavorable interaction between the hydrophobic methyl group (on PAF acetyl group) and the polar side chain of E169. The possibility of a water-bridged interaction between E169 and the polar oxygen atoms on PAF could again mitigate this apparent contradiction between modeling predictions and experimental results. One mutant (F275A) had no observable catalytic activity against PAF16:0. As for LPC, this residue is located less than 4.5 Å from the choline head group of PAF16:0, and is oriented to make a cation-pi interaction. Such an interaction is not possible in the alanine mutant, consistent with the loss of activity upon mutation. Three mutants (L107F, Y142A and E169Q) exhibited higher V_{max} and k_{cat} values than the wild type enzyme. L107F and E169Q also had higher K_m values but L107F also had a much higher V_{max} (thus k_{cat}) value that led to a k_{cat}/K_m value above that of the wild type enzyme. In contrast E169Q had a higher K_m value that led to a lower specificity constant than that of wild type enzyme. Y142A had a lower K_m value than that of wild type enzyme and this combined with the higher k_{cat} value led to a k_{cat}/K_m value higher than that of wild type enzyme. The L107F, Y142A and E169Q effects can be similarly explained as in the case of LPC.

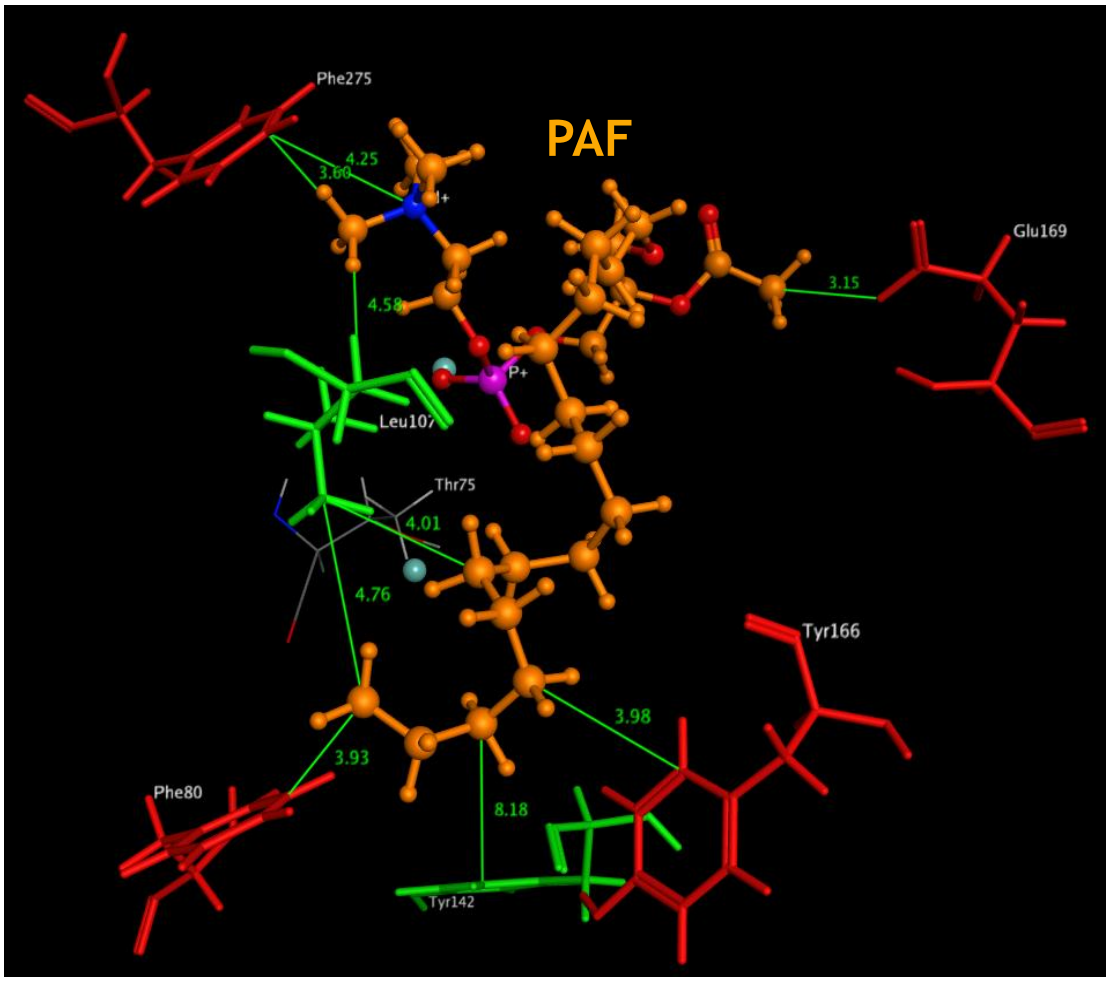

Fig. 4.5. PAF docked into the NPP7 active site. PAF (16:0) is shown as gold ball and stick. Only mutated residues are shown (sticks) with those that increased k_{cat}/K_m in green and those that decreased k_{cat}/K_m in red. The distance (Å) of each residue from the closest interaction point on the substrate is also shown.

Table 4.4 Kinetic parameters for hydrolysis of PAF16:0.

Enzyme	K_m (μM)	V_{max} (μM/sec)(x 10^{-2})	k_{cat} (sec^{-1})	k_{cat}/K_m ($M^{-1}sec^{-1}$) (x 10^4)
Y142A	75 ± 2	2.0 ± 0.03	2.5 ± 0.04	3.3 ± 0.6
L107F	94 ± 3	2.4 ± 0.3	2.9 ± 0.3	3.1 ± 0.2
Wild type	82 ± 2	1.3 ± 0.02	1.6 ± 0.02	2.0 ± 0.8
E169Q	130 ± 8	1.9 ± 0.1	2.3 ± 0.2	1.7 ± 0.2
F80A	120 ± 3	1.2 ± 0.03	1.4 ± 0.03	1.2 ± 0.4
E169A	95 ± 6	0.8 ± 0.02	0.80 ± 0.02	1.0 ± 0.2
Y166A	200 ± 10	0.7 ± 0.02	0.80 ± 0.04	0.4 ± 0.2
F275A	Not enough activity to study kinetics			

4.4.6 Effect of mutations on hydrolysis of SM

Fig. 4.6 shows the lowest energy docked conformation of SM (shown in blue ball and stick) in the NPP7 active site with mutated residues displayed as stick. Mutants of residues colored green hydrolyzed SM with a higher overall k_{cat}/K_m than wild type NPP7ExFLAG. Mutants of residues colored red hydrolyzed SM at a lower k_{cat}/K_m than did NPP7ExFLAG. Residue E169 is colored partially red and partially green because two mutations were made and each had an opposite effect compared to the wild type enzyme. All kinetic parameters obtained from activity assays are presented in Table 4.5. Wild type NPP7ExFLAG had an apparent V_{max} of 3.0 μM/sec and a k_{cat} value of 3.7 sec^{-1}. Four mutants (F80A, Y166A, E169A and F275A) exhibited lower V_{max} and k_{cat} values than the wild type enzyme. Interestingly, all these mutants exhibited lower K_m (14 μM for

F80A, 17 μM for E169A and 12 μM for F275A and Y166A) values meaning they bound SM better than the wild type enzyme (23 μM). However, E169A and F275A had lower k_{cat}/K_m values due to their much more reduced k_{cat} values. These two mutants bound SM more tightly than wild type enzyme but were the least efficient in converting the substrate to product as seen from the drastically reduced k_{cat}/K_m values. F80A had a k_{cat}/K_m value slightly higher than that of wild type enzyme. In the model, F80 and Y166 are located 4 Å or less from the non polar sphingoid chain of SM. Mutation to the smaller alanine residue would increase this contact distance and was predicted to have a detrimental effect on enzyme function (Table 4.2). F275 is about 4 Å away from the choline group of SM and its mutation to an alanine was predicted to have detrimental effects due to elimination of a cation-pi interaction. The results obtained match this prediction but the low K_m value was unexpected and indicates that the change led to better binding affinity for SM but without generation of much product. E169 was closer to the sphingoid chain (second hydrophobic chain) chain of SM and evidently has a hydrogen bond with a hydroxyl group on the substrate. Replacement of the glutamate with an alanine eliminated this hydrogen bond and led to the observed reduction in hydrolysis. Three other mutants (Y142A, Y166A and E169Q) exhibited V_{max} and k_{cat} values that were essentially similar to the wild type enzyme. Of these, Y142A had a K_m value twice that of wild type enzyme meaning it had half the binding affinity compared to that of wild type enzyme for SM while Y166A and E169Q had reduced K_m values and accordingly exhibited higher specificities for the substrate (about 2.5×10^5 $M^{-1}sec^{-1}$) compared to that of wild type enzyme (1.6×10^5 $M^{-1}sec^{-1}$). In the model, L107 is less than 4.5 Å from the interaction sites with SM (choline head group and sphingoid chain). Its change to the

larger, more hydrophobic phenylanine improved the van der Waal's interactions with the palmitate chain and introduced a cation-pi interaction with the choline head group leading to the observed increase in the V_{max} and k_{cat} values for SM hydrolysis by L107F. However, the higher K_m and k_{cat}/K_m values indicate poorer binding and lower specificity for the substrate and this is probably because the larger phenylanine residue reduced the space needed for the bulky SM substrate. In the model, Both Y166 and E169 are within less than 4 Å of the hydrophobic chains of SM. They both had drastically reduced K_m values that led to higher k_{cat}/K_m values. Changing Y166 to alanine may have allowed SM to better fit into the binding pocket and hence the reduced K_m value. Replacing E169 with a glutamine replaced a negatively charged side chain with an uncharged amide side chain close to the hydrophobic portion of the substrate leading to better binding because the hydrogen bond was retained with the glutamine in place of a glutamate.

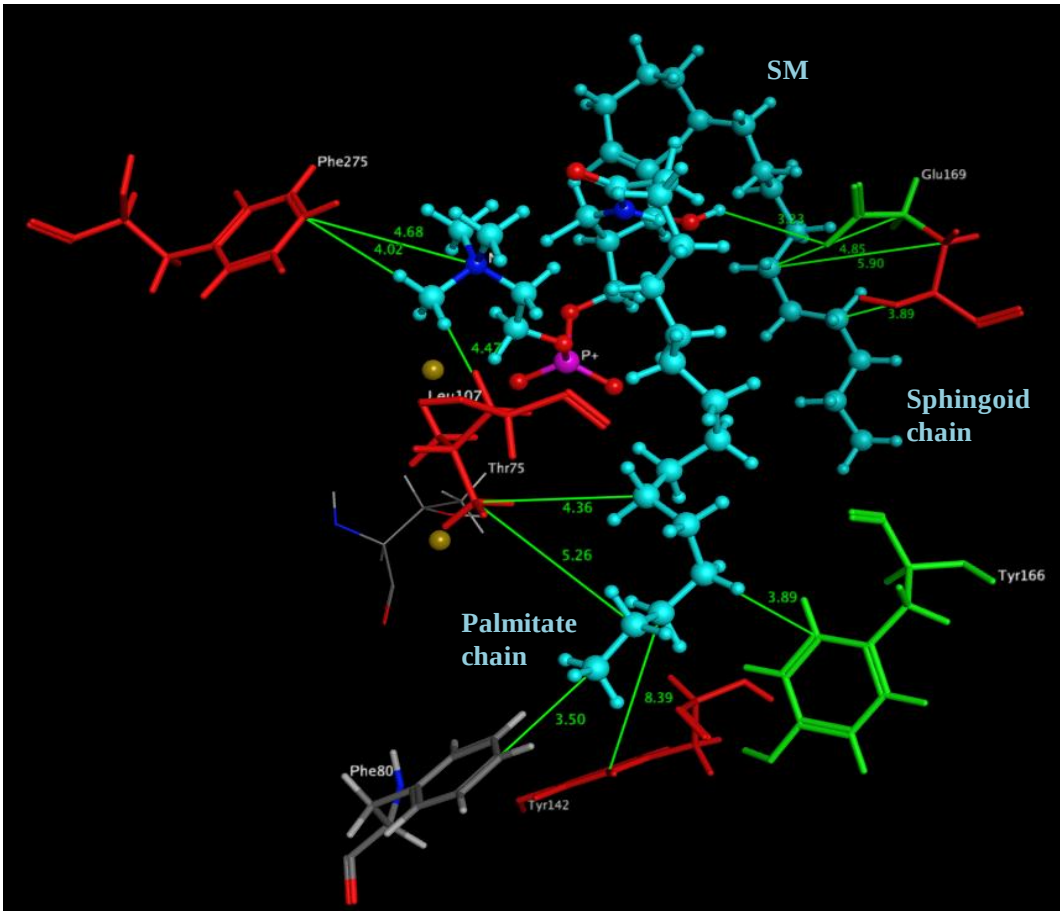

Fig. 4.6. SM docked into the NPP7 active site. SM is shown as blue ball and stick. All mutation points are shown with those that increased k_{cat}/K_m in green and those that decreased k_{cat}/K_m in red. The distance (Å) of each residue from the closest interaction point on the substrate is also shown.

Table 4.5 Kinetic parameters for hydrolysis of SM.

Enzyme	K_m (μM)	V_{max} (μM/sec) (x 10^{-2})	k_{cat} (sec^{-1})	k_{cat}/K_m ($M^{-1}sec^{-1}$) (x 10^4)
E169Q	15 ± 5	3.2 ± 0.08	3.8 ± 0.1	25.0 ± 6.0
Y166A	12 ± 0.4	2.6 ± 0.01	3.1 ± 0.2	25.8 ± 5.0
F80A	14 ± 6	2.2 ± 0.3	2.6 ± 0.3	18.6 ± 5.0
Wild type	23 ± 3	3.0 ± 0.1	3.7 ± 0.2	16.5 ± 4.0
E169A	17 ± 2	1.8 ± 0.1	2.2 ± 0.2	11.6 ± 2.0
L107F	37 ± 3	3.5 ± 0.1	4.2 ± 0.1	11.4 ± 4.0
Y142A	47 ± 7	3.1 ± 0.2	3.7 ± 0.2	7.9 ± 3.0
F275A	12 ± 1	0.7 ± 0.1	0.9 ± 0.2	7.5 ± 2.0

4.4.7 Effect of mutations on hydrolysis of pNPPC

Fig. 4.10 shows the lowest energy docked conformation of pNPPC (shown in yellow ball and stick) in the NPP7 active site with mutated residues displayed as stick. Mutants of residues colored green hydrolyzed pNPPC with a higher k_{cat}/K_m than the wild type NPP7ExFLAG enzyme. Mutants of residues colored red hydrolyzed pNPPC at a lower k_{cat}/K_m than did NPP7ExFLAG. Residue E169 is left in natural element colors because two mutations were made and each had an opposite effect compared to the wild type enzyme. All kinetic parameters obtained from activity assays are presented in Table 4.6. Wild type NPP7ExFLAG had an apparent V_{max} of 1.1 μM/sec and a k_{cat} value of 1.4 sec^{-1}. Four mutants (F80A, Y166A, E169A and F275A) exhibited lower V_{max} and k_{cat} values, as well as higher K_m values, and accordingly had lower specificities than the wild

type enzyme. From the model, F80 and Y166 are too far away from the substrate and were predicted not to have effects when mutated to alanine. The contradictory effects may indicate that their mutations led to allosteric effects that affected recognition of this substrate. It is also possible that this model did not correctly depict pNPPC since we emphasized mostly the three natural substrates that were known at the time the model was generated. Two mutants (L107F and Y142A) exhibited V_{max} and k_{cat} values above those obtained with the wild type enzyme. L107F also had a slightly lower K_m value than that of wild type enzyme and thus a higher k_{cat}/K_m value for pNPPC. Y142A on the other hand had a higher K_m value than wild type enzyme but similar specificity constant due to an improved k_{cat} value. In the model, L107F less than 4.5 Å away from the choline headgroup of pNPPC and thus its mutation to a phenylanine introduced a cation-pi interaction yielding the expected effects. Y142A was too far away and its effects here, as with the other substrates, were minimal. One mutant (E169Q) had V_{max} and k_{cat} values similar to those obtained with wild type enzyme and as seen from the model, E169 is located about 6 Å away from the substrate and its mutation was accordingly predicted to have minimal effect.

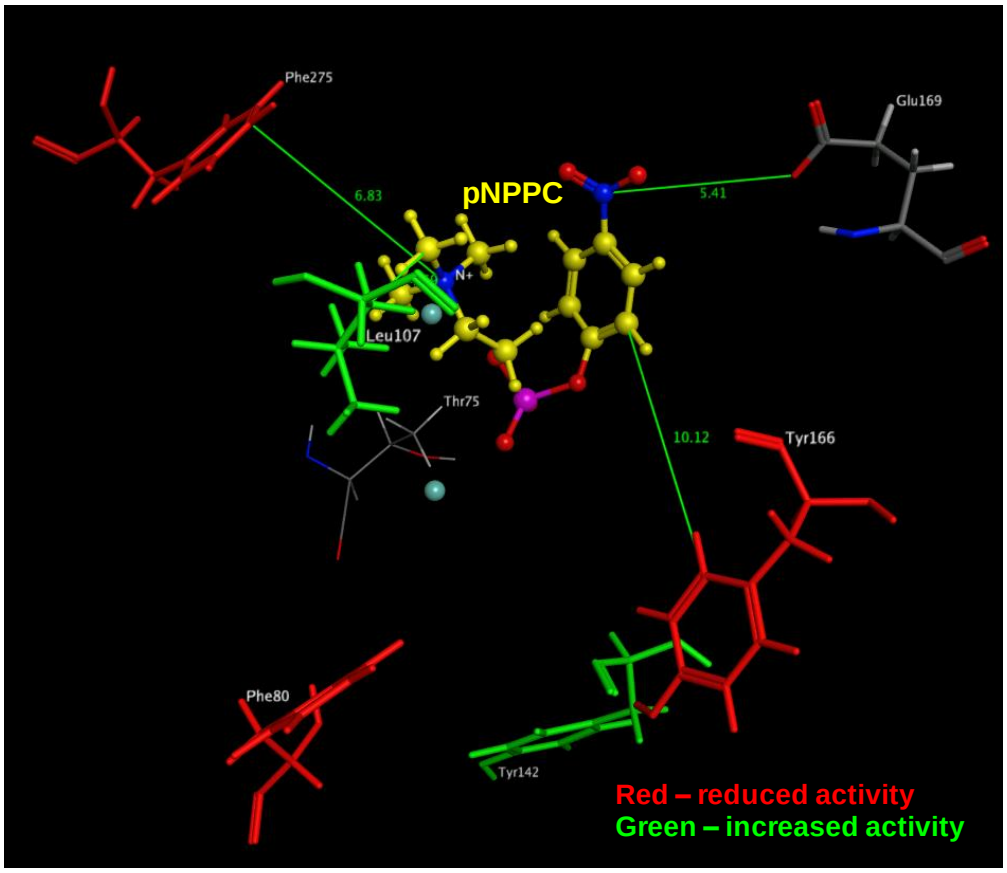

Fig. 4.7. pNPPC docked into the NPP7 active site. pNPPC is shown as yellow ball and stick. Only mutated residues are shown (sticks) with those that increased k_{cat}/K_m in green and those that decreased k_{cat}/K_m in red. The distance (Å) of each residue from the closest interaction point on the substrate is also shown.

Table 4.6 Kinetic parameters for hydrolysis of pNPPC.

Enzyme	K_m (μM)	V_{max} (μM/sec) (x 10^{-2})	k_{cat} (sec^{-1})	k_{cat}/K_m (sec^{-1} M^{-1}) (x 10^4)
L107F	310 ± 5.0	1.4 ± 0.05	1.7 ± 0.1	0.60 ± 0.02
Wild type	360 ± 8.0	1.1 ± 0.01	1.4 ± 0.1	0.40 ± 0.03
Y142A	400 ± 4.0	1.4 ± 0.01	1.7 ± 0.1	0.40 ± 0.02
F80A	450 ± 10.0	0.63 ± 0.04	0.8 ± 0.1	0.20 ± 0.1
E169A	170 ± 30.0	0.42 ± 0.03	0.5 ± 0.03	0.30 ± 0.02
E169Q	440 ± 5.0	1.2 ± 0.02	1.4 ± 0.1	0.30 ± 0.02
Y166A	820 ± 20.0	0.62 ± 0.03	0.7 ± 0.04	0.09 ± 0.01
F275A	120 ± 5.0	0.23 ± 0.03	0.3 ± 0.03	0.03 ± 0.01

4.5 Discussion

NPP enzymes have been reported to possess well-defined substrate specificity but it is not known what determines this property (Stefan et al., 2005). Separate substrate recognition surveys have been performed for NPP2 (Clair et al. 2003) and NPP6 (Sakagami et al. 2005) and established the ability of these two phosphodiesterases to discriminate between substrates with very small structural variations. For instance NPP2 hydrolyzes LPC and SPC but not PAF. Likewise, NPP6 readily recognizes and hydrolyzes LPC and lysoPAF but not PAF. We recently conducted a detailed survey of substrate recognition by NPP7 and identified lysoPAF and SPC as endogenous phospholipid substrates in addition to the previously known LPC, PAF and SM. These findings made NPP7 the only NPP isoform that has the ability to hydrolyze lipids with

one or two long hydrophobic tails. In this study, we have used molecular modeling and experimental mutagenesis to identify and characterize amino acid residues that determine NPP7 substrate recognition. We have further used experimental mutagenesis to validate these computational results and characterize the role of each identified residue in determining NPP7 substrate recognition and preferences.

The use of homology modeling to study NPP7 is a challenging task and has not been previously reported likely because none of the NPP isoforms have a publicly available solved crystal structure. The only crystal structure currently available is the bacterial *Xac* NPP (Zalatan et al., 2005) structure which was found to share 34% identity with human NPP7. Experimental validation of the modeling predictions was therefore an important aspect of this study. Results for the hydrolysis of LPC16:0 show a match with computational predictions for all predicted amino acids with the exception of E169A which led to an unexpected decrease in k_{cat}/K_m. However, this discrepancy can be logically mitigated if there exists a water-bridged interaction between the residue E169 and the polar glycerol backbone of LPC16:0 since water molecules were not including in our modeling system. This fact is further reinforced by the E169Q mutation which led to only a small decrease in k_{cat}/K_m value. The glutamine replacement in this case retained the ability to hydrogen bond (water-bridged) with the glycerol backbone of LPC16:0 although to a lesser extent than a glutamate would. The Y142A mutant had a k_{cat}/K_m value that was essentially the same as that of the wild type enzyme. This was computationally expected as this residue was approximately 8 Å away from the possible interaction point with LPC. The modeling predictions with residues F80A, Y166A, E169A and F275A having a reduction in catalytic function (increased K_m, reduced V_{max},

k_{cat} and k_{cat}/K_m) and L107F having an overall increase in function (although with a slight increase in K_m value) were experimentally observed. All computational predictions for the hydrolysis of PAF16:0 were matched by experimental results with all mutants except for Y142A. The contradictory results in the case of Y142A with PAF16:0 could be due to an allosteric effect that led to faster product generation even with lower substrate affinity than the wild type enzyme. With both substrates, there was an increase in the K_m value with mutations that generally led to improved V_{max} and k_{cat} values probably because of minimally altered folding of the protein. Ultimately, the experimental results for hydrolysis of LPC16:0 and PAF16:0 show that the homology model and the predictions made from it are valid and we can therefore conclude that LPC16:0 and PAF16:0 occupy a common binding pocket within the active site of NPP7.

The effects on the hydrolysis of SM were significantly different compared to LPC16:0 and PAF16:0. Y166A, one of the three mutations that had detrimental effects on hydrolysis of LPC16:0 and PAF16:0 had a significant enhancement in the hydrolysis of SM. This contradiction in computational predictions and experimental results is likely due to the bulky size of SM which which necessarily requires more space to fit within the NPP7 active site. This explains the positive effect observed when the larger tyrosine 166 residue is replaced with a much smaller alanine residue. L107F, which led to an increase in hydrolysis of LPC16:0 and PAF16:0 as was predicted by modeling, only slightly increased the V_{max} and k_{cat} against SM but also increased the K_m value, leading to lower specificity for this substrate. This also can be explained if the bulky size of SM is considered. The smaller L107 residue was replaced by a much larger phenylalanine that could be sterically unfavorable for SM binding. This indicates that SM may not bind in

exactly the same binding pocket as LPC16:0 and PAF16:0 or that the residues selected do not interact with SM as they do with LPC and PAF. Another interesting mutation site with regard to SM hydrolysis was E169. E169A led to a significant reduction in all kinetic parameters except K_m whereas E169Q led to a significant decrease in K_m and an increase in V_{max}, k_{cat}, and k_{cat}/K_m values leading to an overall better catalytic function of E169Q than the wild type. Effects observed for both of these mutations clearly indicate the importance of this site in the recognition of SM by NPP7. The drastic reduction in performance with the E169A mutation is evidence of elimination of the important hydrogen bond between E169 and SM (Figure 4.6). The significant improvement in performance with the E169Q is evidence not only of the H-bond between glutamine and SM but also of the improved electrostatic interactions when a negatively charged side chain (E169) was replaced with a neutral residue (Q169). E169 mutants had the largest effect on hydrolysis of SM compared to the other mutants made and since SM is currently the only substrate with two long hydrophobic chains, we can conclude that the second chain of SM plays an essential role in its recognition by NPP7. The reversal in effects on hydrolysis of SM with majority of the mutants in comparison to hydrolysis of the other substrates is a strong indication that the manual manipulation of the palmitate chain led to a biased model of SM and more refinement needs to be done in the future to identify the exact binding pocket for this substrate.

Para-nitrophenylphosphorylcholine (pNPPC) is a synthetic compound recently identified as a substrate for NPP7. It is much smaller in size than the three known lipid substrates with much lower degree of flexibility. The mutants made were mainly based on the docking results of the three lipid substrates but experiments run with pNPPC

showed that mostof computational predictions were matched by experimental results. This indicates that pNPPC, PAF and LPC, all bind in a common binding pocket within the NPP7 active site. However the model for pNPPC needs refinement as some the mutations had unexpected effects although they matched those of PAF and LPC. In its current conformation (Fig. 4.7), residues F80 and Y166 are located more than 10Å away from pNPPC but experimentally had a significant reduction in overall performance of the enzyme. This indicates that pNPPC binds in the same pocket as LPC and PAF but may do so with a different conformation than that shown in the model to account for the mutation effects.

To identify substrate-binding determinants, the magnitude and/or direction of effect of each mutation was compared for the different substrates. Fig. 4.8 summarizes the k_{cat}/ K_m values for each mutant normalized to that of wild type against the same substrate. Out of all the mutations made, only F275A led to loss of activity against some of the substrates (LPC and PAF) and retained minimal activity against SM and pNPPC. This residue was predicted to make a cation/pi interaction with the choline groups of all substrates tested. It would have been interesting to investigate its effects on a substrate without a choline head group but unfortunately, all currently known substrates for NPP7 have this common functional group. Y166A led to large reduction in recognition of LPC, PAF and pNPPC (reduced k_{cat}/K_m values) but increased SM recognition (increased k_{cat}/K_m value). Since SM is bulkier than all the other three substrates, the replacement of Y166 with an alanine may have allowed more space to accommodate substrate in the binding pocket. These data show that Y166 is important in LPC, PAF and pNPPC recognition but not in the recognition of SM by NPP7. Conversely, L107F led to a

significant increase in k_{cat} /K_m of PAF, LPC and pNPPC but reduced the k_{cat}/K_m for SM indicating that L107 is important for SM recognition but probably not as essential for the recognition of the other three substrates.

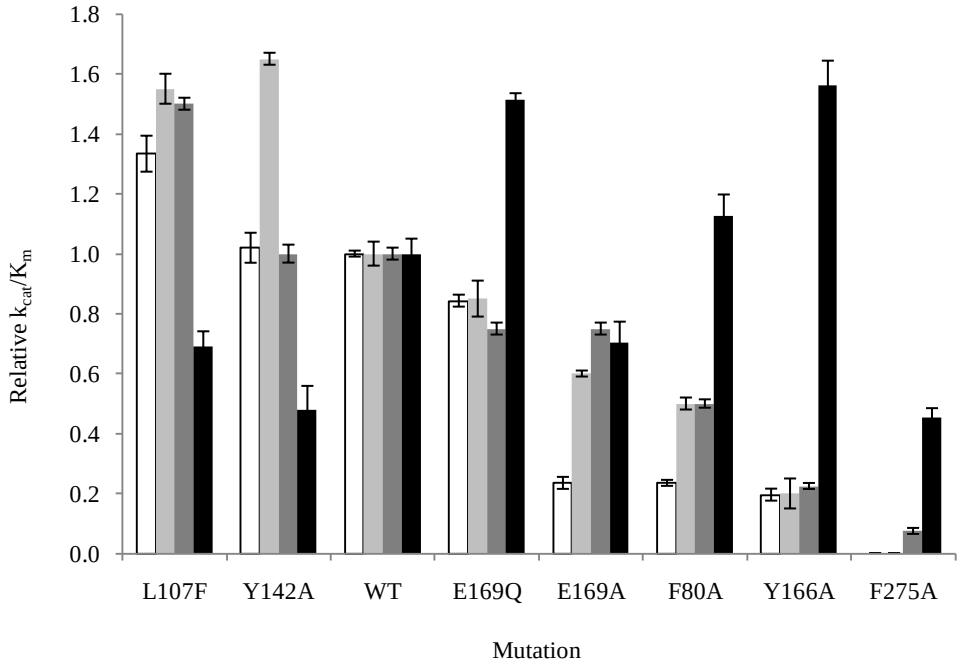

Fig. 4.8. Relative k_{cat}/K_m values of all mutants for hydrolysis of all substrates, LPC (white bars), PAF16:0 (light grey bars), pNPPC (dark grey bars and SM (black bars). The relative k_{cat}/K_m values were obtained by dividing the K_m value of each mutant with that of wild type enzyme against the same substrate.

To analyze substrate specifying determinants for NPP7 as opposed to other NPP isoforms, an alignment of the amino acid sequences of all NPP enzymes was done and the residues in other NPP isoforms that aligned with the NPP7 mutation sites were identified as shown in Table 4.5. An interesting observation is that three (F80, L107, and Y142,) of the six NPP7 mutation sites identified by computational modeling were

Table 4.7 NPP7 mutation sites aligned with all human NPP isoforms

Isoform	Active site	Mutation site					
NPP7	**T75**	**F80A**	**L107F**	**Y142A**	**Y166A**	**E169A/Q**	**F275A**
NPP6	S71	Y76	F103	W139	D163	F166	Q265
NPP5	T72	Y77	F104	W139	F163	R166	T262
NPP4	T70	Y75	F102	W136	F160	R163	T261
NPP3	T205	Y210	F237	W271	F295	R298	F396
NPP2	T210	Y215	F242	W276	H282	R285	I435
NPP1	T256	Y261	F288	W322	F346	R349	I446

conserved in all other NPPs but were different in NPP7. Additionally, one residue (E169) was a conserved arginine in all NPPs except NPP6 which had a phenylanine. Only one mutation (L107F) was changed to the residue in the other NPP isoforms and experimental results indicate its importance in SM recognition. NPP7 is the only NPP enzyme that hydrolyzes SM. From Table 4.5, we can conclude that L107 and E169 provide for the specificity for SM by NPP7. In place of E169, NPP6 has a phenylalanine while the other five isoforms contain an arginine. Both phenylalanine and arginine are much bulkier than the glutamate in NPP7 which further accounts for the ability of NPP7 to bind this larger substrate that is not recognized by NPP2 and NPP6. Mutation of the other five NPP7 mutation sites to those aligned in other isoforms may shed more light on

specificity among these enzymes. It would be interesting to see if F166E and R285E can lead to SM recognition by NPP6 and NPP2, respectively.

In conclusion, this work is the first of its kind where homology modeling has been used to study structure-activity relationships in the NPP7. Although the template used had only 34% amino acid identity with the NPP7 target sequence, validation results have proved the model valid and helped analyze NPP7substrate recognition elements.

4.6 References

Asada, T., Gouda, H. & Kollman, P. A. (2002). Molecular dynamics simulation study of the negative correlation in antibody AZ28-catalyzed oxy-cope rearrangement. *J Am Chem Soc* **124**, 12535-42.

Berman, H. M., Westbrook, J., Feng, Z., Gilliland, G., Bhat, T. N., Weissig, H., Shindyalov, I. N. & Bourne, P. E. (2000). The Protein Data Bank. *Nucleic Acids Res* **28**, 235-42.

Bollen, M., Gijsbers, R., Ceulemans, H., Stalmans, W. & Stefan, C. (2000). Nucleotide pyrophosphatases/phosphodiesterases on the move. *Crit Rev Biochem Mol Biol* **35**, 393-432.

Clair, T., Aoki, J., Koh, E., Bandle, R. W., Nam, S. W., Ptaszynska, M. M., Mills, G. B., Schiffmann, E., Liotta, L. A. & Stracke, M. L. (2003). Autotaxin hydrolyzes sphingosylphosphorylcholine to produce the regulator of migration, sphingosine-1-phosphate. *Cancer Res* **63**, 5446-53.

Clair, T., Lee, H. Y., Liotta, L. A. & Stracke, M. L. (1997). Autotaxin is an exoenzyme possessing 5'-nucleotide phosphodiesterase/ATP pyrophosphatase and ATPase activities. *J Biol Chem* **272**, 996-1001.

Duan, R. (2003). Identification of human intestinal alkaline sphingomyelinase as a a novel ecto-enzyme related to the nucleotide phosohodiesterase family. *Biological chemistry* **278**, 38528-38536.

Duan, R. D. (2006). Alkaline sphingomyelinase: an old enzyme with novel implications. *Biochim Biophys Acta* **1761**, 281-91.

Gijsbers, R., Ceulemans, H. & Bollen, M. (2003). Functional characterization of the non-catalytic ectodomains of the nucleotide pyrophosphatase/phosphodiesterase NPP1. *Biochem J* **371**, 321-30.

Gijsbers, R., Ceulemans, H., Stalmans, W. & Bollen, M. (2001). Structural and catalytic similarities between nucleotide pyrophosphatases/phosphodiesterases and alkaline phosphatases. *J Biol Chem* **276**, 1361-8.

Hornak, V., Abel, R., Okur, A., Strockbine, B., Roitberg, A. & Simmerling, C. (2006). Comparison of multiple Amber force fields and development of improved protein backbone parameters. *Proteins* **65**, 712-25.

Kanda, H., Newton, R., Klein, R., Morita, Y., Gunn, M. D. & Rosen, S. D. (2008). Autotaxin, an ectoenzyme that produces lysophosphatidic acid, promotes the entry of lymphocytes into secondary lymphoid organs. *Nat Immunol* **9**, 415-23.

Nilsson. (1969). The presence of sphingomyelin- and ceramide-cleaving enzymes in the small intestinal tract. *Biochimica biophysica Acta* **176**, 339-47.

Nyberg, L., Duan, R. D., Axelson, J. & Nilsson, A. (1996). Identification of an alkaline sphingomyelinase activity in human bile. *Biochim Biophys Acta* **1300**, 42-8.

Sakagami, H., Aoki, J., Natori, Y., Nishikawa, K., Kakehi, Y. & Arai, H. (2005). Biochemical and molecular characterization of a novel choline-specific glycerophosphodiester phosphodiesterase belonging to the nucleotide pyrophosphatase/phosphodiesterase family. *J Biol Chem* **280**, 23084-93.

Stefan, C., Jansen, S. & Bollen, M. (2005). NPP-type ectophosphodiesterases: unity in diversity. *Trends Biochem Sci* **30**, 542-50.

Umezu-Goto, M., Kishi, Y., Taira, A., Hama, K., Dohmae, N., Takio, K., Yamori, T., Mills, G. B., Inoue, K., Aoki, J. & Arai, H. (2002). Autotaxin has lysophospholipase D activity leading to tumor cell growth and motility by lysophosphatidic acid production. *J Cell Biol* **158**, 227-33.

Wang, J., Cieplak, P., Kollman, P.A.,. (2000). How well does a restrained electrostatic potential (RESP) model perform in calculating conformational energies of organic and biological molecules? *J comput. Chem* **21**, 1049 - 1074.

Wu, J., Hansen, G. H., Nilsson, A. & Duan, R. D. (2005). Functional studies of human intestinal alkaline sphingomyelinase by deglycosylation and mutagenesis. *Biochem J* **386**, 153-60.

Wu, J., Nilsson, A., Jonsson, B. A., Stenstad, H., Agace, W., Cheng, Y. & Duan, R. D. (2006). Intestinal alkaline sphingomyelinase hydrolyses and inactivates platelet-activating factor by a phospholipase C activity. *Biochem J* **394**, 299-308.

Zalatan, J. G., Fenn, T. D., Brunger, A. T. & Herschlag, D. (2006). Structural and functional comparisons of nucleotide pyrophosphatase/phosphodiesterase and alkaline phosphatase: implications for mechanism and evolution. *Biochemistry* **45**, 9788-803.

CHAPTER 5

THE ROLE OF DIVALENT METAL CATIONS IN NPP7

5.1 Introduction

Like all known NPP isoforms, NPP7 is presumed to be a metalloenzyme that depends on the presence of specific divalent metal cations for its catalytic function (1, 2). The catalytic cycle for the seven known NPP enzymes has been described based on that of the related and well studied phospho- and sulfo-coordinating enzymes which includes the alkaline phosphatase superfamily (3, 4). Here we describe the use of circular dichroism spectroscopy and enzyme activity determination to investigate whether the active site divalent metal cations play solely functional or a combined structural and functional role in NPP7. Our results show that these active site divalent metal cations play only a functional role in this isoform. These experiments were performed in parallel with the NPP2 and NPP6 isoforms as part of a comparative survey. Similar results were obtained for all three isoforms studied, thus similar conclusions were reached concerning the functional role of divalent cations in these related isoforms. Here the focus will be on studies of NPP7 with discussion of those pertaining to NPP2 and NPP6 when appropriate. The comparative survey, in its entirety, is a manuscript co-authored by Truc Chi T. Pham, Irene W. Wanjala, Angela, L. Howard, Abby L. Parill, and Daniel L. Baker which is to be submitted to the *Biochemical Journal*.

Previously published data suggested that the catalytic activity of NPP7 was inhibited by the presence of 0.25 mM zinc cations and that this inhibitory effect was

prevented by the addition of 2 mM ethylene diaminetetraacetic acid (EDTA) (1). These findings are hard to rationalize based on the fact that NPP7, like all NPP isoforms, is a metalloenzyme that requires divalent metal cations for catalytic function (2-5). As part of a comparative analysis to determine the role (structural and/ or functional) of divalent metal cations in the three known lysophospholipid preferring NPP isoforms, NPP2, NPP6, and NPP7, experiments detailing the effect of divalent metal ions on the structure and function of NPP7 were performed. Results indicated that all three NPP isoforms are inhibited by EDTA at an enzyme:EDTA molar ratio greator or equal to 1:120 and that the addition of divalent metal cations (including cobalt, nickel and zinc for NPP7) to these inactivated enzymes can restore most of the lost activity. We also show that neither EDTA (which inhibited the enzyme) nor the divalent metal cations (which restored enzyme activity) altered the secondary structure of the enzyme.

5.2 Experimental Design

5.2.1 EDTA treatment

Human NPP7ExFLAG protein was expressed and purified using the baculovirus-Sf9 insect cell system described in Chapter 2, sections 2.3.2-2.3.4. Affinity purified protein was used with stock solutions of varying ETDA concentrations to generate samples with increasing molar ratios of NPP7 protein to chelator (NPP7:EDTA ratios of 1:0, 1:1, 1:2, 1:4, 1:8, 1:20, and 1:120). To prepare these samples, equal volumes (5 μL) of NPP7ExFLAG (8 μM) was mixed with EDTA stocks in CD buffer (10 mM Tris, 10 mM NaCl, pH 7.4) at 0 μM, 8 μM, 16 μM, 32 μM, 64 μM, 160 μM and 720 μM. Duplicate samples were made for each EDTA treatment. One set of the samples was

immediately incubated at 4°C for 30 minutes while the other set was incubated for 16 hours. Following the incubation period, the catalytic activity of NPP7 was examined using *para*-nitrophenylphosphocholine (pNPPC, Sigma-Aldrich, St. Louis, MO, USA) as the substrate. NPP7ExFLAG:EDTA samples were diluted to an enzyme concentration of 30 nM in NPP7 assay buffer (50 mM Tris-HCl, 150 mM NaCl, 10mM sodium taurocholate, pH 7.4) before addition onto the plate. Each reaction well contained a total of 60 µL consisting of 20 µL each of 30 nM enzyme sample, 500 µM pNPPC and NPP7 assay buffer. In this activity assay, the absorbance of the *para*-nitrophenolate anion product generated by the lysophospholipase C activity of NPP7 was monitored at 405 nm every minute for a period of one hour using a Synergy-2 plate reader (BioTek, Winooski, VT, USA). The relative responses of all enzyme/EDTA samples were determined at the 60^{th} minute of the assay where responses were linear. All data were normalized to the zero EDTA control.

5.2.2 Metal ion restoration

Samples containing NPP7ExFLAG and EDTA in a 1:120 molar ratio were prepared by adding 10 µL of purified NPP7ExFLAG (6 µM) to 10 µL of EDTA solution (720 µM). This mixture was incubated for 16 hours at 4 °C and diluted 1:100 with NPP7 assay buffer (50 mM tris-HCl, 150 mM NaCl, and 10mM sodium taurocholate, pH 7.4). These working stocks contained 30 nM NPP7ExFLAG and 3.6 µM EDTA (maintaining the 1:120 molar ratio). Solutions (30 mM) of divalent metal chlorides (Ca^{2+}, Co^{2+}, Cu^{2+}, Fe^{2+}, Mg^{2+}, Mn^{2+}, Ni^{2+}, Zn^{2+}) were prepared in NPP7 assay buffer. Equal volumes of the enzyme:EDTA working stock were then combined with each metal chloride solution

resulting in a solution with final enzyme:EDTA:metal molar ratios of 1:120:1 x 10^6 thus constituting saturating amounts of EDTA compared to enzyme and metal cation compared to EDTA. These mixtures were incubated at 4 ^oC for either 30 minutes or 16 hours. At the end of the incubation periods, the catalytic activity of the enzyme was monitored as described using *para*-nitrophenylphosphocholine as substrate.

5.2.3 Structural studies using CD spectroscopy

To determine the effect of metal ion removal by EDTA treatment and of the restoration of divalent metals on the secondary structure of NPP7ExFLAG, the following sets of samples were prepared. First, NPP7ExFLAG (8 µM, 10 µL) was diluted with 10 µL of CD buffer (control sample). Second, additional samples were generated by mixing NPP7ExFLAG (8 µM, 10 µL) with 10 µL of 960 µM EDTA in CD buffer, pH 7.4 (pH 7.0 for the Zn sample). All samples were incubated for 16 hours at 4°C. Addition of 280 µL of CD buffer to the control and one of the ETDA treated samples made up the volumes to 300 µL that were analyzed for secondary structural compositions on a model 410 CD spectrophotometer (Aviv biomedical Inc., Lakewood, NJ, USA). Wavelength scans were done at 25 °C from 190 to 260 nm in a 1 mm cuvet (zinc samples were studied in 10 mm cuvettes). The 300 µL samples used for the wavelength scan were diluted to 3 mL using CD buffer followed by CD thermal scans at 222 nm from 20 to 100 °C using a 10 mm cuvet. Metal treatment samples were prepared by diluting with 200 µL of 200 mM stocks of $CaCl_2$, $CoCl_2$, or $NiCl_2$ (instead of CD buffer used for controls) and were incubated for either 30 minutes or 16 hours at 4°C. Wavelength and thermal scans were then done as described previously for the control samples. Since Zn^{2+} readily

formed insoluble $Zn(OH)_2$ at pH values higher than 7.0, all CD experiments in the presence of Zn^{2+} were performed at pH 7.0. EDTA treated working stocks were prepared as described previously with the exception that the CD buffer was pH 7.0 rather than pH 7.4 for the zinc-treated samples.

5.3 Results

5.3.1 EDTA treatment

Fig. 5.1 shows the effect of EDTA treatment on the activity of recombinant, purified NPP7ExFLAG. Treatment of NPP7 with EDTA up to a 120 fold excess (30 minute incubation) showed ≥ 90% of the untreated enzyme activity using pNPPC as substrate. Similarly, 16 hour incubation with molar ratios of EDTA lower than 1:20 had little impact on enzyme activity. In contrast, 16 hours of exposure to EDTA at a 1:20 molar ratio decreased activity by approximately 30%, whereas EDTA treatment at a 1:120 molar ratio led to a reduction in activity of approximately 90% in NPP7ExFLAG mediated hydrolysis of pNPPC.

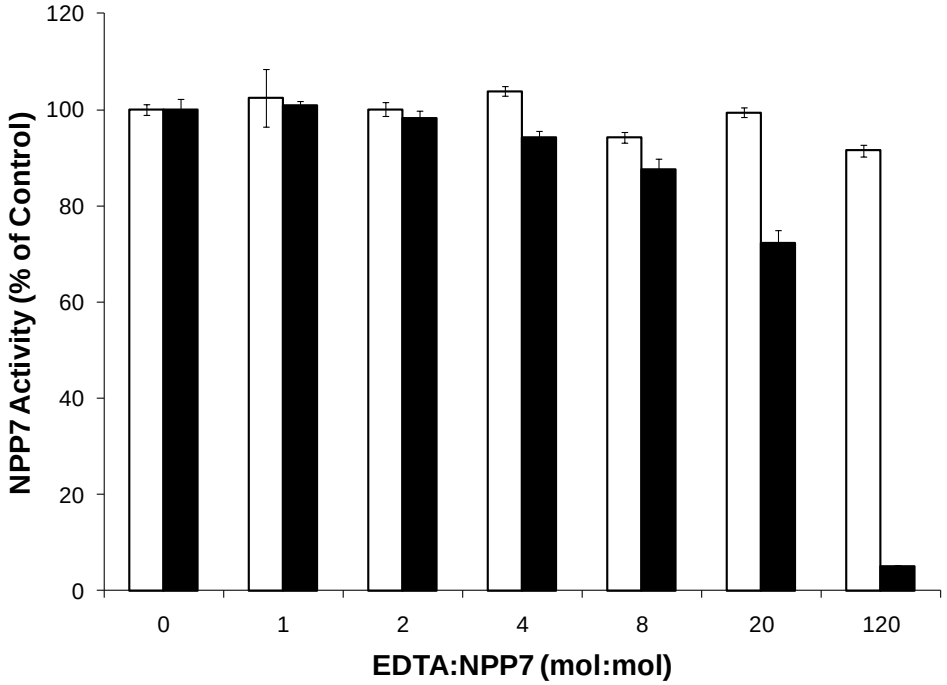

Fig. 5.1. The effect of EDTA on the catalytic activity of NPP7ExFLAG. NPP7ExFLAG was treated with EDTA at various molar ratios of 1:0, 1:1, 1:2, 1:4, 1:8, 1:20, and 1:120 at 4^{o}C for 30 minutes (white bars) or 16 hours (black bars). Following dilution, the catalytic activity of NPP7ExFLAG was determined using pNPPC as substrate.

5.3.2 Metal ion restoration

Sixteen hours of treatment with EDTA at a 1:120 molar ratio significantly inhibited NPP7ExFLAG activity. We speculate this was due to the loss of one or more of the required, active site divalent metals. To address whether this effect on enzyme activity was reversible or not, divalent metals were added back to EDTA-treated NPP7ExFLAG protein and enzymatic function was determined using pNPPC as substrate. Fig. 5.2 shows that four (Ca^{2+}, Co^{2+}, Ni^{2+}, and Zn^{2+}) out of the seven divalent metals tested restored activity of EDTA-treated NPP7ExFLAG above 20% within 30

minutes. Cobalt treated NPP7ExFLAG had the greatest activityas compared to the untreated control (118%), followed by Ni^{2+} and Zn^{2+} at (65 and 79%), respectively. It is interesting to note that the effect of Ca^{2+} improved with additional incubation time to 16 hours, whereas the effect of Co^{2+} and Ni^{2+} did not change appreciably, whereas the effect of Zn^{2+} decreased significantly. The decrease in activity with prolonged exposure was reproducible but our experiments were not adequate to establish why this was the case. Further research is is ongoing to investigate the possibility of the divalent metal cations binding the enzyme at other sites other than the known metal coordination sites.

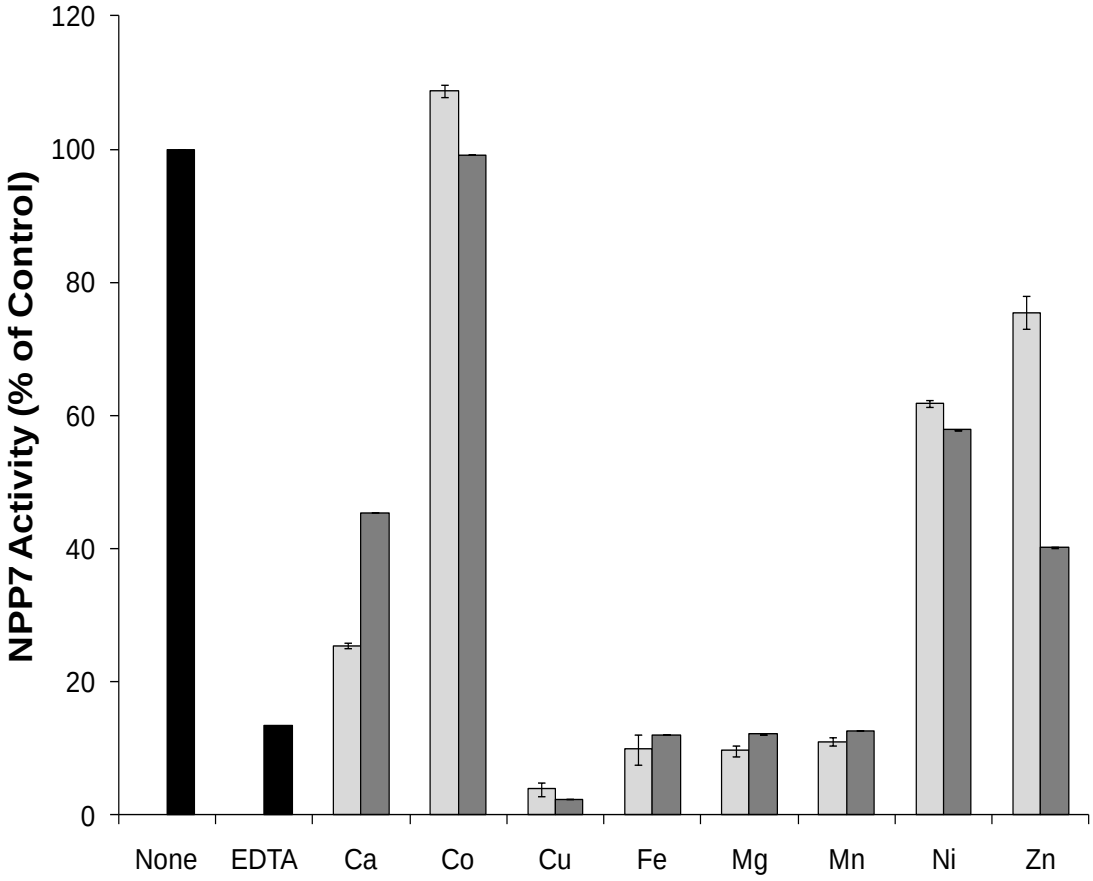

Fig. 5.2. Restoration of catalytic activity of NPP7ExFLAG by divalent metals. NPP7ExFLAG treated with EDTA for 16 hours was exposed to various divalent metal cations and incubated at 4^{o}C for either 30 minutes (light grey bars) or 16 hours (dark grey bars). The catalytic activity of the EDTA-metal-treated NPP7 was determined using pNPPC as substrate.

5.3.3 Secondary structural analysis by CD spectroscopy

Circular dichroism (CD) spectroscopy was employed to study the effect of EDTA chelation and divalent metal add back on the global secondary structure of NPP7ExFLAG. Wavelength scan data from CD characterization of NPP7ExFLAG (untreated control, EDTA treated for 16 hours and EDTA treated with metal ion add back for 30 minutes) are shown in Fig. 5.3. No significant difference was noted in spectra

obtained between 190-260 nm for any of the sample treatments indicating similar global secondary structural compositions.

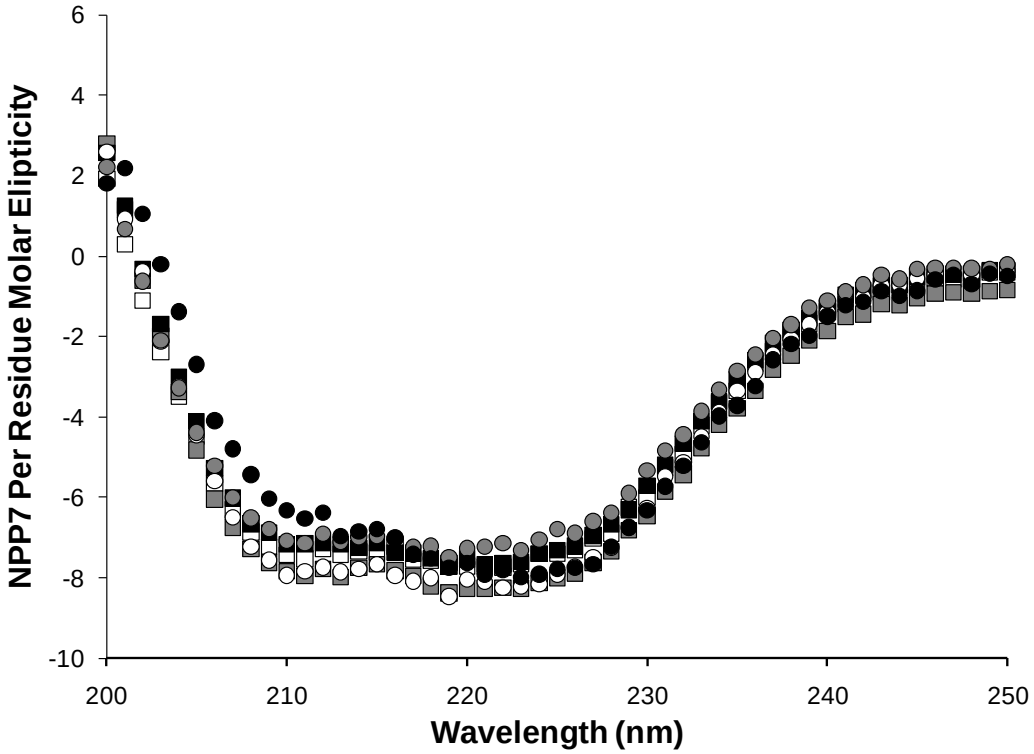

Fig. 5.3. Secondary structural effects of EDTA and divalent metals. NPP7ExFLAG treated with EDTA for 16 hours was then incubated for 30 minutes with Ca^{2+}(grey squares), Co^{2+} (white squares), Ni^{2+}(grey circles), Zn^{2+} (full black circles) or just EDTA (white circles) before dilution and CD determination. A molar ratio of 1:120:1E6 for Enzyme:EDTA:metal was used in each experiment.

The data obtained from these spectra was deconvoluted using default CDSSTR settings on the DicroWeb server accessed at http://dicroweb.cryst.bbk.ac.uk. The percent secondary structural compositions calculated for each sample are shown in Table 5.1. For

the results to be meaningful, the CDSSTR algorithms have a maximum set error of 0.2. The errors shown in Table 5.1 indicate the high confidence in the results obtained using this algorithm.

Table 5.1. Secondary structural components of EDTA/metal-treated NPP7ExFLAG

Element	% Secondary Structural Composition					
	Untreated	EDTA	Ca^{2+}	Co^{2+}	Ni^{2+}	Zn^{2+}
α-helix	31	31	31	32	31	30
β-sheet	12	11	14	12	13	20
Random coil	57	57	55	56	55	50
Max. Error	0.122	0.122	0.182	0.122	0.182	0.182

5.3.4 Effect of EDTA and divalent metals on thermal stability

Thermal scans were obtained at 222 nm for the same sample set used to characterize global secondary structure. Data was collected at every degree between 20 and 100°C and was converted to a measure of the folded/unfolded fraction using the equation (Folded fraction = $([\theta]^{obs} - [\theta]^{den}) / ([\theta]^{nat} - [\theta]^{den})$ based on the work of Luthra *et. al.* (6) where $[\theta]^{obs}$ is the ellipticity at any temperature, $[\theta]^{den}$ is the ellipticity at highest temperature, and $[\theta]^{nat}$ is the ellipticity at lowest temperature. Plots of the unfolded fraction (1-folded fraction) versus temperature (°C) are shown in Fig. 5.4. The point at which the protein is half unfolded is defined as T_{50}. Table 5.2 is a compilation of the T_{50} values obtained for each sample. The T_{50} of the untreated protein was determined to be

approximately 70°C. EDTA-treated NPP7ExFLAG had the highest T_{50} value (75°C), whereas the zinc-, nickel-, and cobalt-treated samples had T_{50} values lower than that of the untreated sample (60°C, 65°C and 68°C respectively). The T_{50} of the protein remained essentially unchanged with calcium treatment.

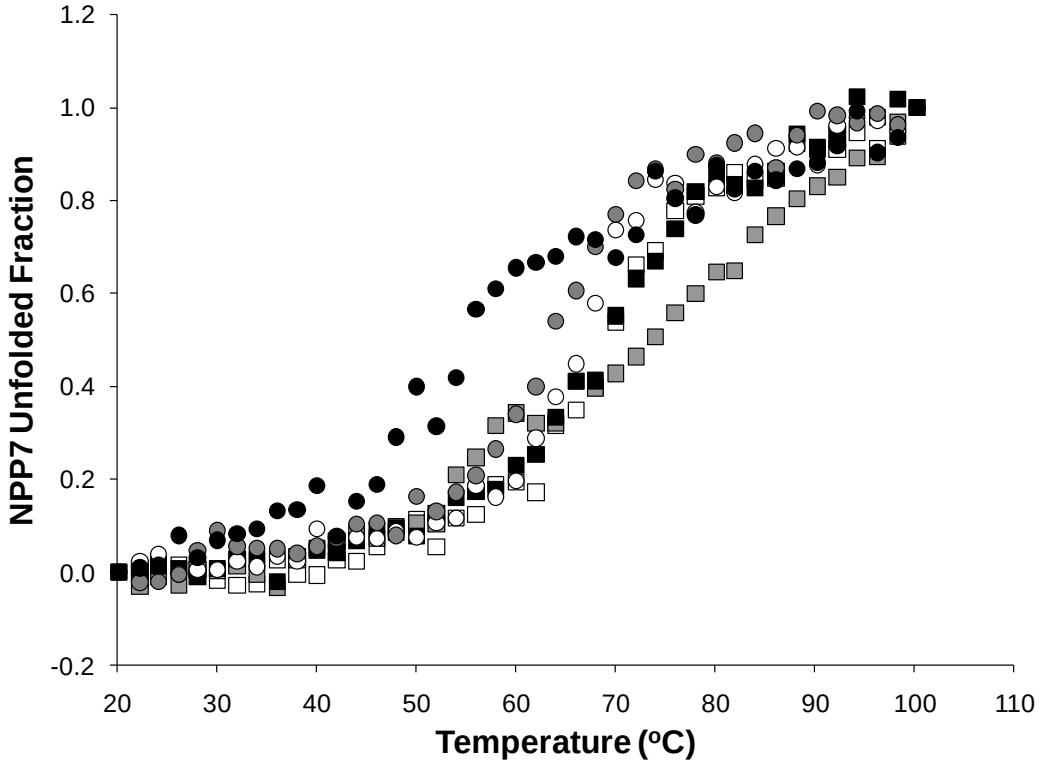

Fig. 5.4. Effect of EDTA and divalent metals on the thermal stability of NPP7ExFLAG. Thermal denaturation was studied at 222 nm. Samples shown were pretreated with EDTA for 16 hours then treated with the divalent metals calcium (white squares), cobalt (white circles), nickel (grey circles), zinc (black circles) or CD buffer (grey squares). The temperature was steadily increased from 20°C to100°C.

Table 5.2. Melting temperatures of EDTA/metal-treated NPP7ExFLAG.

Sample treatment	Untreated	EDTA	Ca^{2+}	Co^{2+}	Ni^{2+}	Zn^{2+}
NPP7	70	75	71	68	65	60

5.4 Discussion

A requirement of divalent metal cations for catalytic activity is a general feature of all NPP isoforms (1). Although the specific identity of the metal(s) present in each individual NPP isoform has not yet been determined conclusively, several divalent metals have previously been shown to restore the activity of NPP2, NPP6 and NPP7 (3, 7, 8). Duan *et al* reported that NPP7 was significantly inhibited by Zn^{2+} and that the inhibitory effect could be prevented by the addition of 2 mM EDTA (1, 5). It is important to note that the experimental conditions under which these previous experiments were performed were not detailed in the literature. In the current work we have established that, contrary to these earlier reports, NPP7 is inhibited by EDTA at concentrations in the micromolar range, although the inhibition takes time. Since the length of the ETDA treatment was not included in the methods described by Duan and coworkers, we cannot be sure if this is the root of the differences noted. We have also established that the catalytic activity of this EDTA-treated enzyme is restored by the addition of cobalt, nickel and zinc, suggesting that EDTA may have inhibited activity by either abstracting or chelating the endogenous divalent metal cations making it unavailable for coordination within the

enzyme's active site. However our studies were not sufficient to distinguish between these possibilities. All metals tested were added in excess at a 1:1 x 10^6 enzyme to metal molar ratio but further work is ongoing where varying concentrations of divalent metal cations coupled with dialysis to remove excess metal will be done before studying the behavior of the enzyme. Our results showed that cobalt, nickel and zinc were able to restore catalytic function after EDTA treatment. Despite these results, it remains unknown if any of these three candidates is one or more of the divalent, active site metals in endogenously expressed NPP7. Further experimentation using atomic absorption spectroscopy is currently ongoing to establish the identity and stoichiometry of the metals in the NPP7 active site.

In exploring the specific role of divalent metals in NPP7ExFLAG function, we have established that the secondary structure of the enzyme does not change in the presence or absence of the metals in its active site. Results from our CD experiments established that the secondary structural composition of the enzyme remains the same regardless of EDTA treatment and metal ion add back (Figure 5.3, Table 5.1). Since catalytic function is effectively abolished with EDTA treatment over 16 hours (presumably via endogenous metal removal) we conclude that the divalent metal cations play a functional but not a structural role in this enzyme. Our work is not exhaustive in the study of metal-binding by NPP7 because our experiments were designed with no intermediate metal concentrations used. According to the proposed mechanism, NPP7 requires two divalent metal cations in the active site for activity and thus should not need a large excess of metals for restoration of its activity. Future studies with lower metal concentrations in addition to isothermal titration calorimetry experiments may shed light

on whether the metals bind at sites other than the known coordination sites and if so are there any effects associated with such interactions.

Interesting data were obtained for the influence of EDTA and divalent metal cations on the thermal stability of NPP7ExFLAG. EDTA treated NPP7ExFLAG, which exhibited significantly reduced catalytic activity, had a higher melting temperature than the untreated control. These data suggest that EDTA treatment stabilized the enzyme although the secondary structure composition was not altered. On the other hand, addition of the divalent metal cations cobalt, nickel, and zinc (all shown to significant restore NPP7 activity following EDTA treatment) led to a decrease in experimentally determined T_{50} of the protein. Calcium add back restored less activity than cobalt, nickel, and zinc but the T_{50} for this treatment was nearly unchanged from the control. These results suggest that the cations may help provide molecular flexibility required for function. This phenomenon requires further investigation as it is clear from the wavelength spectra that none of these metals had a significant impact on the protein's secondary structure.

5.5 References

1. Duan, R., 2003. Identification of human intestinal alkaline sphingomyelinase as a a novel ecto-enzyme related to the nucleotide phosohodiesterase family, *Biological chemistry*, **278**: 38528-38536.
2. Gijsbers, R., J. Aoki, H. Arai and M. Bollen. 2003. The hydrolysis of lysophospholipids and nucleotides by autotaxin (NPP2) involves a single catalytic site, *FEBS Lett*, **538**: 60-4.

3. Gijsbers, R., H. Ceulemans, W. Stalmans and M. Bollen. 2001. Structural and catalytic similarities between nucleotide pyrophosphatases/phosphodiesterases and alkaline phosphatases, *J Biol Chem*, **276**: 1361-8.

4. Zalatan, J. G., T. D. Fenn, A. T. Brunger and D. Herschlag. 2006. Structural and functional comparisons of nucleotide pyrophosphatase/phosphodiesterase and alkaline phosphatase: implications for mechanism and evolution, *Biochemistry*, **45**: 9788-803.

5. Duan, R. D., T. Bergman, N. Xu, J. Wu, Y. Cheng, J. Duan, S. Nelander, C. Palmberg and A. Nilsson. 2003. Identification of human intestinal alkaline sphingomyelinase as a novel ecto-enzyme related to the nucleotide phosphodiesterase family, *J Biol Chem*, **278**: 38528-36.

6. Luthra A., S. S. Malik and R. Ramachandran. 2008. Cloning, purification and comparative structural analysis of two hypothetical proteins from *mycobacterium tuberclosis* found in the human granuloma during persistence and highly up-regulated under carbon-starvation conditions, *Protein Expr Purif*, **62**: 64-74.

7. Sakagami, H., J. Aoki, Y. Natori, K. Nishikawa, Y. Kakehi and H. Arai. 2005. Biochemical and molecular characterization of a novel choline-specific glycerophosphodiester phosphodiesterase belonging to the nucleotide pyrophosphatase/phosphodiesterase family, *J Biol Chem*, **280**: 23084-93.

8. Wu, J., G. H. Hansen, A. Nilsson and R. D. Duan. 2005. Functional studies of human intestinal alkaline sphingomyelinase by deglycosylation and mutagenesis, *Biochem J*, **386**: 153-60.

CHAPTER 6

ACCOMPLISHMENTS AND CONCLUSIONS

Forty-one years have passed since the first paper was published detailing the discovery, by Swedish scientist Ake Nilsson, of the protein that would eventually be known as nucleotide pyrophosphatase/ phosphodiesterase (NPP) 7 (1). Duan and colleagues purified the enzyme from human bile in 1997 (2). Their characterization quickly excluded the enzyme from the sphingomyelinase family due to lack of functional and structural similarities with known members including the acid and neutral sphingomyelinases. Successive reports in 2002 and 2003 (3, 4) led to the association of this Alk-SMase with the nucleotide pyrophosphatase/ phosphodiesterase (NPP) sub-family of alkaline phosphatase enzymes. More than thirty years after its discovery, the complete cDNA sequence of Alk-SMase was successfully determined (Genbank #AY20633) and the enzyme became the most recently identified member of the NPP family and it was renamed NPP7 (3). NPP7 was shown to possess lysolipid phosphodiesterase activity similar to the NPP2 and NPP6 isoforms (5) . NPP7 was further classified as a lysophospholipase C (along with NPP6) due to its ability to cleave phosphocholine from choline-containing lysolipid phosphodiesters substrates. To date, NPP7 is the only known NPP isoform associated with anticancer effects which are proposed to result from the hydrolysis of three endogenous substrates lysophosphatidylcholine (LPC), platelet activating factor (PAF), and sphingomyelin (SM) (6). Moreover, NPP7 has been associated with physiological processes such as

cholesterol absorption and maturation of the intestinal tract as well as pathological processes such as atherosclerosis and inflammatory bowel disease (7). Despite considerable characterization of this enzyme, almost exclusively conducted by Duan and coworkers, several unresolved questions remained about the structure and function of NPP7. Our work has attempted to address questions of substrate specificity using novel assay methods, with subsequent kinetic analysis. Questions concerning the role of divalent metal cations and substrate specifying determinants were addressed using a combination of CD spectroscopy, computational modeling, site-directed mutagenesis and kinetic analysis.

The work to further characterize known and novel NPP7 substrates started with application of a previously described Amplex Red-based assay to the analysis of NPP7 activity in a multi-well format. This method allowed for the kinetic characterization of NPP7 activity using unmodified known and novel substrates. Using this approach we identified two additional endogenous NPP7 substrates, lyso platelet activating factor (lysoPAF) and sphingosylphosphorylcholine (SPC). In addition, one non-lipid substrate, *para*-nitrophenylphosphocholine (pNPPC) was also identified and used with an adapted absorbance assay to further examine NPP7 catalytic function. These methods are important advances for NPP7 as multi-well assays were not described previously. As such, cumbersome and expensive assays (such as radiolabeled substrates with TLC and autoradiography) were previously the only choice.

The study of structure-activity relationships of NPP isoforms has been slowed due a lack of physical structural data on NPP7. The only available crystal structure to use as a template at the onset of this work was that of the bacterial *Xac NPP* (8). A homology

model was generated based on this template that was used to analyze enzyme-substrate interactions as a guide to site-directed mutagenesis. Our results identified F275 as an essential residue for NPP7 recognition of all choline containing substrates. These efforts are not exhaustive, but highlight further work needed in this area. With regard to substrate identification, all the substrates tested here were choline phosphodiesters but a survey of other lysophospholipids such as LPI, LPE, and LPG may also help understand NPP7 function. In fact, since we found NPP7 to be less discriminating than NPP2 and NPP6, it would be worthwhile testing additional analogs such as PE, PI, and PS as well. Characterization of additional lipids will be helpful in understanding the role of F275 since its interaction point in the model complexes was with the choline group of all tested substrates. More work is needed to completely understand substrate specifying determinants of NPP7. The work described herein sets the stage for future experimental site-directed mutagenesis of NPP7. A next logical step would be to examine the role of specific sites by mutating them to their complementary residues in other NPP isoforms as shown by Table 4.7. This approach would allow analysis of similarities and differences in NPP substrate specificities and regioselectivies.

All NPP isoforms are known to be inactivated in the absence of divalent metal cations. However, the identity of these metals remained unknown. Likewise, it was not known whether these metals play only functional, or in addition, structural roles. Using a combination of EDTA treatment, metal ion add back, functional analysis and circular dichroism, we have established that the divalent metal cations play only functional and not structural roles in NPP7. Experimental data showed that cobalt, nickel and zinc restored activity of EDTA-treated NPP7 without significant effects on secondary

structure. Future efforts can be focused on identification of the divalent metals present in endogenous NPP7 by atomic absorption spectroscopy and characterization of metals such as cobalt in the active site using electron paramagenetic resonance spectroscopy.

In conclusion, this work has addressed three significant areas associated with human NPP7. The major legacy of this work has been the methodology generated that will allow for future characterization of this important enzyme.

6.1 References

1. Nilsson. 1969. The presence of sphingomyelin- and ceramide-cleaving enzymes in the small intestinal tract. *Biochimica biophysica Acta* **176**: 339-347.
2. Hertervig, E., A. Nilsson, L. Nyberg, and R. D. Duan. 1997. Alkaline sphingomyelinase activity is decreased in human colorectal carcinoma. *Cancer* **79**: 448-453.
3. Duan, R. 2003. Identification of human intestinal alkaline sphingomyelinase as a a novel ecto-enzyme related to the nucleotide phosohodiesterase family. *Biological chemistry* **278**: 38528-38536.
4. Cheng, Y. 2002. Purification, localization and expression of human intestinal alkaline sphingomyelinase. *Lipid Research* **44**: 316-324.
5. Stefan, C., S. Jansen, and M. Bollen. 2005. NPP-type ectophosphodiesterases: unity in diversity. *Trends Biochem Sci* **30**: 542-550.
6. Wu, J., G. H. Hansen, A. Nilsson, and R. D. Duan. 2005. Functional studies of human intestinal alkaline sphingomyelinase by deglycosylation and mutagenesis. *Biochem J* **386**: 153-160.

7. Duan, R. D. 2006. Alkaline sphingomyelinase: an old enzyme with novel implications. *Biochim Biophys Acta* **1761**: 281-291.

8. Zalatan, J. G., T. D. Fenn, A. T. Brunger, and D. Herschlag. 2006. Structural and functional comparisons of nucleotide pyrophosphatase/phosphodiesterase and alkaline phosphatase: implications for mechanism and evolution. *Biochemistry* **45**: 9788-9803.

APPENDIX

Human NPP7 (full length wild type)
Vectors: pcDNA3.1(+) and pFASTBac1, (upstream: BamH1, downstream: Not1)

Amino Acid Sequence

MRGPAVLLTV ALATLLAPGA GAPVQSQGSQ NKLLLVSFDG FRWNYDQDVD TPNLDAMARD
GVKARYMTPA FVTMTSPCHF TLVTGKYIEN HGVVHNMYYN TTSKVKLPYH ATLGIQRWWD
NGSVPIWITA QRQGLRAGSF FYPGGNVTYQ GVAVTRSRKE GIAHNYKNET EWRANIDTVM
AWFTEEDLDL VTLYFGEPDS TGHRYGPESP ERREMVRQVD RTVGYLRESI ARNHLTDRLN
LIITSDHGMT TVDKRAGDLV EFHKFPNFTF RDIEFELLDY GPNGMLLPKE GRLEKVYDAL
KDAHPKLHVY KKEAFPEAFH YANNPRVTPL LMYSDLGYVI HGRINVQFNN GEHGFDNKDM
DMKTIFRAVG PSFRAGLEVE PFESVHVYEL MCRLLGIVPE ANDGHLATLL PMLHTESALP
PDGRPTLLPK GRSALPPSSR PLLVMGLLGT VILLSEVA

Nucleotide Sequence

atgagaggcc cggccgtcct cctcactgtg gctctggcca cgctcctggc tcccggggcc
ggagcaccgg tacaaagtca gggctcccag aacaagctgc tcctggtgtc cttcgacggc
ttccgctgga actacgacca ggacgtggac acccccaacc tggacgccat ggcccgagac
ggggtgaagg cacgctacat gacccccgcc tttgtcacca tgaccagccc ctgccacttc
accctggtca ccggcaaata tatcgagaac cacggggtgg ttcacaacat gtactacaac
accaccagca aggtgaagct gccctaccac gccacgctgg gcatccagag gtggtgggac
aacggcagcg tgcccatctg gatcacagcc cagaggcagg gcctgagggc tggctccttc
ttctacccgg gcgggaacgt cacctaccaa ggggtggctg tgacgcggag ccggaaagaa
ggcatcgcac acaactacaa aaatgagacg gagtggagag cgaacatcga cacagtgatg
gcgtggttca cagaggagga cctggatctg gtcacactct acttcgggga gccggactcc
acgggccaca ggtacggccc cgagtccccg gagaggaggg agatggtgcg gcaggtggac
cggaccgtgg gctacctccg ggagagcatc gcgcgcaacc acctcacaga ccgcctcaac
ctgatcatca catccgacca cggcatgacg accgtggaca aacgggctgg cgacctggtt
gaattccaca agttccccaa cttcaccttc cgggacatcg agtttgagct cctggactac
ggaccaaacg ggatgctgct ccctaaagaa gggaggctgg agaaggtgta cgatgccctc
aaggacgccc accccaagct ccacgtctac aagaaggagg cgttccccga ggccttccac
tacgccaaca accccagggt cacacccctg ctgatgtaca gcgaccttgg ctacgtcatc
catgggagaa ttaacgtcca gttcaacaat ggggagcacg gctttgacaa caaggacatg
gacatgaaga ccatcttccg cgctgtgggc cctagcttca gggcgggcct ggaggtggag
ccctttgaga gcgtccacgt gtacgagctc atgtgccggc tgctgggcat cgtgcccgag
gccaacgatg ggcacctagc tactctgctg cccatgctgc acacagaatc tgctcttccg
cctgatggaa ggcctactct cctgcccaag ggaagatctg ctctcccgcc cagcagcagg
cccctcctcg tgatgggact gctggggacc gtgattcttc tgtctgaggt cgca

Appendix 1.1. Human NPP7 (full length). Complete amino acid (top) and verified nucleotide (bottom) sequences are shown. For reference the catalytic (T75) residue is highlighted in black. The region highlighted in grey is cutoff to make the T415Ex construct.

Human NPP7ExFLAG

Vectors: pcDNA3.1(+) and pFASTBac1, (upstream: BamH1, downstream: Not1)

Amino Acid Sequence

MRGPAVLLTV ALATLLAPGA GAPVQSQGSQ NKLLLVSFDG FRWNYDQDVD TPNLDAMARD
GVKARYMTPA FVTMTSPCHF TLVTGKYIEN HGVVHNMYYN TTSKVKLPYH ATLGIQRWWD
NGSVPIWITA QRQGLRAGSF FYPGGNVTYQ GVAVTRSRKE GIAHNYKNET EWRANIDTVM
AWFTEEDLDL VTLYFGEPDS TGHRYGPESP ERREMVRQVD RTVGYLRESI ARNHLTDRLN
LIITSDHGMT TVDKRAGDLV EFHKFPNFTF RDIEFELLDY GPNGMLLPKE GRLEKVYDAL
KDAHPKLHVY KKEAFPEAFH YANNPRVTPL LMYSDLGYVI HGRINVQFNN GEHGFDNKDM
DMKTIFRAVG PSFRAGLEVE PFESVHVYEL MCRLLGIVPE ANDGHLATLL PMLHTDYKDD
DDK

Nucleotide Sequence

atgagaggcc cggccgtcct cctcactgtg gctctggcca cgctcctggc tcccggggcc
ggagcaccgg tacaaagtca gggctcccag aacaagctgc tcctggtgtc cttcgacggc
ttccgctgga actacgacca ggacgtggac acccccaacc tggacgccat ggcccgagac
ggggtgaagg cacgctacat gacccccgcc tttgtcacca tgaccagccc ctgccacttc
accctggtca ccggcaaata tatcgagaac cacggggtgg ttcacaacat gtactacaac
accaccagca aggtgaagct gccctaccac gccacgctgg gcatccagag gtggtgggac
aacggcagcg tgcccatctg gatcacagcc cagaggcagg gcctgagggc tggctccttc
ttctacccgg gcgggaacgt cacctaccaa ggggtggctg tgacgcggag ccggaaagaa
ggcatcgcac acaactacaa aaatgagacg gagtggagag cgaacatcga cacagtgatg
gcgtggttca cagaggagga cctggatctg gtcacactct acttcgggga gccggactcc
acgggccaca ggtacggccc cgagtccccg gagaggaggg agatggtgcg gcaggtggac
cggaccgtgg gctacctccg ggagagcatc gcgcgcaacc acctcacaga ccgcctcaac
ctgatcatca catccgacca cggcatgacg accgtggaca aacgggctgg cgacctggtt
gaattccaca agttccccaa cttcaccttc cgggacatcg agtttgagct cctggactac
ggaccaaacg ggatgctgct ccctaaagaa gggaggctgg agaaggtgta cgatgccctc
aaggacgccc accccaagct ccacgtctac aagaaggagg cgttccccga ggccttccac
tacgccaaca accccagggt cacacccctg ctgatgtaca gcgaccttgg ctacgtcatc
catgggagaa ttaacgtcca gttcaacaat ggggagcacg gctttgacaa caaggacatg
gacatgaaga ccatcttccg cgctgtgggc cctagcttca gggcgggcct ggaggtggag
ccctttgaga gcgtccacgt gtacgagctc atgtgccggc tgctgggcat cgtgcccgag
gccaacgatg ggcacctagc tactctgctg cccatgctgc acacagacta caaggacgac
gatgacaag

Appendix 1.2. Human NPP7ExFLAG. Complete amino acid (top) and verified nucleotide (bottom) sequences are shown. For reference the catalytic (T75) residue is highlighted in black and the FLAG affinity tag is highlighted in grey.

Human NPP7ExFLAG-F80A

Vectors: pcDNA3.1(+) and pFASTBac1, (upstream: BamH1, downstream: Not1)

Amino acid Sequence

MRGPAVLLTV ALATLLAPGA GAPVQSQGSQ NKLLLVSFDG FRWNYDQDVD TPNLDAMARD
GVKARYMTPA FVTMTSPCHA TLVTGKYIEN HGVVHNMYYN TTSKVKLPYH ATLGIQRWWD
NGSVPIWITA QRQGLRAGSF FYPGGNVTYQ GVAVTRSRKE GIAHNYKNET EWRANIDTVM
AWFTEEDLDL VTLYFGEPDS TGHRYGPESP ERREMVRQVD RTVGYLRESI ARNHLTDRLN
LIITSDHGMT TVDKRAGDLV EFHKFPNFTF RDIEFELLDY GPNGMLLPKE GRLEKVYDAL
KDAHPKLHVY KKEAFPEAFH YANNPRVTPL LMYSDLGYVI HGRINVQFNN GEHGFDNKDM
DMKTIFRAVG PSFRAGLEVE PFESVHVYEL MCRLLGIVPE ANDGHLATLL PMLHTDYKDD
DDK

Nucleotide Sequence

atgagaggcc cggccgtcct cctcactgtg gctctggcca cgctcctggc tcccggggcc
ggagcaccgg tacaaagtca gggctcccag aacaagctgc tcctggtgtc cttcgacggc
ttccgctgga actacgacca ggacgtggac acccccaacc tggacgccat ggcccgagac
ggggtgaagg cacgctacat gacccccgcc tttgtcacca tgaccagccc ctgccacgcc
accctggtca ccggcaaata tatcgagaac cacggggtgg ttcacaacat gtactacaac
accaccagca aggtgaagct gccctaccac gccacgctgg gcatccagag gtggtgggac
aacggcagcg tgcccatctg gatcacagcc cagaggcagg gcctgagggc tggctccttc
ttctacccgg gcgggaacgt cacctaccaa ggggtggctg tgacgcggag ccggaaagaa
ggcatcgcac acaactacaa aaatgagacg gagtggagag cgaacatcga cacagtgatg
gcgtggttca cagaggagga cctggatctg gtcacactct acttcgggga gccggactcc
acgggccaca ggtacggccc cgagtccccg gagaggaggg agatggtgcg gcaggtggac
cggaccgtgg gctacctccg ggagagcatc gcgcgcaacc acctcacaga ccgcctcaac
ctgatcatca catccgacca cggcatgacg accgtggaca aacgggctgg cgacctggtt
gaattccaca agttccccaa cttcaccttc cgggacatcg agtttgagct cctggactac
ggaccaaacg ggatgctgct ccctaaagaa gggaggctgg agaaggtgta cgatgccctc
aaggacgccc accccaagct ccacgtctac aagaaggagg cgttccccga ggccttccac
tacgccaaca accccagggt cacacccctg ctgatgtaca gcgaccttgg ctacgtcatc
catgggagaa ttaacgtcca gttcaacaat ggggagcacg gctttgacaa caaggacatg
gacatgaaga ccatcttccg cgctgtgggc cctagcttca gggcgggcct ggaggtggag
ccctttgaga gcgtccacgt gtacgagctc atgtgccggc tgctgggcat cgtgcccgag
gccaacgatg ggcacctagc tactctgctg cccatgctgc acacagacta caaggacgac
gatgacaag

Appendix 1.3. Human NPP7ExFLAG-F80A. Complete amino acid (top) and verified nucleotide (bottom) sequences are shown. For reference the catalytic (T75) residue is highlighted in black and the FLAG affinity tag is highlighted in grey. The mutation site is highlighted in blue.

Human NPP7ExFLAG-L107F

Vectors: pcDNA3.1(+) and pFASTBac1, (upstream: BamH1, downstream: Not1)

Amino acid Sequence

MRGPAVLLTV ALATLLAPGA GAPVQSQGSQ NKLLLVSFDG FRWNYDQDVD TPNLDAMARD
GVKARYMTPA FVTMTSPCHF TLVTGKYIEN HGVVHNMYYN TTSKVKFPYH ATLGIQRWWD
NGSVPIWITA QRQGLRAGSF FYPGGNVTYQ GVAVTRSRKE GIAHNYKNET EWRANIDTVM
AWFTEEDLDL VTLYFGEPDS TGHRYGPESP ERREMVRQVD RTVGYLRESI ARNHLTDRLN
LIITSDHGMT TVDKRAGDLV EFHKFPNFTF RDIEFELLDY GPNGMLLPKE GRLEKVYDAL
KDAHPKLHVY KKEAFPEAFH YANNPRVTPL LMYSDLGYVI HGRINVQFNN GEHGFDNKDM
DMKTIFRAVG PSFRAGLEVE PFESVHVYEL MCRLLGIVPE ANDGHLATLL PMLHTDYKDD
DDK

Nucleotide Sequence

atgagaggcc cggccgtcct cctcactgtg gctctggcca cgctcctggc tcccggggcc
ggagcaccgg tacaaagtca gggctcccag aacaagctgc tcctggtgtc cttcgacggc
ttccgctgga actacgacca ggacgtggac acccccaacc tggacgccat ggcccgagac
ggggtgaagg cacgctacat gacccccgcc tttgtcacca tgaccagccc ctgccacttc
accctggtca ccggcaaata tatcgagaac cacggggtgg ttcacaacat gtactacaac
accaccagca aggtgaagtt cccctaccac gccacgctgg gcatccagag gtggtgggac
aacggcagcg tgcccatctg gatcacagcc cagaggcagg gcctgagggc tggctccttc
ttctacccgg gcgggaacgt cacctaccaa ggggtggctg tgacgcggag ccggaaagaa
ggcatcgcac acaactacaa aaatgagacg gagtggagag cgaacatcga cacagtgatg
gcgtggttca cagaggagga cctggatctg gtcacactct acttcgggga gccggactcc
acgggccaca ggtacggccc cgagtccccg gagaggaggg agatggtgcg gcaggtggac
cggaccgtgg gctacctccg ggagagcatc gcgcgcaacc acctcacaga ccgcctcaac
ctgatcatca catccgacca cggcatgacg accgtggaca aacgggctgg cgacctggtt
gaattccaca agttccccaa cttcaccttc cgggacatcg agtttgagct cctggactac
ggaccaaacg ggatgctgct ccctaaagaa gggaggctgg agaaggtgta cgatgccctc
aaggacgccc accccaagct ccacgtctac aagaaggagg cgttccccga ggccttccac
tacgccaaca accccagggt cacacccctg ctgatgtaca gcgaccttgg ctacgtcatc
catgggagaa ttaacgtcca gttcaacaat ggggagcacg gctttgacaa caaggacatg
gacatgaaga ccatcttccg cgctgtgggc cctagcttca gggcgggcct ggaggtggag
ccctttgaga gcgtccacgt gtacgagctc atgtgccggc tgctgggcat cgtgcccgag
gccaacgatg ggcacctagc tactctgctg cccatgctgc acacagacta caaggacgac
gatgacaag

Appendix 1.4. Human NPP7ExFLAG- L107F. Complete amino acid (top) and verified nucleotide (bottom) sequences are shown. For reference the catalytic (T75) residue is highlighted in black and the FLAG affinity tag is highlighted in grey. The mutation site is highlighted in blue.

Human NPP7ExFLAG-Y142A

Vectors: pcDNA3.1(+) and pFASTBac1, (upstream: BamH1, downstream: Not1)

Amino acid Sequence

MRGPAVLLTV ALATLLAPGA GAPVQSQGSQ NKLLLVSFDG FRWNYDQDVD TPNLDAMARD
GVKARYMTPA FVTMTSPCHF TLVTGKYIEN HGVVHNMYYN TTSKVKLPYH ATLGIQRWWD
NGSVPIWITA QRQGLRAGSF FAPGGNVTYQ GVAVTRSRKE GIAHNYKNET EWRANIDTVM
AWFTEEDLDL VTLYFGEPDS TGHRYGPESP ERREMVRQVD RTVGYLRESI ARNHLTDRLN
LIITSDHGMT TVDKRAGDLV EFHKFPNFTF RDIEFELLDY GPNGMLLPKE GRLEKVYDAL
KDAHPKLHVY KKEAFPEAFH YANNPRVTPL LMYSDLGYVI HGRINVQFNN GEHGFDNKDM
DMKTIFRAVG PSFRAGLEVE PFESVHVYEL MCRLLGIVPE ANDGHLATLL PMLHTDYKDD
DDK

Nucleotide Sequence

atgagaggcc cggccgtcct cctcactgtg gctctggcca cgctcctggc tcccggggcc
ggagcaccgg tacaaagtca gggctcccag aacaagctgc tcctggtgtc cttcgacggc
ttccgctgga actacgacca ggacgtggac acccccaacc tggacgccat ggcccgagac
ggggtgaagg cacgctacat gacccccgcc tttgtcacca tgaccagccc ctgccacttc
accctggtca ccggcaaata tatcgagaac cacggggtgg ttcacaacat gtactacaac
accaccagca aggtgaagct gccctaccac gccacgctgg gcatccagag gtggtgggac
aacggcagcg tgcccatctg gatcacagcc cagaggcagg gcctgagggc tggctccttc
ttcgccccgg gcgggaacgt cacctaccaa ggggtggctg tgacgcggag ccggaaagaa
ggcatcgcac acaactacaa aaatgagacg gagtggagag cgaacatcga cacagtgatg
gcgtggttca cagaggagga cctggatctg gtcacactct acttcgggga gccggactcc
acgggccaca ggtacggccc cgagtccccg gagaggaggg agatggtgcg gcaggtggac
cggaccgtgg gctacctccg ggagagcatc gcgcgcaacc acctcacaga ccgcctcaac
ctgatcatca catccgacca cggcatgacg accgtggaca aacgggctgg cgacctggtt
gaattccaca agttccccaa cttcaccttc cgggacatcg agtttgagct cctggactac
ggaccaaacg ggatgctgct ccctaaagaa gggaggctgg agaaggtgta cgatgccctc
aaggacgccc accccaagct ccacgtctac aagaaggagg cgttccccga ggccttccac
tacgccaaca accccagggt cacacccctg ctgatgtaca gcgaccttgg ctacgtcatc
catgggagaa ttaacgtcca gttcaacaat ggggagcacg gctttgacaa caaggacatg
gacatgaaga ccatcttccg cgctgtgggc cctagcttca gggcgggcct ggaggtggag
ccctttgaga gcgtccacgt gtacgagctc atgtgccggc tgctgggcat cgtgcccgag
gccaacgatg ggcacctagc tactctgctg cccatgctgc acacagacta caaggacgac
gatgacaag

Appendix 1.5. Human NPP7ExFLAG- Y142A. Complete amino acid (top) and verified nucleotide (bottom) sequences are shown. For reference the catalytic (T75) residue is highlighted in black and the FLAG affinity tag is highlighted in grey. The mutation site is highlighted in blue.

Human NPP7ExFLAG-Y166A

Vectors: pcDNA3.1(+) and pFASTBac1, (upstream: BamH1, downstream: Not1)

Amino acid Sequence

MRGPAVLLTV ALATLLAPGA GAPVQSQGSQ NKLLLVSFDG FRWNYDQDVD TPNLDAMARD
GVKARYMTPA FVTMTSPCHF TLVTGKYIEN HGVVHNMYYN TTSKVKLPYH ATLGIQRWWD
NGSVPIWITA QRQGLRAGSF FYPGGNVTYQ GVAVTRSRKE GIAHNAKNET EWRANIDTVM
AWFTEEDLDL VTLYFGEPDS TGHRYGPESP ERREMVRQVD RTVGYLRESI ARNHLTDRLN
LIITSDHGMT TVDKRAGDLV EFHKFPNFTF RDIEFELLDY GPNGMLLPKE GRLEKVYDAL
KDAHPKLHVY KKEAFPEAFH YANNPRVTPL LMYSDLGYVI HGRINVQFNN GEHGFDNKDM
DMKTIFRAVG PSFRAGLEVE PFESVHVYEL MCRLLGIVPE ANDGHLATLL PMLHTDYKDD
DDK

Nucleotide Sequence

atgagaggcc cggccgtcct cctcactgtg gctctggcca cgctcctggc tcccggggcc
ggagcaccgg tacaaagtca gggctcccag aacaagctgc tcctggtgtc cttcgacggc
ttccgctgga actacgacca ggacgtggac acccccaacc tggacgccat ggcccgagac
ggggtgaagg cacgctacat gacccccgcc tttgtcacca tgaccagccc ctgccacttc
accctggtca ccggcaaata tatcgagaac cacggggtgg ttcacaacat gtactacaac
accaccagca aggtgaagct gccctaccac gccacgctgg gcatccagag gtggtgggac
aacggcagcg tgcccatctg gatcacagcc cagaggcagg gcctgagggc tggctccttc
ttctacccgg gcgggaacgt cacctaccaa ggggtggctg tgacgcggag ccggaaagaa
ggcatcgcac acaacgccaa aaatgagacg gagtggagag cgaacatcga cacagtgatg
gcgtggttca cagaggagga cctggatctg gtcacactct acttcgggga gccggactcc
acgggccaca ggtacggccc cgagtccccg gagaggaggg agatggtgcg gcaggtggac
cggaccgtgg gctacctccg ggagagcatc gcgcgcaacc acctcacaga ccgcctcaac
ctgatcatca catccgacca cggcatgacg accgtggaca aacgggctgg cgacctggtt
gaattccaca agttccccaa cttcaccttc cgggacatcg agtttgagct cctggactac
ggaccaaacg ggatgctgct ccctaaagaa gggaggctgg agaaggtgta cgatgccctc
aaggacgccc accccaagct ccacgtctac aagaaggagg cgttccccga ggccttccac
tacgccaaca accccagggt cacacccctg ctgatgtaca gcgaccttgg ctacgtcatc
catgggagaa ttaacgtcca gttcaacaat ggggagcacg gctttgacaa caaggacatg
gacatgaaga ccatcttccg cgctgtgggc cctagcttca gggcgggcct ggaggtggag
ccctttgaga gcgtccacgt gtacgagctc atgtgccggc tgctgggcat cgtgcccgag
gccaacgatg ggcacctagc tactctgctg cccatgctgc acacagacta caaggacgac
gatgacaag

Appendix 1.6. Human NPP7ExFLAG- Y166A. Complete amino acid (top) and verified nucleotide (bottom) sequences are shown. For reference the catalytic (T75) residue is highlighted in black and the FLAG affinity tag is highlighted in grey. The mutation site is highlighted in blue.

Human NPP7ExFLAG-E169A

Vectors: pcDNA3.1(+) and pFASTBac1, (upstream: BamH1, downstream: Not1)

Amino acid Sequence

MRGPAVLLTV ALATLLAPGA GAPVQSQGSQ NKLLLVSFDG FRWNYDQDVD TPNLDAMARD
GVKARYMTPA FVTMTSPCHF TLVTGKYIEN HGVVHNMYYN TTSKVKLPYH ATLGIQRWWD
NGSVPIWITA QRQGLRAGSF FYPGGNVTYQ GVAVTRSRKE GIAHNYKNAT EWRANIDTVM
AWFTEEDLDL VTLYFGEPDS TGHRYGPESP ERREMVRQVD RTVGYLRESI ARNHLTDRLN
LIITSDHGMT TVDKRAGDLV EFHKFPNFTF RDIEFELLDY GPNGMLLPKE GRLEKVYDAL
KDAHPKLHVY KKEAFPEAFH YANNPRVTPL LMYSDLGYVI HGRINVQFNN GEHGFDNKDM
DMKTIFRAVG PSFRAGLEVE PFESVHVYEL MCRLLGIVPE ANDGHLATLL PMLHTDYKDD
DDK

Nucleotide Sequence

atgagaggcc cggccgtcct cctcactgtg gctctggcca cgctcctggc tcccggggcc
ggagcaccgg tacaaagtca gggctcccag aacaagctgc tcctggtgtc cttcgacggc
ttccgctgga actacgacca ggacgtggac acccccaacc tggacgccat ggcccgagac
ggggtgaagg cacgctacat gacccccgcc tttgtcacca tgaccagccc ctgccacttc
accctggtca ccggcaaata tatcgagaac cacggggtgg ttcacaacat gtactacaac
accaccagca aggtgaagct gccctaccac gccacgctgg gcatccagag gtggtgggac
aacggcagcg tgcccatctg gatcacagcc cagaggcagg gcctgagggc tggctccttc
ttctacccgg gcgggaacgt cacctaccaa ggggtggctg tgacgcggag ccggaaagaa
ggcatcgcac acaactacaa aaatgcgacg gagtggagag cgaacatcga cacagtgatg
gcgtggttca cagaggagga cctggatctg gtcacactct acttcgggga gccggactcc
acgggccaca ggtacggccc cgagtccccg gagaggaggg agatggtgcg gcaggtggac
cggaccgtgg gctacctccg ggagagcatc gcgcgcaacc acctcacaga ccgcctcaac
ctgatcatca catccgacca cggcatgacg accgtggaca aacgggctgg cgacctggtt
gaattccaca agttccccaa cttcaccttc cgggacatcg agtttgagct cctggactac
ggaccaaacg ggatgctgct ccctaaagaa gggaggctgg agaaggtgta cgatgccctc
aaggacgccc accccaagct ccacgtctac aagaaggagg cgttccccga ggccttccac
tacgccaaca accccagggt cacacccctg ctgatgtaca gcgaccttgg ctacgtcatc
catgggagaa ttaacgtcca gttcaacaat ggggagcacg gctttgacaa caaggacatg
gacatgaaga ccatcttccg cgctgtgggc cctagcttca gggcgggcct ggaggtggag
ccctttgaga gcgtccacgt gtacgagctc atgtgccggc tgctgggcat cgtgcccgag
gccaacgatg ggcacctagc tactctgctg cccatgctgc acacagacta caaggacgac
gatgacaag

Appendix 1.7. Human NPP7ExFLAG- E169A. Complete amino acid (top) and verified nucleotide (bottom) sequences are shown. For reference the catalytic (T75) residue is highlighted in black and the FLAG affinity tag is highlighted in grey. The mutation site is highlighted in blue.

Human NPP7ExFLAG-E169Q

Vectors: pcDNA3.1(+) and pFASTBac1, (upstream: BamH1, downstream: Not1)

Amino acid Sequence

MRGPAVLLTV ALATLLAPGA GAPVQSQGSQ NKLLLVSFDG FRWNYDQDVD TPNLDAMARD
GVKARYMTPA FVTMTSPCHF TLVTGKYIEN HGVVHNMYYN TTSKVKLPYH ATLGIQRWWD
NGSVPIWITA QRQGLRAGSF FYPGGNVTYQ GVAVTRSRKE GIAHNYKNCT EWRANIDTVM
AWFTEEDLDL VTLYFGEPDS TGHRYGPESP ERREMVRQVD RTVGYLRESI ARNHLTDRLN
LIITSDHGMT TVDKRAGDLV EFHKFPNFTF RDIEFELLDY GPNGMLLPKE GRLEKVYDAL
KDAHPKLHVY KKEAFPEAFH YANNPRVTPL LMYSDLGYVI HGRINVQFNN GEHGFDNKDM
DMKTIFRAVG PSFRAGLEVE PFESVHVYEL MCRLLGIVPE ANDGHLATLL PMLHTDYKDD
DDK

Nucleotide Sequence

atgagaggcc cggccgtcct cctcactgtg gctctggcca cgctcctggc tcccggggcc
ggagcaccgg tacaaagtca gggctcccag aacaagctgc tcctggtgtc cttcgacggc
ttccgctgga actacgacca ggacgtggac acccccaacc tggacgccat ggcccgagac
ggggtgaagg cacgctacat gacccccgcc tttgtcacca tgaccagccc ctgccacttc
accctggtca ccggcaaata tatcgagaac cacggggtgg ttcacaacat gtactacaac
accaccagca aggtgaagct gccctaccac gccacgctgg gcatccagag gtggtgggac
aacggcagcg tgcccatctg gatcacagcc cagaggcagg gcctgagggc tggctccttc
ttctacccgg gcgggaacgt cacctaccaa ggggtggctg tgacgcggag ccggaaagaa
ggcatcgcac acaactacaa aaatcagacg gagtggagag cgaacatcga cacagtgatg
gcgtggttca cagaggagga cctggatctg gtcacactct acttcgggga gccggactcc
acgggccaca ggtacggccc cgagtccccg gagaggaggg agatggtgcg gcaggtggac
cggaccgtgg gctacctccg ggagagcatc gcgcgcaacc acctcacaga ccgcctcaac
ctgatcatca catccgacca cggcatgacg accgtggaca aacgggctgg cgacctggtt
gaattccaca agttccccaa cttcaccttc cgggacatcg agtttgagct cctggactac
ggaccaaacg ggatgctgct ccctaaagaa gggaggctgg agaaggtgta cgatgccctc
aaggacgccc accccaagct ccacgtctac aagaaggagg cgttccccga ggccttccac
tacgccaaca accccagggt cacacccctg ctgatgtaca gcgaccttgg ctacgtcatc
catgggagaa ttaacgtcca gttcaacaat ggggagcacg gctttgacaa caaggacatg
gacatgaaga ccatcttccg cgctgtgggc cctagcttca gggcgggcct ggaggtggag
ccctttgaga gcgtccacgt gtacgagctc atgtgccggc tgctgggcat cgtgcccgag
gccaacgatg ggcacctagc tactctgctg cccatgctgc acacagacta caaggacgac
gatgacaag

Appendix 1.8. Human NPP7ExFLAG- E169Q. Complete amino acid (top) and verified nucleotide (bottom) sequences are shown. For reference the catalytic (T75) residue is highlighted in black and the FLAG affinity tag is highlighted in grey. The mutation site is highlighted in blue.

Human NPP7ExFLAG-F275A

Vectors: pcDNA3.1(+) and pFASTBac1, (upstream: BamH1, downstream: Not1)

Amino acid Sequence

MRGPAVLLTV ALATLLAPGA GAPVQSQGSQ NKLLLVSFDG FRWNYDQDVD TPNLDAMARD
GVKARYMTPA FVTMTSPCHF TLVTGKYIEN HGVVHNMYYN TTSKVKLPYH ATLGIQRWWD
NGSVPIWITA QRQGLRAGSF FYPGGNVTYQ GVAVTRSRKE GIAHNYKNET EWRANIDTVM
AWFTEEDLDL VTLYFGEPDS TGHRYGPESP ERREMVRQVD RTVGYLRESI ARNHLTDRLN
LIITSDHGMT TVDKRAGDLV EFHKFPNFTF RDIEFELLDY GPNGMLLPKE GRLEKVYDAL
KDAHPKLHVY KKEAFPEAFH YANNPRVTPL LMYSDLGYVI HGRINVQFNN GEHGFDNKDM
DMKTIFRAVG PSFRAGLEVE PFESVHVYEL MCRLLGIVPE ANDGHLATLL PMLHTDYKDD
DDK

Nucleotide Sequence

atgagaggcc cggccgtcct cctcactgtg gctctggcca cgctcctggc tcccggggcc
ggagcaccgg tacaaagtca gggctcccag aacaagctgc tcctggtgtc cttcgacggc
ttccgctgga actacgacca ggacgtggac acccccaacc tggacgccat ggcccgagac
ggggtgaagg cacgctacat gacccccgcc tttgtcacca tgaccagccc ctgccacttc
accctggtca ccggcaaata tatcgagaac cacggggtgg ttcacaacat gtactacaac
accaccagca aggtgaagct gccctaccac gccacgctgg gcatccagag gtggtgggac
aacggcagcg tgcccatctg gatcacagcc cagaggcagg gcctgagggc tggctccttc
ttctacccgg gcgggaacgt cacctaccaa ggggtggctg tgacgcggag ccggaaagaa
ggcatcgcac acaactacaa aaatgagacg gagtggagag cgaacatcga cacagtgatg
gcgtggttca cagaggagga cctggatctg gtcacactct acttcgggga gccggactcc
acgggccaca ggtacggccc cgagtccccg gagaggaggg agatggtgcg gcaggtggac
cggaccgtgg gctacctccg ggagagcatc gcgcgcaacc acctcacaga ccgcctcaac
ctgatcatca catccgacca cggcatgacg accgtggaca aacgggctgg cgacctggtt
gaattccaca agttccccaa cttcaccttc cgggacatcg aggctgagct cctggactac
ggaccaaacg ggatgctgct ccctaaagaa gggaggctgg agaaggtgta cgatgccctc
aaggacgccc accccaagct ccacgtctac aagaaggagg cgttccccga ggccttccac
tacgccaaca accccagggt cacacccctg ctgatgtaca gcgaccttgg ctacgtcatc
catgggagaa ttaacgtcca gttcaacaat ggggagcacg gctttgacaa caaggacatg
gacatgaaga ccatcttccg cgctgtgggc cctagcttca gggcgggcct ggaggtggag
ccctttgaga gcgtccacgt gtacgagctc atgtgccggc tgctgggcat cgtgcccgag
gccaacgatg ggcacctagc tactctgctg cccatgctgc acacagacta caaggacgac
gatgacaag

Appendix 1.9. Human NPP7ExFLAG- F275A. Complete amino acid (top) and verified nucleotide (bottom) sequences are shown. For reference the catalytic (T75) residue is highlighted in black and the FLAG affinity tag is highlighted in grey. The mutation site is highlighted in blue.